NTNU

Norwegian University of
Science and Technology

Entrainment of Bed Sediments by Debris Flow

Bigyan Sherchan

Geotechnics and Geohazards
Submission date: June 2016
Supervisor: Steinar Nordal, BAT
Co-supervisor: Ashenafi Lulseged Yifru, BAT

Norwegian University of Science and Technology
Department of Civil and Transport Engineering

NTNU
Norwegian University of Science and Technology

Entrainment of Bed Sediments by Debris Flow

Bigyan Sherchan

Geotechnics and Geohazards

Submission date: June 2016

Supervisor: Steinar Nordal, BAT

Co-supervisors: Petter Fornes, BAT

Ashenafi Lulseged Yifru, BAT

Norwegian University of Science and Technology

Department of Civil and Transport Engineering

NORWEGIAN UNIVERSITY OF SCIENCE AND TECHNOLOGY

DEPARTMENT OF CIVIL AND TRANSPORT ENGINEERING

Report Title: ENTRAINMENT OF BED SEDIMENTS BY DEBRIS FLOW	Date: 10.06.2016 Number of pages (incl. appendices): 116			
	Master Thesis	X	Project Work	
Name: Bigyan Sherchan				
Professor in charge/supervisor: Steinar Nordal, NTNU				
Other external professional contacts/supervisors: Petter Fornes, NTNU; Ashenafi L. Yifru, NTNU				

Abstract:

Debris flows have proved to be a major worldwide hazard for more than 100 years causing destruction of lives, property and infrastructures. This occurrence of debris flows is likely to increase in the future due to the impending climate change. The large runout distance of the debris flow due to its ability to entrain materials along its way is one of the main causes for destruction.

The objective of this study was to research the mechanism of entrainment in debris flows and to investigate the different methods that can be used for debris flow modelling. While empirical methods are mostly used to model debris flows due to their simplicity, numerical methods can be advantageous in representing debris flows with more accuracy. Literature study was carried out on the existing attempts to include entrainment in these methods and it was found that the mechanism of entrainment is not fully understood and hence used in terms of empirical coefficients or user defined entrainment rates. RAMMS was used for the numerical modelling of debris flows and a detailed explanation of the software and its governing equations was presented.

Two debris flows, one of a physical model prepared in the laboratory and another of a real event in Almåskroken, Sør-Trøndelag were back calculated using RAMMS. These events were used first for the calibration of the input parameters applying the Voellmy rheology followed by the sensitivity analysis of the calibrated input parameters. RAMMS was able to replicate the runout distance of the physical model and the Almåskroken debris flow. The runout distance was found to be most sensitive to the friction coefficient μ, followed by the turbulent coefficient ξ. Entrainment was included in the simulation of the real case event. Although RAMMS was not completely successful to simulate the final deposit volume, the volume of simulated eroded materials was most sensitive to the entrainment coefficient K used in RAMMS.

Thus RAMMS can be a useful tool to for numerical modelling of debris flows due to the applicability of its Voellmy rheology to debris flows but for a complete understanding of the entrainment mechanism, more theoretical studies and laboratory experiments are essential.

Keywords: Debris Flow, Entrainment, Numerical Modelling, RAMMS

Bigyan Sherchan

Abstract

Debris flows have proved to be a major worldwide hazard for more than 100 years causing destruction of lives, property and infrastructures. This occurrence of debris flows is likely to increase in the future due to the impending climate change. The large runout distance of the debris flow due to its ability to entrain materials along its way is one of the main causes for destruction.

The objective of this study was to research the mechanism of entrainment in debris flows and to investigate the different methods that can be used for debris flow modelling. While empirical methods are mostly used to model debris flows due to their simplicity, numerical methods can be advantageous in representing debris flows with more accuracy. Literature study was carried out on the existing attempts to include entrainment in these methods and it was found that the mechanism of entrainment is not fully understood and hence used in terms of empirical coefficients or user defined entrainment rates. RAMMS was used for the numerical modelling of debris flows and a detailed explanation of the software and its governing equations was presented.

Two debris flows, one of a physical model prepared in the laboratory and another of a real event in Almåskroken, Sør-Trøndelag were back calculated using RAMMS. These events were used first for the calibration of the input parameters applying the Voellmy rheology followed by the sensitivity analysis of the calibrated input parameters. RAMMS was able to replicate the runout distance of the physical model and the Almåskroken debris flow. The runout distance was found to be most sensitive to the friction coefficient μ, followed by the turbulent coefficient ξ. Entrainment was included in the simulation of the real case event. Although RAMMS was not completely successful to simulate the final deposit volume, the volume of simulated eroded materials was most sensitive to the entrainment coefficient K used in RAMMS.

Thus, RAMMS can be a useful tool to for numerical modelling of debris flows due to the applicability of its Voellmy rheology to debris flows but for a complete understanding of the entrainment mechanism, more theoretical study and laboratory experiments are essential.

Preface

This thesis is submitted in the partial fulfillment for the Master of Science (MSc) degree in Geotechnics and Geohazards at the Department of Civil and Transport Engineering, Norwegian University of Science and Technology (NTNU). It was carried out in the spring of 2016.

First, I would like to thank Professor Steinar Nordal, my supervisor at NTNU, for his continuous supervision and guidance throughout my work. His suggestions and support have been very helpful which provided me much insight about the research. I am grateful to have him as my supervisor.

Next, I would like to thank my co-supervisors, Petter Fornes, PhD candidate at NTNU and Ashenafi L. Yifru, Research Assistant at NTNU for their assistance during my entire thesis. My gratitude goes to their advice on the execution of this thesis. They have contributed with great enthusiasm and discussion during this study from helping me with running the simulations to commenting on my report.

I am in debt to Martine Frekhaug, Statens Vegvesen for providing me the digital terrain model of the Almåskroken area and other relevant photographs. She helped me a great deal with the confusions I had regarding anything about the site.

Next, I would like to thank Kenneth Sundli for his help in purchase of the RAMMS software along with Steinar and Ashenafi, and providing me a workstation at the university.

My thanks go to Marc Christen at the Swiss Federal Institute for Snow and Avalanche Research and his recommendations on how to use the software.

I am grateful to my friends, Emilie Laache and Mingbo Yang, for sharing their data with me for this study.

I am thankful for my friends and family for their constant love and support during these two years. Finally, special mention to all the Norwegians who helped me during my stay here in Norway and made this a time to remember. I will cherish every moment of it.

Bigyan Sherchan

June 2016

Trondheim, Norway

TABLE OF CONTENTS

List of Figures

List of Tables

1 Introduction

1.1 Background

Debris flow can be defined as the depiction of flood in a mountainous terrain transporting the suspended loads and varying quantities of bed materials (Stiny, 1910). As the concentration of the sediment in the flow increases, "*at a certain limit, it changes into a viscous flow consisting of water, soil, sand, gravel, rocks, and wood mixed together, which flows like lava into a valley*" (Stiny, 1910). The sediment concentrations can exceed 40 percent by volume with maximum speeds exceeding 10 m/s and sizes ranging up to 10^9 m^3 (Iverson, 2014).

Debris flows involve smearing of unsorted soil, such as glacier transported moraine material, and in addition, often a high content of organic matter in the form of logs and other vegetation types (Hungr et al., 2001). Earthquake and rainfall are the major triggering factors of debris flows and the flow takes place on a terrain typically steeper than 25 degrees. In Norway where climate research expects more precipitation over the next century (Frekhaug, 2015) and more than 6.7 percent of the country has a steeper terrain than 30 degrees (Jaedicke et al., 2009), debris flows can cause a major damage to the infrastructure.

Preventive measures of debris flows include careful location of facilities away from hazard zones or by building protective measures. Based on the concept of acceptable risk, building new development in hazard zones is tolerable. However, to recommend the acceptable level of risk is not the scope of debris flow study, it is to predict the probability of occurrence, magnitudes, runout distances, velocities, impact forces and associated potential damage and other parameters necessary to quantify risk. (Hungr and Jakob, 2005)

Initiation of debris flows can take place through various processes as they descend down the channels by entraining sediment, including mobilization of separate landslides and high concentration of surface-water flow (Cannon et al., 2001, Coe et al., 2008, Godt and Coe, 2007, Wang et al., 2003). Debris flows can prove to be a great hazard especially due to the entrainment of sediments which result in increased volume, velocities and runout distances (Reid et al., 2011). Research about entrainment in debris flows has been carried out in the past, ranging from deriving empirical formulas to account for entrainment and building large scale physical models and analyzing the entrainment mechanism to represent the debris flows occurring in the field. Dynamic numerical modelling is another method to model the

entrainment processes in the debris flow. Back calculations of previous events of debris flows can prove to be helpful in characterizing the sensitivity of different input parameters affecting the debris flow. Still, the entrainment mechanism is not fully understood and a lot of research needs to be done.

The aim of this thesis is to study the mechanism of sediment entrainment in debris flow. While a brief discussion is provided about debris flows in general and the analytical, empirical and physical approaches for debris flow modelling, this thesis mainly focuses on the numerical approach using a dynamic numerical model with an entrainment module, RAMMS-2D. A sensitivity analysis is carried out of the different rheological and entrainment parameters on the debris flow output like the runout distance, flow height, velocity and eroded volume.

1.2 Objectives of the Study

The main objective of this study is to gain knowledge about entrainment of bed sediments by debris flow through different methods. This thesis helps to reproduce previous events with the help of a numerical modelling software, RAMMS and analyze how entrainment is implemented into it.

A number of sub-objectives have been formed to reach the aim of the study.

1. Literature review of debris flows and their mechanism of entrainment of bed sediments.
2. Literature review of different approaches of debris flow modelling and how they implement entrainment.
3. Detailed analysis of the numerical software, RAMMS with analysis of its principles and governing equations.
4. To evaluate the suitability of rheological Voellmy model implemented in RAMMS to model debris flows.
5. To perform a model calibration by conducting a parameterization of the input parameters based on back calculation of past debris flows.
6. To perform a sensitivity analysis of the rheological parameters and the entrainment parameters on the debris runout distance, flow height, flow velocity and the eroded volume.
7. To assess the applicability of RAMMS for the analysis of bed sediment entrainment mechanism in debris flows including evaluation of the different entrainment laws.

1.3 Approach

RAMMS (Rapid Mass Movements Simulation), a dynamic software has been used for the numerical modelling of debris flows in this thesis. RAMMS is a two-dimensional numerical simulation program that calculates the mass movements of a three-dimensional terrain (Christen et al., 2010b). It has developed modules for avalanches, debris flows and rock falls. RAMMS can be used to calculate the flow height, speed and stagnation pressure in every point from start to stop of the flow path. The program was developed in Switzerland by the Swiss Federal Institute for Snow and Avalanche Research (WSL/ SLF). RAMMS describes the friction forces acting on the debris flow using a Voellmy-Salm model, and divides the frictional forces into two parts- the Coulomb friction, μ, which takes into account the friction that occurs due to the fixed part of the landslide and dominates when the flow is close to stopping. The speed-dependent friction, ξ, takes into account the friction arising from the viscous and turbulent forces. (Christen et al., 2010b)

The version used in this research is RAMMS::Debris Flow 1.6.45.

Besides RAMMS, Microsoft Excel was used for preparation of the digital elevation model (DEM) that is to be used in RAMMS. Models with varying resolutions were prepared to get results with suitable detail and accuracy.

1.4 Description of Task

The first part of the study deals with the analysis of debris flows as a whole and sediment entrainment mechanism in particular. A brief explanation of the different analytical and empirical approaches is presented along with existing physical models used to study debris flow entrainment.

Before starting the simulation of debris flows using RAMMS, a detailed discussion on the different features of RAMMS is given. The principles and governing equations of the software are carefully analyzed to understand its functioning.

The next step is the simulation of a physical model prepared in the laboratory by Emilie Laache, a Master student currently doing her thesis in Norwegian University of Science and Technology (NTNU). A DEM representing the laboratory model is prepared and the required input parameters are calibrated to match the output results from RAMMS according to the actual results in the laboratory. During these simulations, the effect of rheological parameters are studied and the applicability of Voellmy Salm model to debris flows is assessed.

The numerical modelling is concluded with the back calculation of a debris flow event that occurred in Almåskroken, Sør-Trøndelag on August 13, 2013. A sensitivity analysis of the input rheological and entrainment parameters on the debris flow results is carried out at the end to conduct a parametric study of the input parameters.

1.5 Structure of the Thesis

Chapter 1 begins with the introduction of the thesis explaining the problem statement and stating the research objectives.

Chapter 2 provides the theoretical background of debris flow and its types discussing the mechanism of sediment entrainment. Different types of approaches for debris flow modelling employing entrainment are briefly discussed.

Chapter 3 gives insight into the numerical software RAMMS::Debris Flow, used for debris flow modelling in this study.

Chapter 4 analyzes the results and discussions of RAMMS simulations of a physical model prepared in the laboratory along with the parametric study and sensitivity analysis of the rheological friction parameters.

Chapter 5 presents the analyses, results and discussions of the back-calculation of a debris flow event that occurred in Almåskroken. Sensitivity analysis of the entrainment parameters is included.

Chapter 6 summarizes this study by presenting the conclusions and limitations and recommending possible areas of study for future work.

2 Literature Review

2.1 Terminology

Debris flows vary in their origins, compositions and appearances from gradually and silently flowing sand slurries to huge surges of rocks along with mud, and hence the varying definitions of debris flows as a result. There is a confusion over the definition of debris flows and its difference from other types of landslides. There are different criteria for defining debris flows-sediment concentrations, grain size distributions, flow velocity and shear strength to name a few. (Iverson, 1997)

The main characteristic of a debris flow is the strong interaction between the solid and fluids in it, i.e. both the solid and fluid forces fundamentally influence its motion separating them from related phenomena like rock avalanches and sediment loaded water forces (Iverson, 1997). In rock avalanches, solid grain forces are dominant and fluid forces primarily influence the mechanism of floods whereas in debris flows, both solid and fluid forces must vitally dominate the process. By this principle, other processes as debris floods, mudflows, slides, and hyper concentrated flows where solid and fluid forces interact can be regarded the same as debris flows. This further strengthens the diversity of debris flows. According to the well-established North American landslide classification system (Cruden and Varnes, 1996, Varnes, 1978), debris flows are "*rapid movements of material as a viscous mass where inter-granular movements predominate over shear surface movements. These can be debris flows, mudflows, rock avalanches, depending upon the nature of the material involved in the movement.*" Hungr et al. (2001) later defined debris flows as "*very rapidly to extremely rapidly flowing saturated non plastic debris in a steep channel with plasticity index less than 5 percent in sand and finer fractions.*"

Table 1 Classification of flow type landslides (Hungr and Jakob, 2005)

Material	Water content[1]	Special condition	Velocity	Name
Silt, Sand, Gravel, Debris (talus)	dry, moist or saturated	- no excess pore-pressure, - limited volume	various	***Non-liquefied sand (silt, gravel, debris) flow***
Silt, Sand, Debris, Weak rock[2]	saturated at rupture surface	- liquefiable material[3], - constant water content	Ex. rapid	***Sand (silt, debris, rock) flow slide***
Sensitive clay	at or above liquid limit	- liquefaction *in situ*,[3] - constant water content[4]	Ex. rapid	***Clay flow slide***
Peat	saturated	- excess pore-pressure	Slow to very rapid	***Peat flow***
Clay or Earth	near plastic limit	- slow movements, - plug flow (sliding)	< Rapid	***Earth flow***
Debris	saturated	- established channel[5], - increased water content[4]	Ex. rapid	***Debris flow***
Mud	at or above liquid limit	-fine-grained debris flow	> Very rapid	***Mud flow***
Debris	free water present	- flood[6]	Ex. rapid	***Debris flood***
Debris	partly or fully saturated	- no established channel[5], - relatively shallow, steep source	Ex. rapid	***Debris avalanche***
Fragmented Rock	various, mainly dry	- intact rock at source, - large volume[7]	Ex. rapid	***Rock avalanche***

[1] Water content of material in the vicinity of the rupture surface at the time of failure.
[2] Highly porous, weak rock (examples: weak Chalk, weathered tuff, pumice)
[3] The presence of full or partial *in situ* liquefaction of the source material of the flow slide may be observed or implied.
[4] Relative to in-situ source material.
[5] Presence or absence of a defined channel over a large part of the path, and an established deposition landform (fan). *Debris flow* is a recurrent phenomenon within its path, while *debris avalanche* is not.
[6] Peak discharge of the same order as that of a major flood or an accidental flood. Significant tractive forces of free flowing water. Presence of floating debris.
[7] Volume greater than 10,000 m^3 approximately. Mass flow, contrasting with fragmental rock fall.

Mudflow, debris flood and debris avalanche are the other flow type landslides similar to debris flows as shown in Table 1. Mud flows have higher water content with plasticity greater than 5 percent, debris floods rapidly surge down a steep channel and debris avalanches are rapid but shallow flow of partially or fully saturated debris on steep slopes without channelization (Hungr and Jakob, 2005).

Irrespective of the different terminologies and definitions used for describing debris flow, the strong interaction between the fluid and solid forces distinguishes it from other types of landslides reinforcing it with its own distinct type of material, movement and velocity.

2.2 Mechanism of Debris Flows

The motion of debris flows involves a transfer of energy which usually begins with an initial inclined movement and ends with deposition (Iverson, 1997). A debris flow path essentially comprises of three parts- an initiation zone, a transport zone and a deposition zone as shown in Figure 2-1.

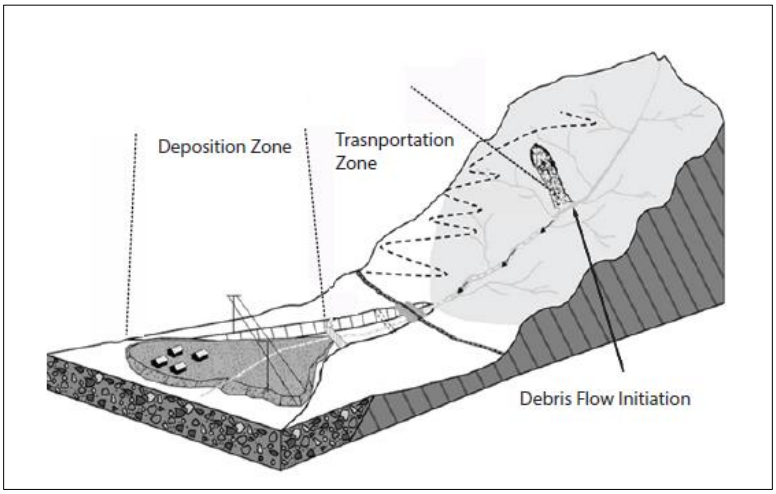

Figure 2-1 A typical debris flow path (Schematic diagram from *www.dnv.org*) (Hussin, 2011)

The initiation zone has a steep slope in between 20 to 45 degrees and is usually a slope failure in the headwall or a sidewall of a stream channel (Hungr and Jakob, 2005). Heavy rainfall is the main triggering factor of debris flows initiation which initially start off as landslides or rock avalanches which transform into debris flow further along the path (Hussin, 2011). The slope failure may also occur due to manmade road fills. Another triggering factor is collapse of the previously formed channel blocking dams (Nettleton et al., 2005). According to Norem and Sandersen (2012), the primary cause of debris flow initiation in Norway is the exceedance of the force of the flowing water over the frictional resistance of the soil leading to increased mobility of mass movement. Another possible factor for debris flow initiation is the mobility of soil due to release or uptake of water body. By release of water, the pore pressure increases resulting in the reduction of soil strength and possible formation of soil slip as shown in Figure 2-2 (Norem and Sandersen, 2012).

Figure 2-2 Soil slip caused by a weak layer, Åby in Telemark County, Norway (Håland, 2012)

After its initiation, debris flows continue downslope and are often characterized by the disintegration and remolding of the flowing mass. Due to this, the volume of the debris flow increases introducing a higher level of saturation. This middle part of the flow is referred to as the transportation zone and has a slope of more than 10 degrees (Hungr and Jakob, 2005). The transportation zone can consist of non-erodible bedrock channels and falls, as well as erodible soil banks. Along the flow path, deposition of the debris flow starts once the slope of the path starts decreasing below a certain value (Iverson, 2005).

The transition from transition to deposition zone takes place when the slope of the terrain is 15-20 degrees (Frekhaug, 2015). Deposition zone usually takes the formation of debris fan and starts at the fan apex. The coarser materials are deposited at the beginning, while the finer materials are subsequently deposited as the flow progresses (Norem and Sandersen, 2012). This is the most hazardous zone with the risk of being hit by the debris flow hazards so proper risk assessment of structures like buildings, bridges and roads lying in this zone should be carried out.

In this research, the term debris flow is used to represent the entire phenomenon- starting from the initiating slide on a precarious slope including the rapid flow along the transportation zone and final deposition on a debris fan.

2.3 Morphology

Debris flows can primarily be distinguished as hillslope (open slope) debris flows and channelized debris flows as shown in Figure 2-3. In hillslopes, debris flows create their own paths normally occurring on open slopes (Glade, 2005) and deposit the materials on gentler slopes (Varnes, 1978). Hillslope debris flows usually begin as soil slip, however they can enter

channel type depressions or form their own channels as they flow (Nettleton et al., 2005). Channelized debris flows on the other hand occur in large gullies and follow existing topographic channel features (Cruden and Varnes, 1996).

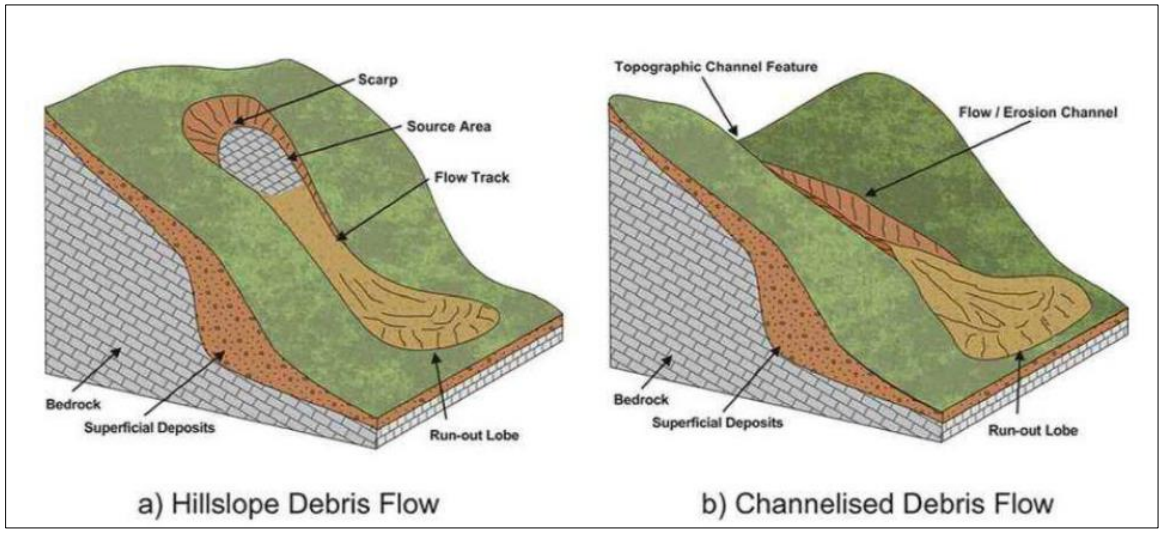

Figure 2-3 Hillslope and Channelized Debris Flows (Nettleton et al., 2005)

2.4 Physics of Debris Flows

2.4.1 Entrainment in Debris Flow

Generally, the starting landslide does not highly influence the final magnitude of the debris flow volume. It is often a rare case that the volume of the deposited material is the same as the volume of the debris flow in the initiation zone. The majority of the volume transported and hence deposited is a result of the material that the flow entrains along its path. Entrainment in debris flows can commonly be defined as incorporation of solid and fluid boundary material which doesn't significantly change the composition of the flow and resulting mostly from the scouring of channel bed and/or banks (Iverson, 2012). There are several cases of entrainment leading to an enormous increase in the debris flow volume. A famous case is shown in Figure 2-4. It shows the 1990 Tsing Shan debris flow where the initiating volume of 400 m^3 led to the final depositing volume of 20000 m^3. This example shows that entrainment is an important factor in determining the final debris flow volume which may lead to longer runout distances and larger deposit volumes.

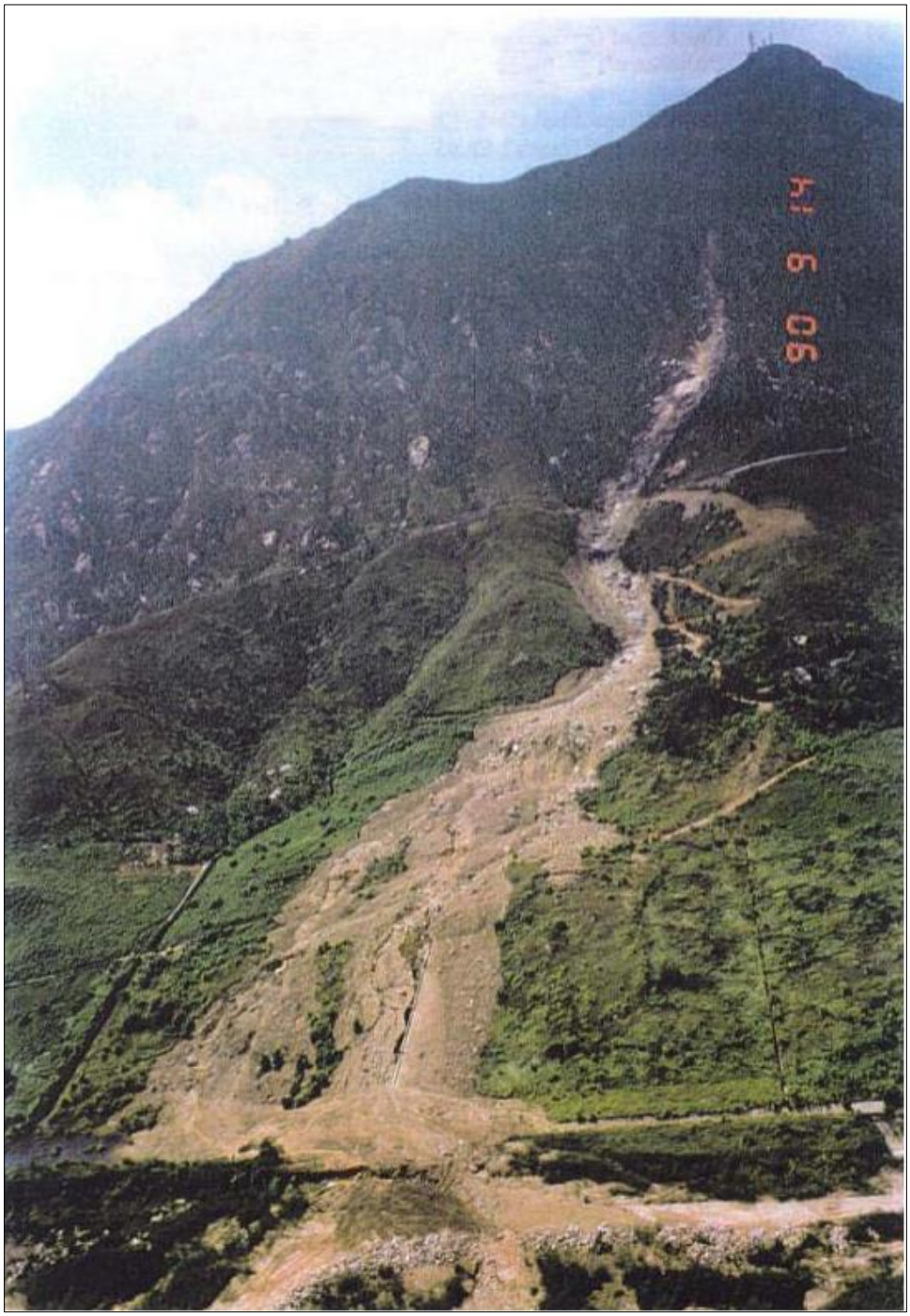

Figure 2-4 The Tsing Shan debris flow (King, 1996)

Debris flows grow in volume by entrainment of bed sediments and water upon descending into steep channel slopes and by scouring of channel beds and banks (Iverson, 2014). The magnitude of a debris flow event can be represented by its run-out distance, peak discharge or volume. Similarly, the impact pressure can also be considered as a magnitude of the debris flow mostly in terms of risk and vulnerability assessment of structures to the incoming debris flows (van Westen, 2009). The run-out distance of a debris flow is the total distance between

the point of initiation and its deposition where the flow completely stops. The peak discharge is the maximum discharge occurring at any point of the flow and is given by the maximum cross-sectional area multiplied by the velocity of the flow at that point. Besides, these are also the output parameters of different debris flow analyses and modelling.

The total volume of a debris flow is given by the following equation,

$$V_{total} = \sum V_{ini} + \sum V_{ent} + \sum V_{dep} \quad (1)$$

where, $\sum V_{ini}$ is the total volume of all the initiation zones combined, $\sum V_{ent}$ is the total volume of the entrained debris and $\sum V_{dep}$ is the total volume of the deposited debris. The total volume of debris flows ranges from 100 m^3 to several hundred thousand cubic meters and to several million cubic meters in some exceptional cases. The debris flow in Venezuela Stream San Julian in December 1999 gave a total volume of 2.6 * 10^6 m^3 (García-Martínez and López, 2005).

2.4.2 Mechanism of Entrainment

Debris flows usually occur due to transportation of bed sediments from channel beds and banks by suspension, moving, sliding or saltation (Easterbrook, 1999). Different physical models have been constructed and simultaneous debris flows have been simulated. In these physical models, the channel bed itself becomes unstable once the slope exceeds a certain value, due to the action of gravitational forces and the drag forces exerted by the over-riding debris flow (Bagnold, 1966). Upon replacing water in this flow by saturated debris, the drag forces increase resulting in the greater entrainment of the bed sediments (Hungr et al., 2005).

There are two mechanisms primarily responsible for material entrainment in debris flows. The first one is bed destabilization and erosion. As a result of the drag forces acting on the base of the flow, the channel bed destabilizes and erosion is assisted by the loss of strength due to rapid undrained loading (Hutchinson and Bhandari, 1971), and liquefaction of the channel fill (Sassa, 1985). As shown in Figure 2-5, this bed destabilization not only affects the bedload at the bottom, but also any erodible bed substrate lying in the channel.

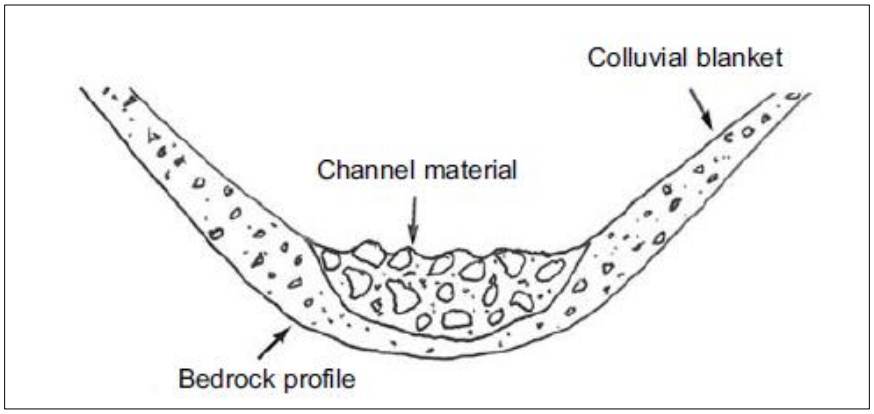

Figure 2-5 Vertical cross section of a debris flow channel (Hungr et al., 2005)

The second mechanism of debris flow entrainment is a direct consequence of the first one. Bed erosion results in the instability of the channel banks which are already in a state of equilibrium. Therefore, any further disturbance in the channel bed level can release a shallow landslide into the surge entraining materials. Additionally, this lowering of the channel bed can also release the landslide with a delay, which can be remobilized later during the next surge (Hungr et al., 2005). There are various reports of debris flows from banks slides briefly forming a dam in the channel only to be eroded by the debris flows later (Johnson, 1970). Figure 2-6 shows a flow channel with a combination of highly erodible bed and banks.

Figure 2-6 Eroded debris flow channel in the Columbia Mountains, British Columbia (Hungr et al., 2005)

Entrainment was first analysed in terms of erosion depth. Bed destabilization during debris flow is a simple extension of infinite slope stability theory (Morgenstern and Sangrey, 1978) but it depends on certain assumptions regarding the pore-water pressure of the bed materials. This theory is identical to the one proposed by Takahashi (1978, 2014) in which a slope parallel seepage in a saturated bed is assumed.

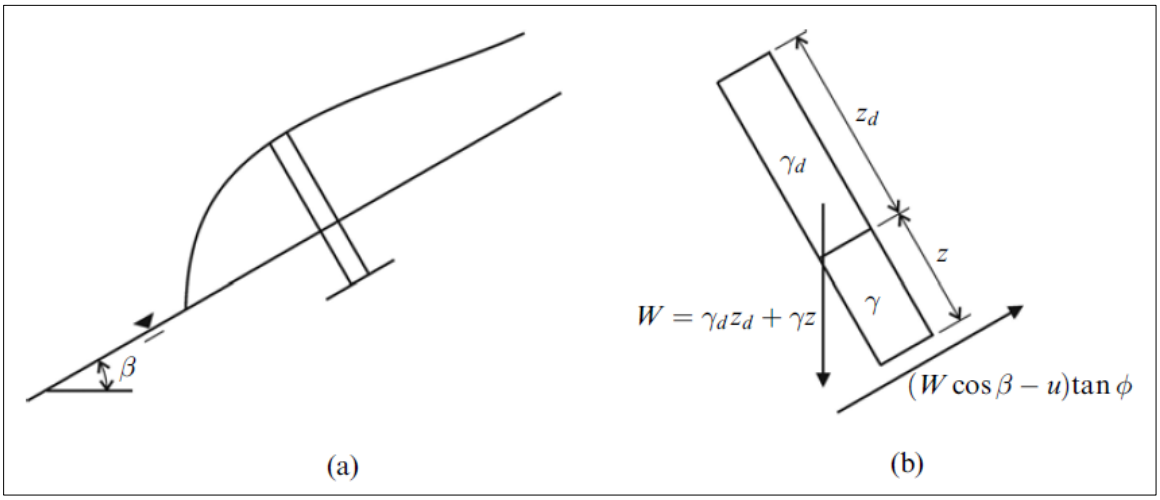

Figure 2-7 (a) Schematic representation of a saturated bed overridden by a debris flow and (b) Forces acting on an elemental column (Hungr et al., 2005)

A debris of thickness z_d flows over a bed of cohesion less material with an inclination angle β (Figure 2-7). The bed becomes unstable to an unknown depth z below the original surface due to the additional tractive force of the debris. As in the case of infinite slope approach, only a typical column on unit length in the downslope direction and its stability is considered.

The weight of the column,

$$W = \gamma_d z_d + \gamma z \quad (2)$$

Where, γ is the saturated unit weight of the bed material (20-23 kN/m^3) and γ_d is the bulk unit weight of the debris (18-20 kN/m^3).

The normal stress at the column base,

$$\sigma = W\cos\beta \quad (3)$$

And the shear stress,

$$\tau = W\sin\beta \quad (4)$$

According to Takahashi theory of slope parallel seepage flow, the pore pressure is hydrostatic flowing in a steady state resulting no excess pore pressure. While this assumption is not fully justified, it is used for this analysis. The pore pressure at the base of the column,

$$u = \gamma_w (z_d + z) \cos\beta \tag{5}$$

Where, γ_w is the unit weight of water and $(z_d + z)\cos\beta$ is the elevation difference along an equipotential line.

The shear strength of the bed sediment is given by the Mohr-Coulomb shear strength equation with friction angle Φ.

$$S = (\sigma - u)\tan\varphi \tag{6}$$

At shear failure, the shear strength is equal to the shear stress giving,

$$(W\cos\beta - u)\tan\varphi = W\sin\beta \tag{7}$$

Substituting W from (2) and u from (5) in (7) and solving for z, we get

$$z = z_d \left[\frac{\frac{\gamma_d}{\gamma}\left(1 - \frac{\tan\beta}{\tan\varphi}\right) - \frac{\gamma_w}{\gamma}}{\frac{\gamma_w}{\gamma} - \left(1 - \frac{\tan\beta}{\tan\varphi}\right)} \right] \tag{8}$$

From (8), it is clear that a certain amount of entrainment is possible for any value of γ_d less than $\frac{\gamma_w}{\left(1-\frac{\tan\beta}{\tan\varphi}\right)}$, whereas more dilute flows will cause instability to greater entrainment depths. For fully developed debris surges, where the bulk density of the flow is nearly equal to the density of the bed material i.e. $\frac{\gamma_d}{\gamma} \approx 1$, no entrainment will be predicted with these assumptions, unless the bed itself is inherently unstable.

A steady seepage condition is unlikely during a debris flow causing building of high pore pressure within the deposit materials. Development of excess pore pressure due to the undrained loading of the debris flow is a more realistic assumption. The pore water pressure in the bed sediment changes to,

$$u = (z_d\,\gamma_d + z\,\gamma_w)\cos\beta \tag{9}$$

And the erosion depth will change accordingly as,

$$z = z_d \left[\frac{\left(-\frac{\gamma_d}{\gamma} \frac{\tan\beta}{\tan\varphi} \right)}{\frac{\gamma_w}{\gamma} - \left(1 - \frac{\tan\beta}{\tan\varphi} \right)} \right] \quad (10)$$

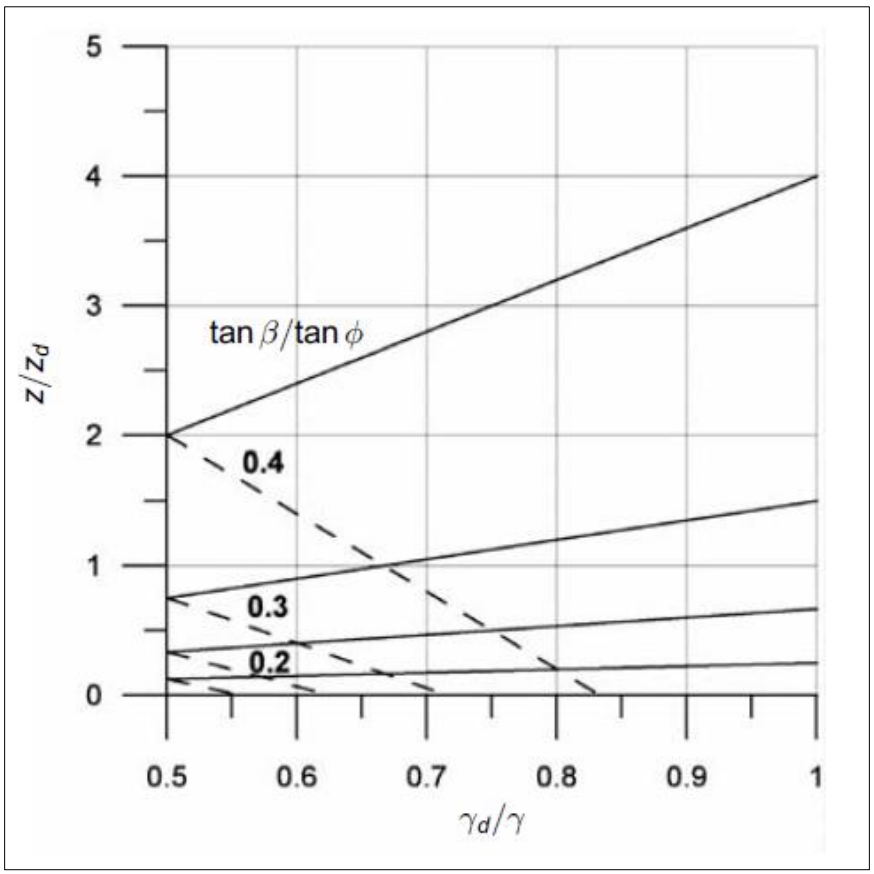

Figure 2-8 Erosion depths predicted by Equation 8 (dashed lines) and Equation 10 (full lines) (Hungr et al., 2005).

Equations 8 and 10 are plotted in Figure 2-8 using dashed and full lines respectively. The new formula predicts entrainment depth for all values of γ_d with the unstable depth increasing with the bulk density of the debris flow as predicted otherwise by equation 8. The actual value of the unstable depth may lie somewhere between the two extremes depicted in Figure 2-8 although it is likely to be closer to the undrained condition (full lines) than to the drained condition (dashed lines). (Hungr et al., 2005)

These results are only important for conceptual purpose but not for practical applications. Shear strength of the bed materials in a debris flow and its variation with depth is very difficult to find. Besides, it is unlikely to predict correctly the pore pressure due to the discharge gradients

and excess gradients that may be generated due to the rapid loading and vibration (Hungr et al., 2005). As a result, new approach is required to study the mechanism of entrainment in debris flow. There are different empirical and numerical approaches which make this process comparatively easier.

Furthermore, elementary theory of entrainment of sediments by debris flow explains erosion in terms of entrainment rate and this entrainment rate E (m/s) can be explicitly predicted by making reasonable assumptions about flow velocity profiles and shear traction profiles (Iverson, 2012). In the case of Coulomb frictional bed resistance, the predicted entrainment rates are sensitive to the pore water pressures that develop in the overridden bed sediments. Considering the simplest scenario where the bed sediment liquefies completely, entrainment rate is given by Iverson (2012) as,

$$E = \frac{2\,\mu_1 g h_1 Cos\theta (1-\lambda_1)}{\bar{v}_1} \tag{11}$$

where, θ is the slope angle, μ_1 is the flow's Coulomb friction coefficient, h_1 is the flow's thickness, λ_1 is the flow's degree of liquefaction and $\bar{v}_1$ is the depth averaged velocity.

According to equation 11, the entrainment rates decrease as basal velocities increase on contrary to the conventional belief of increasing a flow's velocity will enhance the flow's capacity for sediment entrainment.

2.5 Debris Flow Modelling

The runout distance of the debris flow is the primary factor affecting the level of losses and damages caused by the flow. Therefore, prediction of debris flows runout distances can prove to be very useful in assessing the hazard mapping and in determining the debris flow intensity parameters (Rickenmann, 2005). There exists no single universal model for calculating run-out distances but over the past few decades, several methods have been developed by researchers to predict the runout distances of debris flows. Information available from past debris flow events has often proved to be a reliable tool.

Broadly, the methods to predict runout distances and in general debris flow modelling can be divided into three categories.

1. Empirical Approach
2. Physical Modelling
3. Numerical Modelling

This research is focused on the numerical modelling of debris flows hence the other two approaches are briefly described.

2.5.1 Empirical Approach

Empirical models are meaningful where material properties is limited and flow path is controlled by subtle changes in terrain (Fannin and Bowman, 2007). Hence, these are the most widely used techniques to estimate the maximum run out distance and inundation areas. A combination of empirical and statistical approaches was used to predict runout distances using factors like the debris-flow volume (Bianco and Franzi, 2000, Bovis and Jakob, 1999, Glade, 2005, Rickenmann, 1999) and the flow peak discharge (Bovis and Jakob, 1999, Costa, 1988, Mizuyama et al., 1992). Additionally, mass movement volumes were also used to determine the inundation areas (Iverson et al., 1998, Schilling and Iverson, 1997). Based on the correlation of historical data of debris flow events, Rickenmann (1999) has essentially carried out extensive amount of work predicting runout distances by empirical approaches and has found that the empirical relationships between the peak discharge and the deposited volume of debris flows can be described in terms of linear empirical equations. These equations have been derived from a set of peak discharges and deposit volumes of worldwide debris flows.

Some of the well-known empirical approaches in debris flow modelling are as follows:

1. Volume loss rate method
2. Channel geometry method
3. Angle of reach method
4. Geometrical method

However, there are some drawbacks of using empirical approaches for estimating debris flow runouts and deposited volumes. Firstly, they do not incorporate the rheology of the debris flow neither the mechanics of the flow itself. Similarly, adequate field observations should be carried out to correctly derive the empirical relationships (Chen and Lee, 2004). Because of this, these relationships can only be applied to the debris flows with similar flow conditions. There can also be an inaccuracy in the prediction of debris flow parameters with these relationships which Rickenmann (1999) noticed when he found the debris flow volume can be overestimated by a factor of upto 100. Thus, extreme caution is required while using these empirical methods and making a proper geomorphologic assessment in the field is recommended (Franzi and Bianco, 2001, Rickenmann, 1999).

2.5.2 Physical Modelling

Several hypotheses have been proposed to explain the mechanics of bed sediment entrainment by debris flows. Earlier Takahashi (1978, 2014) proposed that saturated bed sediment fails as a masse, rather than progressive downward scour, when loaded by overriding debris flow. He supported this hypothesis with the help of an infinite slope stability analysis where the groundwater pressure in the sediment is in equilibrium to the sloping water table of the overriding debris flow and there is no development of transient excess pore pressure. In contrast, there are other hypotheses where it is suggested that the overriding debris flow will cause an increase in the transient pore pressure of the saturated bed sediment, reducing the shear strength of the bed. Some small-scale laboratory flumes have been set up by different researchers to experiment the entrainment mechanism in debris flows. However, they are not representative of the natural debris flows due to the limitation in the scale dependent properties.

Physical modelling employs controlled field and laboratory experiments to research about the dynamics of debris flows and entrainment. One example is the use of flumes to simulate a debris flow event and careful analysis of the flow with high speed photography or videography by placing sensors at different locations of the flow (Reid et al., 2011).

Reid et al. (2011) has performed large scale debris flow entrainment experiments with minimal scaling problems. The experiment is representative of the natural debris flows, and a number of experiments have been conducted primarily for two cases, on a wetter sediment with high volumetric water content and on a drier sediment with relatively low volumetric water content. The flume is composed of a reinforced concrete channel 95 m long, 2 m wide and 1.2 m deep with an inclination of 31 degrees, an angle representative of terrain where natural debris flows originate (Figure 2-9). The required water content level is reached by sprinkling of the bed sediment by low intensity overhead sprinklers. Both debris flow and bed sediment averaged 37 percent sand, 56 percent gravel and 7 percent mud.

Figure 2-9 Debris flow behavior during a large scale experiment with wet bed sediment (a) Release of the flow (b) Close up of the debris flow entraining bed sediment (c) Debris flow crossing the deposition zone (Reid et al., 2011)

With wetter sediment, significant entrainment occurred with more than 60 percent of the bed sediment and debris flow runout was subsequently enhanced whereas in case of drier sediment, net entrainment was minimal around 20-30 percent of the bed sediment hindering the runout of the debris flow.

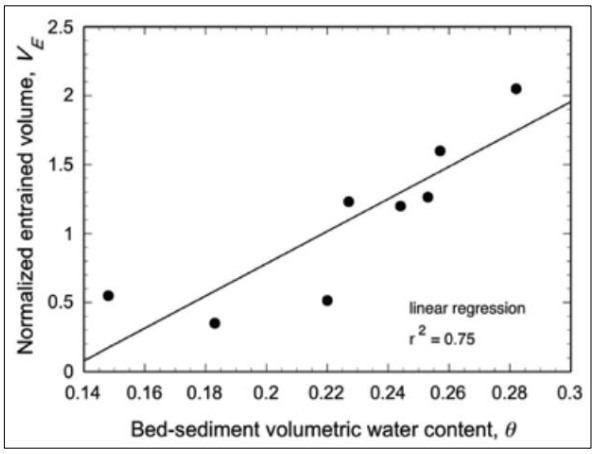

Figure 2-10 Normalized volume of sediment entrained, V_E (entrained volume/control debris flow volume of 6m^3) as a function of bed sediment volumetric water content (Reid et al., 2011)

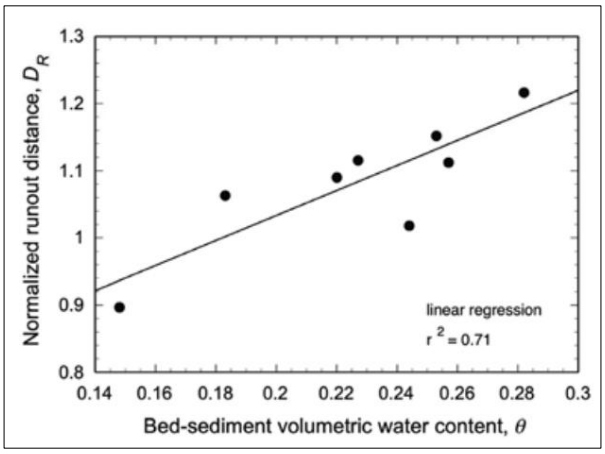

Figure 2-11 Normalized maximum debris flow runout distance, D_R (runout distance relative to that of control experiment) as a function of bed sediment volumetric water content (Reid et al., 2011)

A roughly linear positive relation was obtained between overall bed-sediment volumetric water content θ, and normalized volume of sediment entrained V_E, defined as the ratio of entrained

volume to the control debris flow volume of 6 m^3 (Figure 2-10). It was found that if $\theta > 0.22$, then $V_E > 1$, indicating that the entrained volume exceeded the control debris-flow initial volume. (Reid et al., 2011)

Similarly, flows that overrode wetter bed sediment generally increased in speed by 10-20 percent, whereas those that overrode drier bed sediment had speeds similar to or slower than the speeds measured in control experiments without any bed sediments. A roughly linear positive relation was obtained as shown in Figure 2-11 between overall bed-sediment volumetric water content, θ, and normalized maximum runout distance, D_R, defined as the furthest runout distance relative to that of the control experiments. (Reid et al., 2011)

This rapid pore-pressure increase in wet bed sediment can be caused by contraction and collapse during shear failure promoting debris flow mobilization (Berger et al., 2010). The debris flow moves over the bed sediment and its weight compresses the sediment pores below. As this compression is quicker than the rate of equilibrium of pore pressure, undrained loading may occur. In addition, the loose bed sediment contracted possibly, as it reached the critical state density during shear deformation. A volumetric water content of 0.22 percent seems to be the threshold for rapid pore pressure development and sediment entrainment. (Reid et al., 2011)

On addition of sediment entrainment, it increases the flow mass with zero velocity which would reduce the flow velocity if momentum is conserved and the frictional resistance remaining the same (Reid et al., 2011). This is true and evident when the debris flows slow over a dry sediment. In the case of wet bed sediments, the elevated pore pressures reduce the frictional resistance and increase the flow distance and speed.

Higher volumetric water content of the bed sediment greatly influences the entrainment. Sediment entrainment is significantly greater in wetter sediment than in drier sediment. This entrainment occurs through rapid progressive downward scour with velocity upto 5-10 cm/s instead of mass failure. However, there is a small possibility of failure of very thin and finite-thickness of bed sediment layers that are undetected in the experiments. The pore pressure in the wetter bed sediment increases to lithostatic levels because of overriding debris flows. As a result, debris flows with entrainment of wet sediment are more hazardous than flow without entrainment travelling faster and farther. Rapid increase of the pore pressure and the reduction of intergranular friction to near zero are the major factors for this. (Reid et al., 2011)

2.5.3 Numerical Modelling

While well-tested empirical methods are available to determine runout distances, velocities and flow heights, numerical models now provide cell information on flow height and flow velocity and allow practitioners to predict flow paths in general terrain as well as to model entrainment processes or the breaking effect of forests. An accurate prediction of runout distances, flow velocities and impact pressures in natural three-dimensional terrain is the reason for development of improved dynamics models of debris flow (Christen et al., 2010b).

Dynamic models apply the principle of energy and momentum conservation laws and can be broadly categorized into lumped mass models and continuum based models (Chen and Lee, 2000). In lumped mass models, the motion of the slide is idealized as a single point also called discontinuum models (Hutchinson, 1986). Lumped mass models are limited in being unable to account for the internal deformation (Chen and Lee, 2000). The flow moves in a single dimension and does not account for the dissipation of flow in other directions (Dai et al., 2002).

Continuum based numerical models employ fluid mechanics applying mass, momentum and energy conservation equations for describing the debris flow dynamics. They have an added advantage over lumped mass models in that they allow for the simulation of the deformation of the debris flow along the flow path and the flow can be simulated over an irregular terrain (Quan, 2012). Additionally the behavior of the debris flow is more realistically depicted by using rheology (Brunsden, 1999). Correct rheology and related friction parameters are essential in dynamically modelling a debris flow (Rickenmann, 2005). And although the calibration of suitable flow resistance friction parameters still remain an open problem, back-calculation of well documented debris flows has proven to be the best approach in the calibration of model parameters (Schraml et al., 2015).

The continuum depth averaged method

Savage and Hutter (1989) first developed a continuum mechanical theory that was capable of describing dynamics of motion of a finite mass down an inclined surface. These equations have been generalised to different complex phenomena. The flow is assumed as a one dimensional shallow flow and the equations are derived from depth averaging mass and momentum conservation equations by assuming a Coulomb resistance for basal shear resistance.

Most of these equations developed are based on single phase. The moving mixture of the solid and fluid is replaced by a homogeneous continuum of whose behaviour are governed by the

rheological properties. The flow motion is described by the mass and momentum balance equations given by,

$$\nabla v = 0 \tag{12}$$

$$\rho \left(\frac{\partial v}{\partial t} + v \nabla v\right) = -\nabla\sigma + \rho g \tag{13}$$

where, v = (v_x, v_y, v_z) is the velocity vector in the three different directions of the reference system, σ (x, y, z, t) is the Cauchy stress tensor, ρ is the mass density of the flow and g is the gravitational acceleration.

By assuming that the depth of the debris flow is much smaller than the length of the flow and the flow is incompressible, integration of equations 12 and 13 along the depth helps to obtain the depth-averaged equations of motion.

$$\frac{\partial h}{\partial t} + \frac{\partial h v_x}{\partial x} + \frac{\partial h v_y}{\partial y} = 0 \tag{14}$$

$$\rho\left(\frac{\partial v_x h}{\partial t} + \frac{\partial h v_x^2}{\partial x} + \frac{\partial h v_x v_y}{\partial y}\right) = \frac{\partial(\sigma_{xx} h)}{\partial x} - \tau_{zx} + \rho g_x h \tag{15}$$

$$\rho\left(\frac{\partial v_y h}{\partial t} + \frac{\partial h v_x v_y}{\partial x} + \frac{\partial h v_y^2}{\partial y}\right) = \frac{\partial\left(\sigma_{yy} h\right)}{\partial y} - \tau_{zy} + \rho g_y h \tag{16}$$

where, v_x and v_y are the depth averaged velocities in the x and y-directions, h is the flow depth, τ_{zx} and τ_{zx} are the shear resistance stresses, σ_{xx} and σ_{yy} are the depth averaged normal stresses, g_x and g_y are the x and y components of the gravitational acceleration (Savage and Hutter, 1989).

Equations 14, 15 and 16 are the governing equations of many numerical models including RAMMS solved by different formulations of solution reference frames. The numerical models are based on two-dimensional equations, simulated over a three dimensional terrain.

Rheology

Each continuum mechanics model is associated with a distinct rheology model. Rheology is defined as "*the study of the flow of matter, primarily in the liquid state, but also as 'soft solids' or solids under conditions in which they respond with plastic flow rather than deforming elastically in response to an applied force*" (Schowalter, 1978). The resistance force inside the flow and at the interface is expressed by basal rheology (Quan, 2012). Equations relating the

motion of the flow and the unknown stress state are required to solve the equations for conservation of mass and momentum. Rheological models for debris flows along with snow and rock avalanches use the concept of equivalent fluid and adopt it for modelling the soil masses.

There are few rheological models that have been used to describe the debris flows motion like the Bingham fluid model, in which the fluid acts as a rigid body at low shear stress levels and a viscous fluid at higher rates of shear stress, hence described as a viscous-elastic fluid (Hungr and Jakob, 2005). Thakur et al. (2014) described this rheology as a combination of plastic and viscous behavior and defined a threshold yield strength which separates the viscous and the rigid behavior of the fluid.

The Voellmy model is another rheological model that has been used widely to simulate debris flow events (Ayotte and Hungr, 2000, Hungr and Evans, 1996, Rickenmann et al., 2006). This model was introduced by Voellmy (1955) initially for snow avalanches and successfully applied later to debris flows, and contains a friction term and a turbulence term which is used to model the resistance at the base of the flow.

Various numerical models with respect to the rheology and presence/absence of choice of rheology, approach of solution, reference frame, and presence/absence of entrainment are shown in Table 2.

A brief description of some of the numerical models presented in Table 2 is given in the next section.

Table 2 Summary of numerical models for debris flow modelling (Quan, 2012)

Model	Rheology	Solution approach	Reference frame	Variation of rheology	Entrainment rate
MADFLOW	Frictional, Voellmy and Bingham	Continuum integrated	Lagrangian with mesh	No	Defined
TOCHNOG	Frictional (elastoplastic model)	Continuum differential	Differential (adaptive mesh)	Yes	Process based
RAMMS	Voellmy	Continuum integrated	Eulerian	Yes	Process based and defined
DAN3D	Frictional, Voellmy, Bingham, Newtonian, Plastic	Continuum integrated	Lagrangian meshless	Yes	Defined
FLATMODEL	Frictional, Voellmy	Continuum integrated	Eulerian	No	Process based
SCIDDICA s3-hex	Energy based	Cellular Automata	Eulerian	No	Process based
3dDMM	Frictional, Voellmy	Continuum integrated	Eulerian	Yes	Defined
PASTOR model	Frictional, Voellmy, Bingham	Continuum integrated	Lagrangian meshless	Yes	Defined
MassMov2D	Voellmy, Bingham	Continuum integrated	Eulerian	Yes	Defined
RASH3D	Frictional, Voellmy, Quadratic	Continuum integrated	Eulerian	No	No entrainment rate is used.
FLO-2D	Quadratic	Continuum integrated	Eulerian	No	No entrainment rate is used.
TITAN2D	Frictional	Continuum integrated	Lagrangian meshless	No	No entrainment rate is used.
PFC	Inter-particle and particle wall interaction	Solution of motion of particles by a distinct element method	Distinct element method	No	No entrainment rate is used.
VolcFlow	Frictional, Voellmy	Continuum integrated	Eulerian	No	No entrainment rate is used.

1. Dynamic Analysis (DAN)

Dynamic Analysis (DAN) is a continuum model based on a Lagrangian solution of the equations of motion first developed by Hungr (1995) and was later extended into three dimension as DAN3D by McDougall (2006) for his PhD thesis at University of British Columbia. The governing equations are primarily based on the depth-averaged equations derived from classical principles of continuum mechanics. Although this model is mainly used for modelling snow and rock avalanches, simulations of debris flows can be carried out and the different runout results can be compared against the field results like the maximum runout distance, flow velocity, thickness and distribution of the deposit and flow behaviour in bends and obstacles along the path (Hungr, 1995). One of its distinct features is it provides selection of different material rheologies which may vary along the slide mass or the slide path unlike RAMMS which employs only one fixed rheological model. Plastic, Bingham, friction, Voellmy and Newtonian rheology are the varying rheologies upon which selection can be made for a suitable one according to the flow conditions. Verification of this model was done by laboratory experiments (McDougall, 2006).

The two dimensional set of governing equations are,

$$\frac{\partial h}{\partial t} + h\left(\frac{\partial u_x}{\partial x} + \frac{\partial u_y}{\partial y}\right) = \frac{\partial b}{\partial t} \tag{17}$$

$$\rho h \frac{\partial u_x}{\partial t} = \rho h g_x + k_x \sigma_z \left(\frac{\partial h}{\partial x}\right) + k_{yx} \sigma_z \left(-\frac{\partial h}{\partial y}\right) + \tau_{zx} - \rho u_x \frac{\partial b}{\partial t} \tag{18}$$

$$\rho h \frac{\partial u_y}{\partial t} = \rho h g_y + k_y \sigma_z \left(\frac{\partial h}{\partial y}\right) + k_{yx} \sigma_z \left(-\frac{\partial h}{\partial x}\right) + \tau_{zy} - \rho u_y \frac{\partial b}{\partial t} \tag{19}$$

where, h is the flow height, u_x and u_y are the velocity components in the x and y direction and g_x and g_y are the x and y components of gravitational acceleration. k_x, k_y, k_{xy} and k_{yx} are the tangential stress coefficients. σ_z is the normal stress.

$\frac{\partial b}{\partial t} = Eh\bar{u}$ is the erosion rate where, E is an empirical constant and $\bar{u}$ is the depth averaged speed.

Material is entrained in this model by a volume flux across the basal boundary. The material entrainment physically includes frontal plowing and direct basal scouring as shown in the Figure 2-12. The amount of volume entrained from a point at each time step is added to the

nearest control volume. The erosion depth is user defined and it helps to limit the entrainment amount. The average erosion rate is defined by Hungr and McDougall (2004) as,

$$E_s = \frac{\ln\left(\frac{V_f}{V_o}\right)}{S} \tag{20}$$

where, V_o and V_f are the total volume of the mass flowing before and after entrainment and S is the length of the flow path along the entrainment zone.

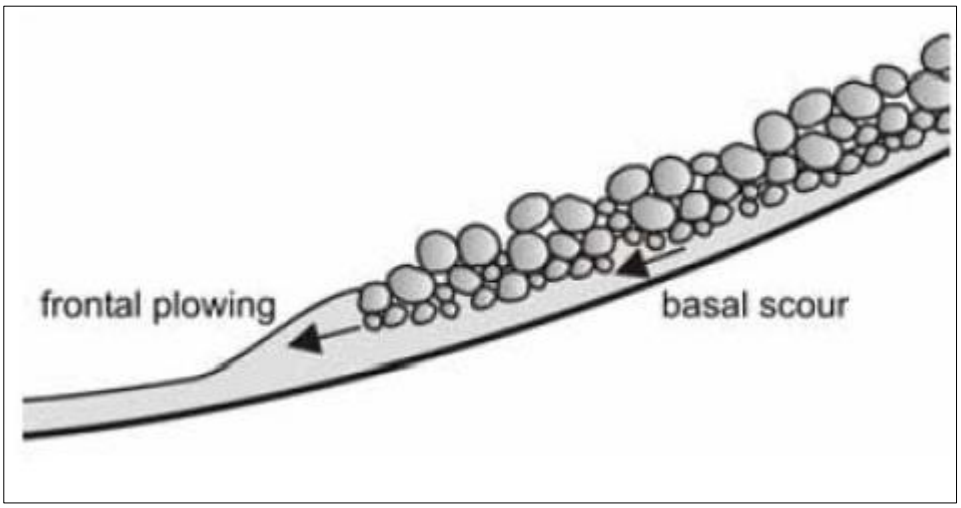

Figure 2-12 Entrainment of material by plowing and erosion at the base (McDougall, 2006)

2. MassMov2D

MassMov2D is a two dimensional model used for the dynamics of mud and debris flow over a complex terrain and was introduced by Begueria et al. (2009a). The model is based on classical Savage and Hutter theory (1989) which assumes the flow as a single phase homogeneous material with rheological behaviour. The flow is modelled as a two dimensional continuum using the depth integrated approximation from which the governing mass and momentum balance equations are derived. It can be used to model both debris flows and rock avalanches. (Beguería et al., 2009b). Due to its implementation in the GIS scripting language PCRaster, preparations of input data and output data are simplified (Quan, 2012). Data from debris flows in Austrian Tyrol and French Alps have been used to estimate the required input parameters for the numerical model. MassMov2D employs two rheology laws, Coulomb-viscous rheology and Voellmy rheology (Beguería et al., 2009a).

The mass and momentum balance equations have been developed with h_s, a new variable representing the soil thickness.

$$\frac{\partial h}{\partial t} + c_x \frac{\partial (hu)}{\partial x} + c_y \frac{\partial (hv)}{\partial y} - \frac{\rho_s}{\rho} \frac{\partial h_s}{\partial t} = 0 \quad (21)$$

$$\frac{\partial u}{\partial t} + c_x u \frac{\partial u}{\partial x} + c_y v \frac{\partial u}{\partial y} = -c_x g \left(S_x + k \frac{\partial (c_x h)}{\partial x} + S_f q_x \right) - \frac{u}{h} \frac{\partial h_s}{\partial t} \quad (22)$$

$$\frac{\partial v}{\partial t} + c_y v \frac{\partial v}{\partial x} + c_x u \frac{\partial v}{\partial y} = -c_y g \left(S_y + k \frac{\partial (c_y h)}{\partial y} + S_f q_y \right) - \frac{v}{h} \frac{\partial h_s}{\partial t} \quad (23)$$

where, h is the flow height normal to the bed, u and v are the x and y components of the velocity, c_x and c_y are the direction cosines of the bed. $\frac{\rho_s}{\rho}$ gives the ratio between the density of the soil and the flowing mass. S_x and S_y are the bed slope gradients in the x and y directions respectively and S_f is the flow resistance gradient, k is the earth pressure coefficient.

Entrainment rate is given in MsssMov2D as $\frac{\partial h_s}{\partial t}$ due to scouring and is proportional to the flow momentum.

$$\frac{\partial h_s}{\partial t} = Eh\sqrt{u^2 + v^2} \quad (24)$$

E is the average entrainment rate which can be determined from field observations as in the case of DAN3D (McDougall and Hungr, 2004).

$$E_s = \frac{\ln\left(\frac{V_f}{V_o}\right)}{S} \quad (25)$$

where, V_o and V_f are the total volume of the mass flowing before and after entrainment respectively and S is the average length of the flow path along the entrainment zone.

A detailed description of the MassMov2D model can be found in Begueria et al. (2009a).

3. FLO-2D

FLO-2D is a model for floods and mudflows which was first developed at Colorado State University in the United States by O'brien et al. (1993). The Rudd Creek mudflow in the US initiated by a landslide and deposited in the urban areas was used for the verification of the model. It solves the differential equations of motion by a central difference scheme, an Eulerian method and is based on the quadratic rheological approach. Channelized flows are modelled in one dimension and less channelized flows are modelled in two dimensions. It is based on a volume conservation model where the flow is routed across a series of tiles and is a combination

of hydrologic and hydraulic models. Although it simulates mostly conventional flooding problems, it can also be used for the simulation of debris flows. The governing equations of the flow are the two dimensional equations of motion and the continuity equation similar to other numerical models. (O'brien et al., 1993)

$$\frac{\partial h}{\partial t} + \frac{\partial hV_x}{\partial x} + \frac{\partial hV_y}{\partial y} = i \tag{26}$$

$$S_{fx} = S_{ox} - \frac{\partial h}{\partial x} - \frac{V_x}{g}\frac{\partial V_x}{\partial x} - \frac{V_y}{g}\frac{\partial V_x}{\partial y} - \frac{1}{g}\frac{\partial V_x}{\partial t} \tag{27}$$

$$S_{fy} = S_{oy} - \frac{\partial h}{\partial y} - \frac{V_y}{g}\frac{\partial V_y}{\partial y} - \frac{V_x}{g}\frac{\partial V_y}{\partial x} - \frac{1}{g}\frac{\partial V_y}{\partial t} \tag{28}$$

where, h is the flow depth, V_x and V_y are the x and y components of depth averaged velocity, i is the excess rainfall intensity which may be 0 on the surface. S_{fx} and S_{fy} are friction slope components which are written as function of bed slope S_{ox} and S_{oy}, pressure gradient and convective and local acceleration terms (O'brien et al., 1993).

No entrainment model is incorporated into FLO-2D and the mass balance equation is equal to the rainfall intensity (O'brien et al., 1993).

3 Numerical Tool

This research is focused on modelling debris flows using the Voellmy rheology model in the continuum based numerical model, RAMMS with the inclusion of entrainment module (Christen et al., 2010b). A detailed explanation of the RAMMS software along with the Voellmy rheology is presented in this chapter.

3.1 RAMMS

RAMMS (RApid Mass Movements Simulation) is a state-of-the-art numerical two dimensional simulation model which can be used to calculate the motion of geophysical mass movements (snow avalanches, debris flows, rock falls) from initiation to runout in a three-dimensional terrain (Bartelt et al., 2013). The application was developed by the RAMMS program group at the Swiss Federal Institute for Snow and Avalanche Research SLF (Christen et al., 2010b).

RAMMS was initially developed to resolve the avalanche -related problems that appear during danger mapping and dimensioning of safeguards. It is a dynamic numerical modelling software originally designed to model snow avalanches (Christen et al., 2010b) and has been later applied in the past to model other types of mass movements like lahars (Luna, 2007) and debris flows (Cesca and D'Agostino, 2006, Christen et al., 2008) as well as rock falls. RAMMS calculates the runout path, flow height, velocities and impact pressure in every point from the beginning to the end of the debris flow path. The entrainment module has been recently added in the later versions. RAMMS has a sophisticated graphic user interface and the visualization of the input file and the output results can be enhanced by superimposing aerial photographs, topographical maps and satellite images. It is a user-friendly software which can also be used in association with a GIS-linked environment.

RAMMS describes the flow resistance acting on the debris flow using a Voellmy-Salm fluid flow continuum model (Salm, 1993) based on the Voellmy- fluid flow law and describes the debris flow as a hydraulic-based depth-average continuum model. This model divides the frictional resistance into two parts, one dry Coulomb friction which is dependent on normal pressure, and another viscous resistance turbulent friction. The entrainment module included in RAMMS is as described by Sovilla et al. (2006).

Since RAMMS was originally developed for hazard mapping in Switzerland, it must be used with regard to existing calculation guidelines in Switzerland (Salm et al., 1990). For this reason, the Voellmy–Salm (VS) model (Salm, 1993) is chosen, which is used in the Swiss Guidelines for avalanche runout calculation. Although the VS model can accurately model the maximum

flow heights and velocities at the head of the avalanche and therefore avalanche runout distances, it cannot model the evolution of velocity over the entire length of the avalanche (Bartelt and Buser, 2010). Because velocity gradients control the distribution of mass within the avalanche body, the VS model works poorly with snow cover entrainment which determines the avalanche growth and size. Therefore, RAMMS includes an additional flow model based on the production, transport and decay of the kinetic energy of the random motion associated with the mass of flowing snow granules, the random kinetic energy (RKE) model. This model can track the evolution of velocity within the avalanche and therefore allows a more realistic modeling of entrainment and deposition. (Christen et al., 2010b)

In this version of RAMMS, the RKE model is not available and the software uses the simple Voellmy Salm model. The software has been calibrated with the help of full-scale avalanche attempts made in the Vallée de la Sionne in Switzerland (Christen et al., 2010b).

3.2 The Voellmy Salm Model

The Voellmy–Salm (VS) model is used for debris flow and avalanche runout calculation. In practical applications, the VS model has proven to be simple as it contains only two flow parameters and numerically accurate. All of the derivations and calculations below have been compiled from the research carried out by Christen et al. (2010b).

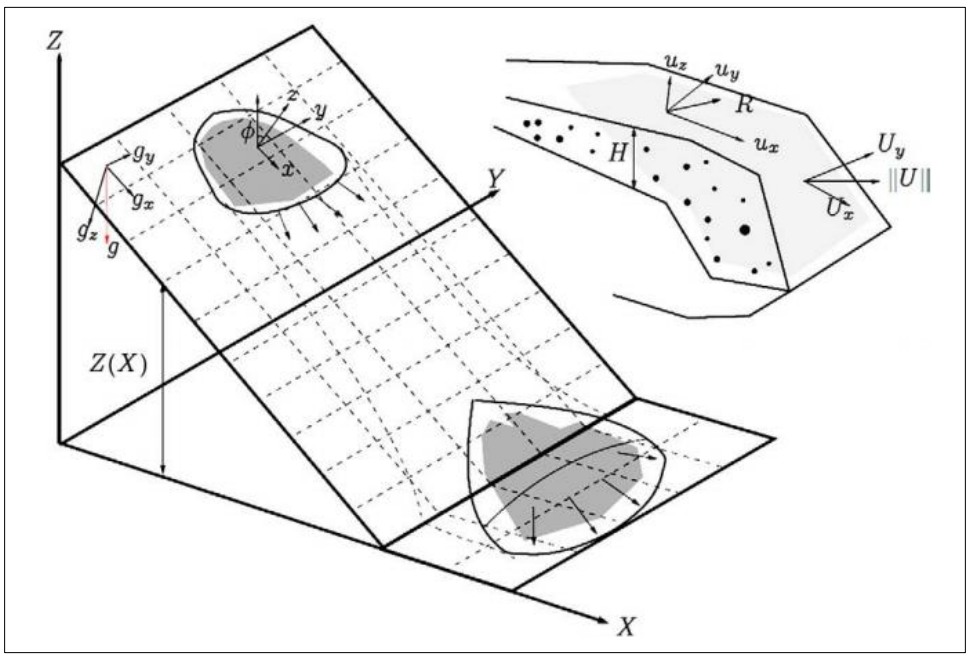

Figure 3-1 Topography Z (X,Y) given in a Cartesian framework (Christen et al., 2010b)

Let X and Y be horizontal coordinates in a fixed Cartesian coordinate system and Z (X, Y) denote a mountain profile parameterized in X and Y as given in Figure 3-1. The coordinates x, y, and z define the surface induced coordinate system. Its orientation varies with the position on the surface, such that the vector of gravitational acceleration $g = (g_x, g_y, g_z)$ has three non-zero components in general, in each case functions of x and y. Time t completes the set of independent variables for the system.

This snow avalanche or debris flow is characterized by unsteady and non-uniform motion with varying height and velocity. The field variables of interest are therefore the avalanche flow height H (x, y, t) and the mean avalanche velocity U (x, y, t).

$$U\ (x, y, t) = (\ U_x\ (x, y, t), U_y\ (x, y, t))^T \tag{29}$$

where, U_x and U_y are the velocities in the x and y directions respectively, and T is used to transpose the matrix of the mean velocity.

The magnitude of the flow velocity is given by:

$$\|\mathrm{U}\| = \sqrt{U_x^2\ + U_y^2} \tag{30}$$

where, the double lines (||) indicate the norm on the velocity, making it a strictly positive velocity. The unit vector of the flow velocity is:

$$n_U = \frac{1}{\|\mathrm{U}\|}(U_x + \ U_y)^T \tag{31}$$

The Voellmy Salm model uses the following mass balance in terms of the height,

$$\delta_t H + \ \delta_x(HU_x) + \ \delta_y\big(HU_y\big) = \dot{Q}\ (x, y, t) \tag{32}$$

where, H is the flow height (m) and $\dot{Q}$ (x, y, t) (kg/m^{2}s) denotes the mass production source term, referred to as the snow entrainment rate ($\dot{Q} > 0$) or the snow deposition rate ($\dot{Q} < 0$). The component wise depth-averaged momentum balance is given by,

$$\delta_t(HU_x) + \ \delta_x\left(c_x HU_x^2 + \ g_z k_{a/p}\frac{H^2}{2}\right) + \ \delta_y\big(HU_x U_y\big) = S_{gx} - \ S_{fx} \tag{33}$$

$$\delta_t\big(HU_y\big) + \ \delta_y\left(c_y HU_y^2 + \ g_z k_{a/p}\frac{H^2}{2}\right) + \ \delta_x\big(HU_x U_y\big) = S_{gy} - \ S_{fy} \tag{34}$$

The velocity profile shape factors c_x and c_y serve as a first-order model correction to account for shear gradients and non-rectangular velocity profiles and g_z is the gravitational acceleration in the vertical direction.

The vertical and horizontal normal stresses are proportional with a proportionality factor given by the earth pressure coefficient, $k_{a/p}$.

$$k_{a/p} = tan^2\left(45^\circ \pm \frac{\varphi}{2}\right) \tag{35}$$

where, φ is the angle of internal friction of the debris flow. We set $k_{a/p}$ = 1 in general when using the standard VS approach and this parameter is called lambda in RAMMS, since $k_{a/p}$ has little influence on the final calculated runout distances and velocities.

The right-hand side terms add up to an effective acceleration.

$$S_{gx} = g_x H \tag{36}$$

$$S_{gy} = g_y H \tag{37}$$

where, S_{gx} and S_{gy} denote the driving, gravitational acceleration in x and y direction, respectively.

The friction in the VS model is given by,

$$S_f = \left(S_{fx}, S_{fy}\right)^T \tag{38}$$

where, S_{fx} and S_{fy} are the frictions in the x and y directions respectively and are given by:

$$S_{fx} = \eta_{U_x}\left[\mu g_z H + \frac{g||U||^2}{\xi}\right] \tag{39}$$

$$S_{fy} = \eta_{U_y}\left[\mu g_z H + \frac{g||U||^2}{\xi}\right] \tag{40}$$

where, η_{U_x} and η_{U_y} are the velocity directional unit vectors in the x and y directions respectively. The total basal friction is divided into a velocity independent dry-Coulomb term which is proportional to the normal stress at the flow bottom (friction coefficient μ) and a velocity dependent "viscous" or "turbulent" friction (turbulent coefficient ξ). In RAMMS, the friction coefficient is denoted by Mu and the turbulent coefficient by Xi.

3.3 Entrainment in RAMMS

The effective entrainment rate $\dot{Q}$ (x, y, t), the entrainment rate at which the mass is moving with the avalanche velocity is given as:

$$\dot{Q}\ (x,y,t) = \begin{cases} 0, & for\ \left[h_s\ (x,y,0) - \int_0^t \dot{Q}\ (x,y,\tau)\partial\tau\right] = 0 \\ \frac{\rho_i^s}{\rho}\ K_i\ U, for & \left[h_s\ (x,y,0) - \int_0^t \dot{Q}(x,y,\tau)\partial\tau\right] > 0 \end{cases} \quad (41)$$

where, ρ (kg/m^3) is the density of the initiated debris flow, τ is the shear stress and h_s (x, y, 0) (m) is the initial height of the debris at position (x, y) and time t = 0. The total height of the entrainment layer in RAMMS can be divided into three separate entrainment layers, so that $h_s = \sum h_i$ and the density of the each layer is given by ρ_i^s (kg/m^3). K_i is the dimensionless entrainment coefficient for each layer. If a single entrainment layer is chosen, K_i can simply be defined as K. Christen et al. (2010b) mentions that the entrainment rate depends on the speed of the incoming flow, but when K > 1, then entrainment is near instantaneous.

3.4 Analysis of Governing Equations

Instead of deriving the governing equations of RAMMS by the previously mentioned depth averaging, a simple strength of material approach is adopted in this study that will reveal only the significant and essential properties of the model. All the derivations and calculations performed in his section are compiled from Pudasaini and Hutter (2007).

Let´s consider a one dimensional flow of granular materials along an inclined plane at an angle α with the horizontal surface as shown in Figure 3-2.

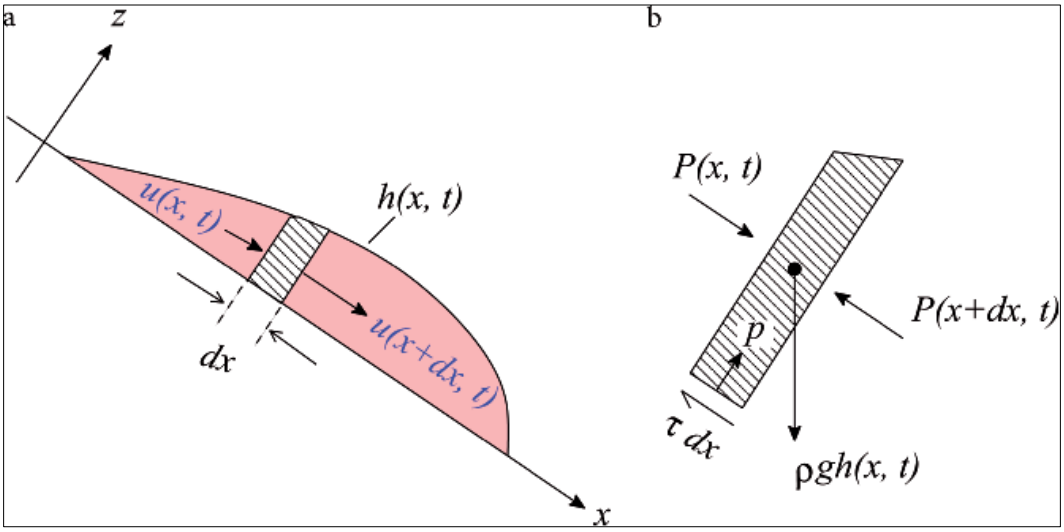

Figure 3-2 Flow of a finite mass of debris flow/avalanches down an inclined plane and free body diagram of an elemental column for which the mass and momentum balances are formulated (Pudasaini and Hutter, 2007)

Assumptions:

1. The moving mass has a constant volume. If it is not constant, subsequent entrainment or deposition will occur as a result.
2. The flow material is cohesionless.
3. The shear stresses lateral to the main flow direction is neglected.
4. The flow takes place in isothermal conditions.
5. The density of the flow is constant, ρ.
6. Constant velocity of the flow over the whole depth, $u = u\,(x,t)$

Isolating a column in the flow of elemental length dx and formulating mass and momentum balance equations on the resulting free body diagram in the x-direction only (Figure 3-2).

The growth rate of the mass within the column will be given by,

$$\frac{\partial}{\partial t}\big(\rho h(x,t)\big)dx = \rho h(x,t)u(x,t) - \rho h(x+dx,t)u(x+dx,t) \tag{42}$$

$$= -\frac{\partial}{\partial x}(\rho h(x,t)u(x,t)dx + O((dx)^2) \tag{43}$$

The above expression is gotten by using a Taylor series expansion and $O((dx)^2)$ refers that the next term will be of the order $(dx)^2$.

Dropping the higher orders of dx, we get from equation 43,

$$\frac{\partial h}{\partial t} + \frac{\partial (hu)}{\partial x} = 0 \tag{44}$$

This is the mass balance equation.

Now, the momentum balance states that the time rate of change of momentum (in the x-direction) is equal to the convected flux of the momentum into and out of the column plus the forces acting on the column.

X-momentum of the column $= mu = \rho hudx$

Time rate of the change of this x-momentum

$$= \frac{\partial}{\partial t}(\rho h(x,t)u(x,t))dx \tag{45}$$

Using Taylor series expansion as in above, the flux of momentum through the column wall is given by

$$= \rho h(x,t)u^2(x,t) - \rho h(x+dx,t)u^2(x+dx,t) \tag{46}$$

$$= -\frac{\partial}{\partial x}((\rho h(x,t)\, u^2(x,t)) + (O(dx)^2) \tag{47}$$

The forces acting on the column are,

1. The gravity force normal to the inclined plane given by,

$$\rho g h \sin\alpha \, dx$$

2. The basal frictional force given by,

$$\tau dx$$

3. The longitudinal pressure in the column given by,

$$\int_0^{h(x,t)} p_L(x,z,t)dz - \int_0^{h(x+dx,t)} p_L(x+dx,z,t)dz$$

Above, the subscript L indicates that the longitudinal pressure, p_L can be different than the overburden pressure. This overburden pressure is given by the force balance in the z-direction.

$$p(x,z,t) = \rho g(h(x,z,t) - z)cos\alpha \tag{48}$$

The longitudinal pressure p_L and overburden pressure p can be related by classical soil mechanics.

$$p_L(x,z,t) = k_{a/p}p(x,z,t) \tag{49}$$

where, $k_{a/p}$ is the earth pressure coefficient.

From 3,

$$-\frac{\rho g}{2}\frac{\partial}{\partial x}\left(k_{\frac{a}{p}}h^2(x,t)\right)cos\alpha dx + O((dx)^2)$$

Applying a Coulomb friction law with internal friction angle δ to the basal friction,

$$\tau = \tan\delta\, p \tag{50}$$

From 2, we get

$$-sgn(u)\rho g h(x,t) tan\delta cos\alpha dx$$

Now adding the forces 1, 2, and 3, the force balance in the x-direction is given by,

$$\left[\rho g h(x,t)(sin\alpha - sgn(u)tan\delta cos\alpha) - \frac{\rho g}{2}\frac{\partial}{\partial x}\left(k_{\frac{a}{p}}h^2(x,t)cos\alpha\right)\right]dx + (O(dx)^2) \tag{51}$$

From the momentum balance law,

Time rate of change of momentum = Flux of momentum of column + Forces acting on the column

This gives,

$$\frac{\partial}{\partial t}\left(\rho h(x,t)u(x,t)\right)dx + \frac{\partial}{\partial x}\left(\left(\rho h(x,t)u^2(x,t)\right)\right) = \left[\rho g h(x,t)(sin\alpha - sgn(u)tan\delta cos\alpha) - \frac{\rho g}{2}\frac{\partial}{\partial x}\left(k_{\frac{a}{p}}h^2(x,t)cos\alpha\right)\right]dx \tag{52}$$

$$\frac{\partial}{\partial t}(hu) + \frac{\partial}{\partial x}(hu^2) = g\left[(sin\alpha - sgn(u)tan\delta cos\alpha)h - \frac{1}{2}\frac{\partial}{\partial x}\left(k_{a/p}h^2 cos\alpha\right)\right] \tag{53}$$

Equations 44 and 53 give the system of two partial differential equations for the flow with thickness h (x, t) and longitudinal velocity u (x, t). This is correct to the order (O (dx) ^{2}).

These equations can be generalized into two dimensions by adding a cross slope direction.

In equation 53, the driving force is the inclined component of the gravity force, g sinα and this force is counteracted by the frictional force, $-sgn(u)tan\delta cos\alpha gh$. This force is modelled by Coulomb type dry friction law. In case of a numerical model using a Voellmy drag, the bed friction law is extended to include the viscous drag given by,

$$S_v = \frac{\rho g}{\xi}|u|u \tag{54}$$

where, ξ is the velocity dependent viscous or turbulent coefficient.

When generalised into a two dimensional flow and considering the viscous drag in addition to the Coulomb friction and after rearranging the terms, equations 44 and 53 will be identical to the governing equations of RAMMS.

In the depth averaged momentum balance equations of RAMMS, c_x and c_y are the velocity profile factors. For a rectangular velocity profile, c_x and c_y are equal to 1.

3.5 Analysis of Entrainment in RAMMS

Due to the complex mechanisms involving entrainment and lack of knowledge of the physical processes characterizing the entrainment phenomenon, a lot of the dynamic numerical models incorporate the entrainment procedure in a simple way through a calibration coefficient or entrainment rates based on empirical rules which estimate the yield erosion rate which can be predefined by the user. Barbolini et al. (2005) and Eglit and Demidov (2005) quantify the erosion rate q, i.e. the eroded snow volume per unit time and area in three manners:

1. The entrainment rate is proportional to the velocity of the debris flow and is given by the product of the flow velocity and an empirical coefficient considering the density of the erodible bed and the flow.

   $$q = au$$

   where, a is a coefficient depending on the snow properties and takes into account the different densities of the snow cover and avalanche, and u is the flow velocity.

2. The entrainment rate is proportional to the flow height and is given by the product of the flow property coefficient and the minimum flow height with a load equal to the shear strength of the bed.

$$q = b\,(h - h_*)$$

where, h is the flow height, h_* is the minimum flow height that produces a load equal to the shear strength of the snow cover and b is a coefficient.

3. The entrainment rate is growing with the square of the flow velocity and is given by the product of the flow property coefficient and a velocity threshold for erosion.

$$q = c\,(u^2 - u_*^2)$$

where, c is a coefficient and u_* is the threshold velocity for erosion.

RAMMS uses a rate-controlled, history-dependent approach in RAMMS which allows us to regulate both the mass uptake and the time delay required to accelerate the mass to the avalanche velocity. It is assumed that when the avalanche hits the snow cover, it first fragments and the speed of the fragmentation front scales with the avalanche velocity as shown in Figure 3-3. At every node n, the fragmentation front moves with speed of the avalanche given by U_n. The effective entrainment rate is K_iU_n where K_i is the effective entrainment coefficient for the i^{th} snow layer. In this two-dimensional depiction, the avalanche is moving in the direction S given by the unit vector n_U.

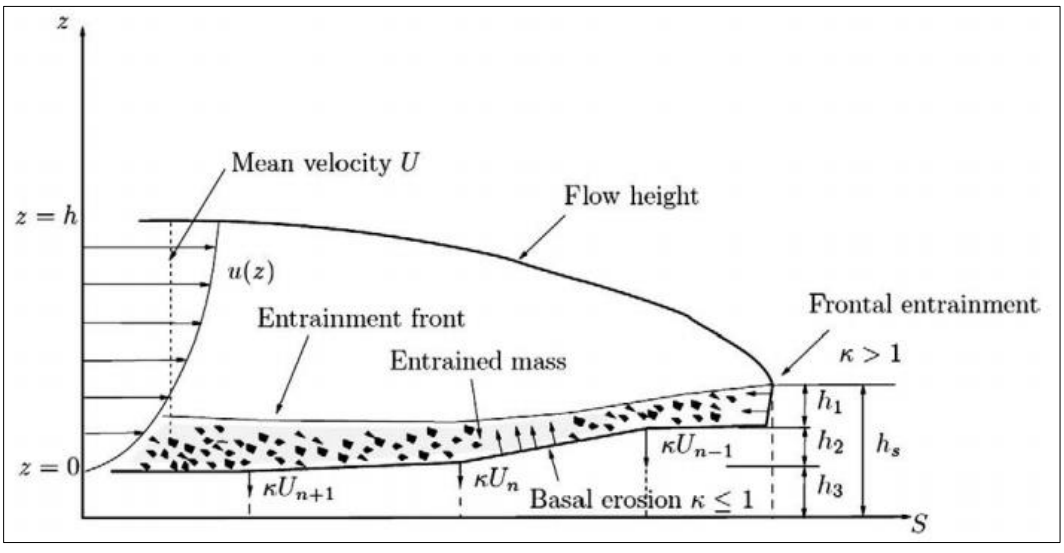

Figure 3-3 Rate controlled entrainment model in RAMMS (Christen et al., 2010b)

For K ≤ 0.5, sediment is entrained into the debris flow, but at a much slower rate. Therefore, different values of *K* correspond to different entrainment mechanisms. For frontal ploughing, it has been found K > 0.5 and for basal erosion K ≤ 0.5. (Christen et al., 2010b)

Three types of erosion laws are included in RAMMS. They are:

1. Velocity driven law
2. Momentum driven law
3. Velocity square driven law

In this version of RAMMS, the entrainment rate is defined in the first manner set as default, i.e. the velocity driven law as specified by Barbolini et al. (2005) and Eglit and Demidov (2005) and only one layer of entrainment layer can be specified in the program instead of three.

3.6 Input Parameters in RAMMS

In this section, a brief explanation of running a simulation in RAMMS is presented. A more detailed guide on how to simulate a RAMMS model is presented in Appendix B. To perform a numerical simulation, three quantities must be specified- topographic data, release zone and release (height), and lastly model friction parameters. Figure 3-4 shows the typical graphical user interface for running a simulation in RAMMS.

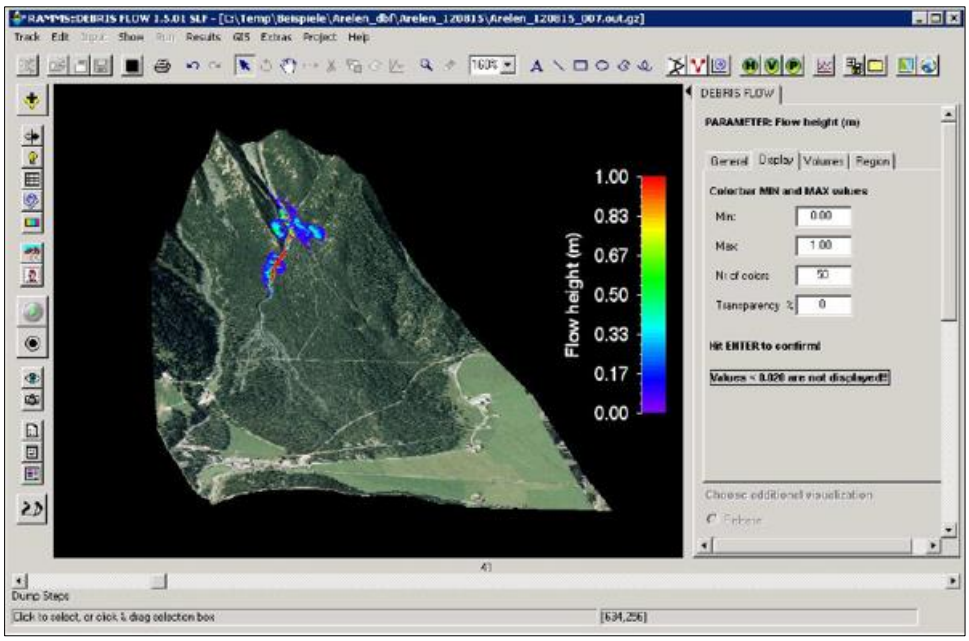

Figure 3-4 Graphical User Interface of RAMMS (Bartelt et al., 2013)

The topographic data is the main input of the simulation procedure that forms the framework of the entire modelling and information about topography is given via digital elevation models

(DEMs). DEMs can be generated from field measurements, for instance terrestrial or aerial laser scanning data or they can be obtained from national geographic information centers. The DEMs can be imported in RAMMS as an ESRI ASCII grid format, which can be made with the help of GIS. Moreover, the grid file should follow the RAMMS format as in, the header of the grid should contain information about the number of rows and columns, the x and y co-ordinates of the lower left corner and grid resolution. The results are very strongly dependent on the resolution and accuracy of the DEMs.

There is an option of importing geo-referenced maps or aerial photographs that can be superimposed upon the DEMs. In this way, the model along with the results are easier to analyze and interpolate.

RAMMS automatically applies a calculation domain around the topography once the DEM and the images are imported. The user can later modify the calculation domain as per need. Calculation time depends on the size of the calculation domain so it is recommended to have a smaller domain covering the relevant area instead of the whole topography. The second step in running a simulation is specifying the initiation area. This is done by specifying a release area along with the release height which gives the initiation volume for the flow. Release areas can be specified using polygon shapefiles directly on the program interface or they can also be drawn in GIS first and then imported into RAMMS. Another option of defining a release area is using input hydrographs which is not applied in this research. The calculation domain is drawn in the same way as the release area.

The next step before running the simulation is the input of friction parameters, friction coefficient (μ) and turbulent coefficient (ξ). Although there are no fixed values for these friction parameters, Table 3 gives a general suggestion for the initial values of μ and ξ which can be used for the calibration procedure.

Table 3 General suggestion for the initial values of the Voellmy friction coefficients used for the calibration procedure (Bartelt et al., 2013)

Initial values of the Voellmy friction coefficients used for calibration with unknown flow type		
Dry-Coulomb type friction	μ	0.2
Viscous-turbulent friction	ξ [m/s^2]	200

One of the methods of predicting the value of the friction coefficient μ is given by Chen and Lee (2003) according to which $\mu = \tan \alpha$, where α is the average inclination of the flow topography. Alternatively, it can also be calculated as $\mu = \tan \Phi$, where Φ is the bulk friction angle (Hungr and Evans, 1996). The value of the turbulent coefficient ξ is harder to predict.

In this version of RAMMS, entrainment is implemented by defining polygons in the transport zone where entrainment would take place. These polygons can be drawn directly in RAMMS or imported as a shape file from GIS similar to a release area. A maximum of two polygons can be defined accounting for different entrainment heights. The process is completed by assigning entrainment height (m), density of the entrainable material (kg/m^3) and the entrainment coefficient K for each entrainment polygon.

3.7 Output Results of RAMMS

After specifying all the input parameters, RAMMS begins the simulation. The simulation takes between 100 seconds to 15 minutes depending on the grid resolution of the DEM and calculation domain of the project. The RAMMS simulation is stopped by using a stop criterion which is based on momentum (kgm/s). RAMMS calculates the sum of momentum at every dump step and compares with the maximum sum of momentum. If this percentage difference is less than the value provided by the user, then the flow is regarded as stopped (Christen et al., 2010b).

The output of the numerical simulation can be viewed in RAMMS itself as well as can be exported to GIS as ESRI shapefiles. A log file is also available as an output for the entire simulation and at different dump steps.

From the Results dropdown menu, it is possible to view the different output results. The important result parameters are- the initiation, entrainment and deposited volume (m^3) at different time steps, flow height (m), flow velocity (m/s), impact pressure (kPa) at different time steps with their maximum and the runout path of the entire flow. Depending on the data available for the actual flow, comparisons can be made while back calculating a debris flow.

In addition to the above parameters, line profile and time plots can be made for each of the above parameters along different sections of the flow. Similarly, an image or GIF animation of the entire flow can be created.

4 Simulation of Laboratory Model

4.1 Introduction

Working with numerical models require proper knowledge about the software. While running simulation of a laboratory model, the first important step is to make sure that the simulated model will give good results for the analysis (Blanc et al., 2011). A simple DEM can help to control the simulation and to understand the analysis and results. Therefore, a sample DEM was prepared and imported to RAMMS and simple analyses were carried out on it before carrying out analysis of the actual laboratory model and the Almåskroken debris flow event. Simulations were carried out with two initiating release volumes, one very high compared to the other. Since this work is repeated with the next two case studies, only a brief summary of these simulations performed on the DEM prepared above is discussed here. A more detailed explanation of the carried out simulations along with its analysis and results is presented in Appendix C.

The most distinct result from the simulations carried out was that the increase in release volume of the initiating landslide increased the runout distance, flow height and velocity of the debris flow. Increasing the release volume of the debris flow from 732 m^3 to 3660 m^3 increased the runout distance by nearly 10 percent and doubled the flow height and the flow velocity. This increase in runout distance will be more in case of larger release volumes.

4.2 Background

Out of different physical models used to simulate debris flow events in the laboratory, flume tests are the closest. Different flume tests have been conducted all around the world in small scales (Papa et al., 2004, Rickenmann et al., 2003) as well as in a large scale (Reid et al., 2011).

A similar kind of flume test has been conducted by Emilie Laache (2016) at the laboratory for her Master's thesis at NTNU this spring. The flume is built of a wooden channel 869 cm long, 60 cm wide and 30 cm deep. The flume has a varying inclination of 23 degrees at the beginning, 13.8 degrees in the middle and it flattens to 1.6 degrees towards the end. A debris flow containing a mixture of sand and water is released from the top as represented by the box in Figure 4-1 and sensors are placed along the flow at different locations enabling measurements of different outputs. The runout distance over the inclined surface and the flow height at different locations are recorded for different cases. The total weight of the flowing material for the debris flow simulation was 100 kg with 80 kg of sand and 20 kg of water (Figure 4-2). The

runout distance of the flow was found to be approximately 550 cm, measured from the release point (Figure 4-1). This runout distance is the average distance measured from three tests conducted for the same laboratory setup. Flow heights were measured at the downstream of the release point along the channel and an average flow height of 4 cm at the deposition zone was found from the experiment.

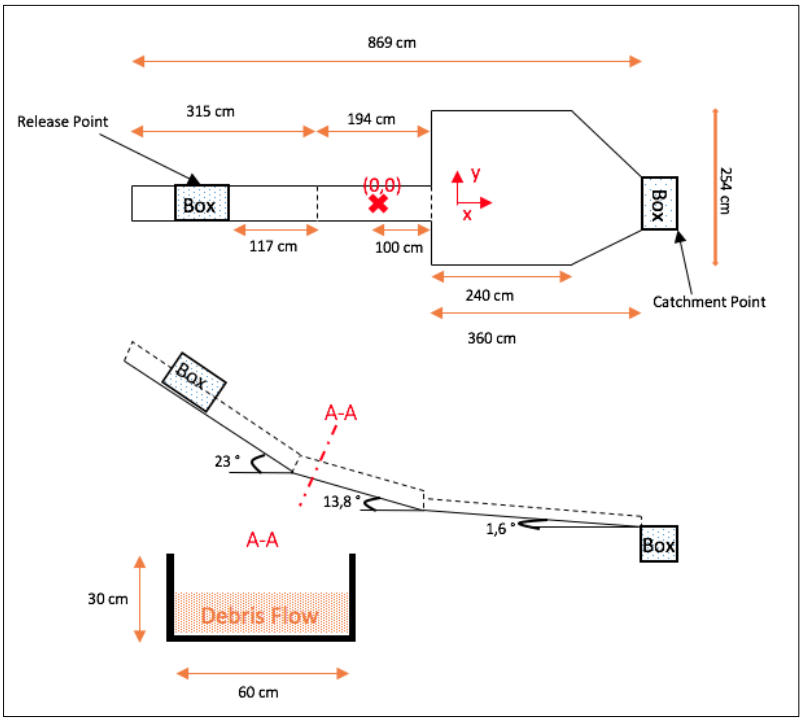

Figure 4-1 Geometry of the flume test (Laache, 2016)

Figure 4-2 Overview of the laboratory model (Hiller and Jenssen, 2009)

4.3 Application of Input Parameters

A hypothetical DEM was prepared in MS-EXCEL first and later imported to RAMMS to represent the laboratory setup. See Appendix A for the sample grid which is to be used as the DEM in RAMMS. Different input parameters are to be defined for the simulation of this test. The density of the materials was determined as $\rho = 2710$ kg/m^3 from the laboratory experiments (Yang, 2016) and the flowing material was considered cohesionless as regular debris flows (Pudasaini and Hutter, 2007). The release volume was defined to represent the release volume in the flume test. In this case, as it was difficult to define the same volume as that of the laboratory experiment in RAMMS, the mass of the material used in the laboratory, 100 kg was used as a control mass. The volume of the release area was modified as to have nearly the same mass of the release materials. The Voellmy coefficients were calibrated against the measured runout distance by beginning with the default values of $\mu = 0.2$ and $\xi = 200$m/s^2 as recommended in the user manual.

The green line represents the automatically defined calculation domain and the red polygon represents the release area as shown in Figure 4-3.

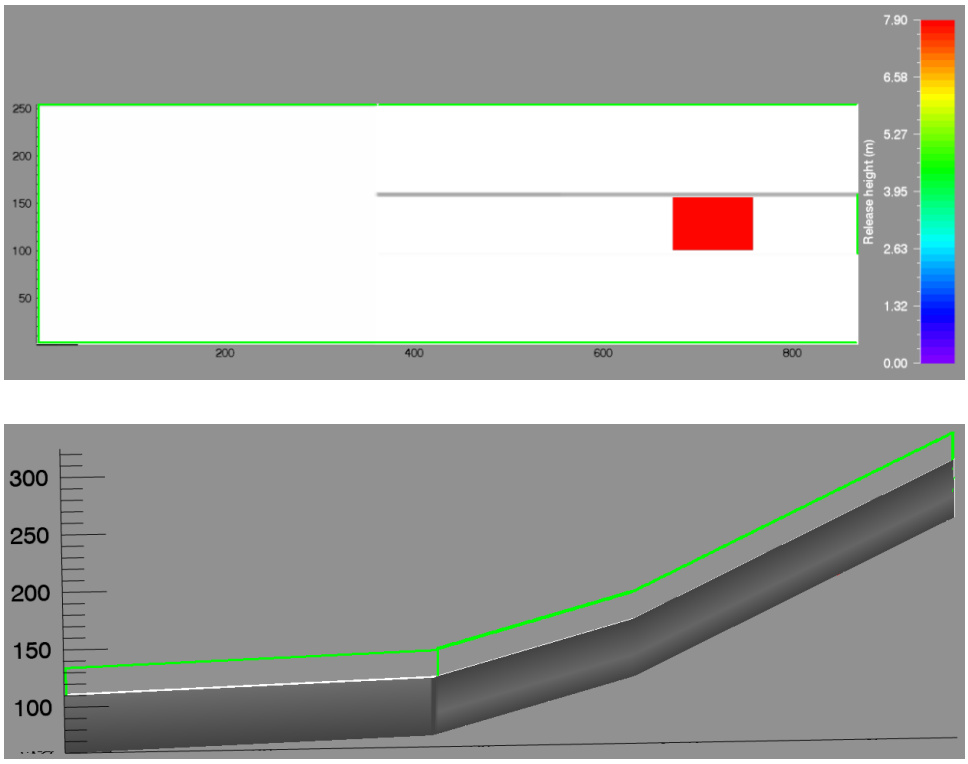

Figure 4-3 Plan (top) and elevation (bottom) view of the laboratory model prepared in RAMMS

A significant difference between the laboratory model and the simulated model was the difference in size. The dimensions of the laboratory setup were difficult to be modelled in

RAMMS. The minimum grid resolution of the DEM to be used in RAMMS is of the order 1 m * 1 m. As a result, the dimensions of the laboratory model were scaled by a factor of 100 to make it convenient to be used for simulation as shown in Table 4.

Table 4 Dimensions of the actual laboratory model and the simulation model

	Actual Size of the Laboratory Model	Model Size used in RAMMS	Scaling Factor
L	869 cm	869 m	100
B	60 cm	60 m	100
H	30 cm	30 m	100

Because of this scaling effect, the runout distance will be expected to increase as a result of additional kinetic energy converted from the additional potential energy of the scaled volume of the release material. Yifru (2014) has previously studied the effect of scaling and found out the effects to be insignificant so its effects were neglected.

4.3.1 Friction Parameters

A number of researchers have previously attempted to calibrate the Voellmy rheology coefficients using real landslide events. Out of these, a comprehensive database of 253 landslide events has been created by back-calculation, with 61% of them being debris flows among which 152 of them have been modeled using a Voellmy rheology (Luna et al., 2010). Parametric study of these events approximated the value of maximum friction coefficient (μ) to lie in the range of 0.05 and 0.2 as shown in Figure 4-4 and the value of maximum turbulent coefficient (ξ) in the range 150 to 600m/s^2 as shown in Figure 4-5, reaching the peak at 500 m/s^2. Similarly, Di Santolo et al. (2009) carried out back calculation of 57 debris flows in Italy employing a Voellmy rheology and found out that most of the channelized debris flows has a friction parameter of 0.06.

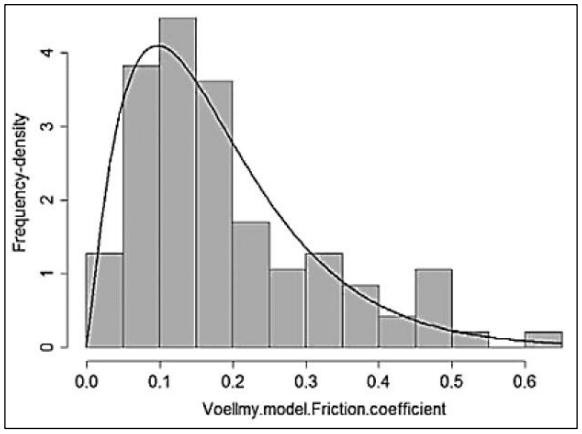

Figure 4-4 Probability density function of friction coefficient (Luna et al., 2010)

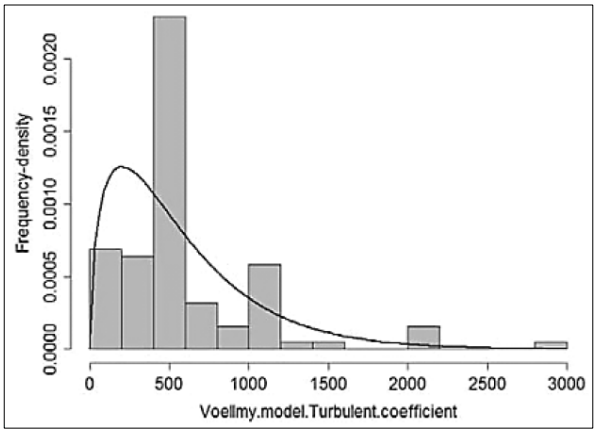

Figure 4-5 Probability density function of turbulent coefficient (Luna et al., 2010)

As entrainment was not considered in the flume test, an exact back calculation could not be performed to reproduce entrainment in the debris flow simulation. The effect of varying entrainment parameters can be studied by defining an entrainment zone and varying the entrainment coefficient, K.

The rest of the parameters were kept constant according to their default values in RAMMS during all the simulations.

A detailed procedure of running the simulation is described in Appendix B.

4.4 Assessment of Output Results

Observed runout distance is the most conveniently defined output parameter for the basement of output results as it can be accurately measured in the laboratory. Although the debris flow may deposit into several small channels during deposition, the flow distance of the main channel is considered as the runout distance.

Similarly, flow height was measured for the debris flow at the upstream of the deposition so this value can also be used for the calibration of the model. No information was available from the flume test regarding other output results like flow velocity and impact pressure. Similar assessment can be carried out in the case of available results.

4.5 Sensitivity Analysis of the Rheological Parameters

Sensitivity analysis of the rheological parameters was conducted by keeping one of the Voellmy coefficients constant while changing the other one and seeing the subsequent change in the output results of the numerical model. According to the RAMMS Debris Flow User

Manual (2013), values of μ exceeding 0.4 rarely provide useful results so a suitable range of μ for sensitivity analysis would be 0.01-0.2. Similarly, a minimum value of 100 m/s^2 and a maximum value of 800 m/s^2 was chosen for the turbulent coefficient, ξ. The range for these rheological parameters were adopted and later modified from suitable literature as described in Section 4.2.1.

4.6 Results

4.6.1 Model Calibration

When the input parameters are not fixed but vary over a certain range, a number of combinations of possible input parameters may lead to the same results also known as principle of equifinality (Hussin, 2011). The model was run several times with different values of each input parameter in a trial and error basis until the required output was reached.

To achieve the best-fit Voellmy friction coefficients, the simulation was initiated with the default values of μ = 0.2 and ξ = 200 m/s^2. These values were varied and finely tuned individually until the simulation results matched with the field observations. In this case, the simulation results were best fitted with the field observations with a friction coefficient, μ = 0.06 and turbulent coefficient, ξ = 500 m/s^2. The result with these parameters keeping all other input parameters constant gave a total runout distance of 530 m (Figure 4-6). This distance is 20 m shorter than the actual runout distance observed in the laboratory. The flow height with these set of rheological parameters was found to be in the range of 3-4 m that is identical to the flow height measured during the laboratory experiment.

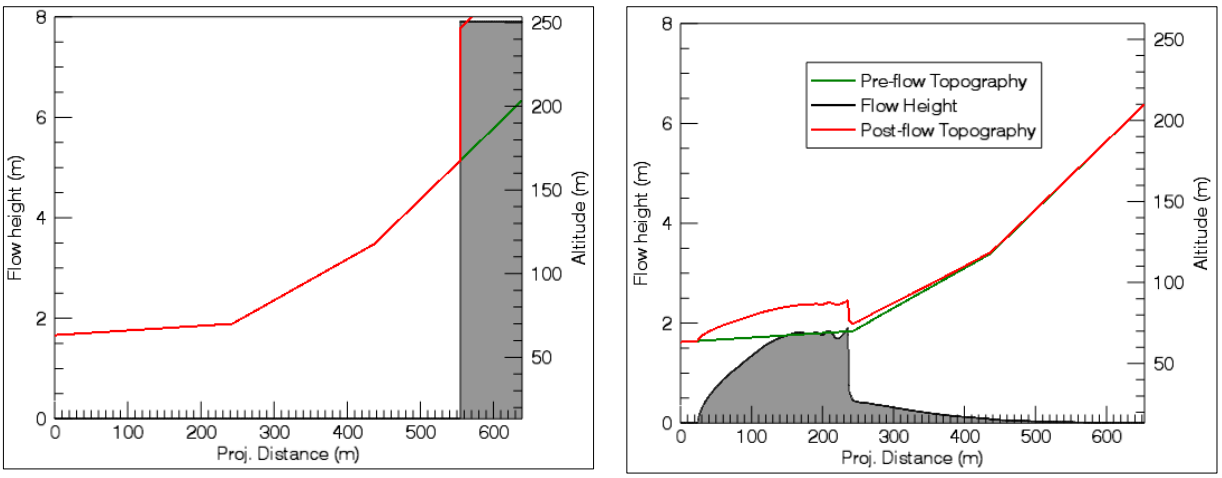

Figure 4-6 Flow Height vs Projected Runout Distance with μ = 0.06 and ξ = 500 m/s^2

In Figure 4-6, the green line is the pre-flow topography and the red line is the post flow topography and the values of the altitude can be read from the right axis. The filled grey area represents the active parameters- flow height with the scale on the left side. The bottom axis is the projected runout distance in m.

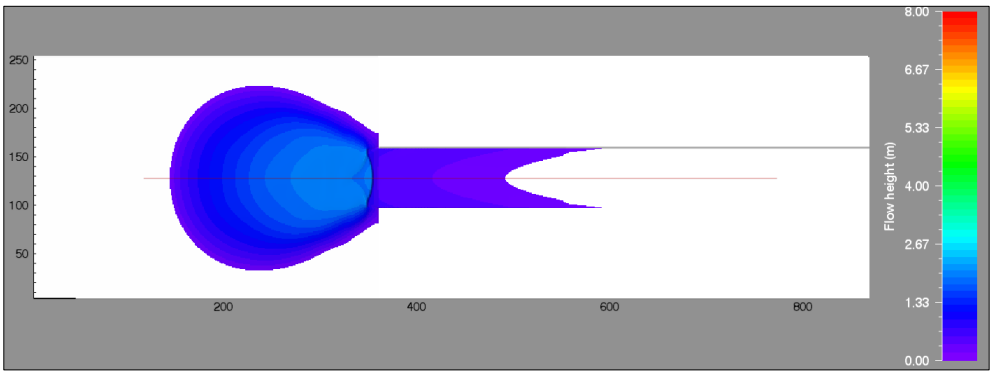

Figure 4-7 Flow Pattern with μ = 0.06 and ξ = 500 m/s^2

Figure 4-8 Flow deposition in the laboratory experiment (Laache, 2016)

The flow pattern and the final deposit pattern of both the simulated model in RAMMS and the laboratory experiment are shown in Figure 4-7 and Figure 4-8 respectively and they follow a similar outline.

4.6.2 Sensitivity analysis of the Rheological Parameters

The only input parameters changed while simulating the physical model were the rheological friction parameters, μ and ξ. All the other inputs were kept constant including the 100 kg of initiating debris flow used for RAMMS simulation. This section shows the effects of keeping either of the friction or turbulent coefficient constant and varying the other within a certain range and the corresponding change in the back-calculated runout distance.

When first simulating the model with the default friction values of μ = 0.2 and ξ = 200 m/s^2, the flow was barely able to reach the lower gentler slope of the flume giving a total runout distance of 355 m also plotted in Figure 4-9. This is 195 m shorter than the actual runout distance of the physical model in the laboratory which is 550 m. Similarly, the deposit flow height was calculated to be approximately 6 m that is greater than the required output of 4 m. Hence, the maximum value of μ was limited to 0.2.

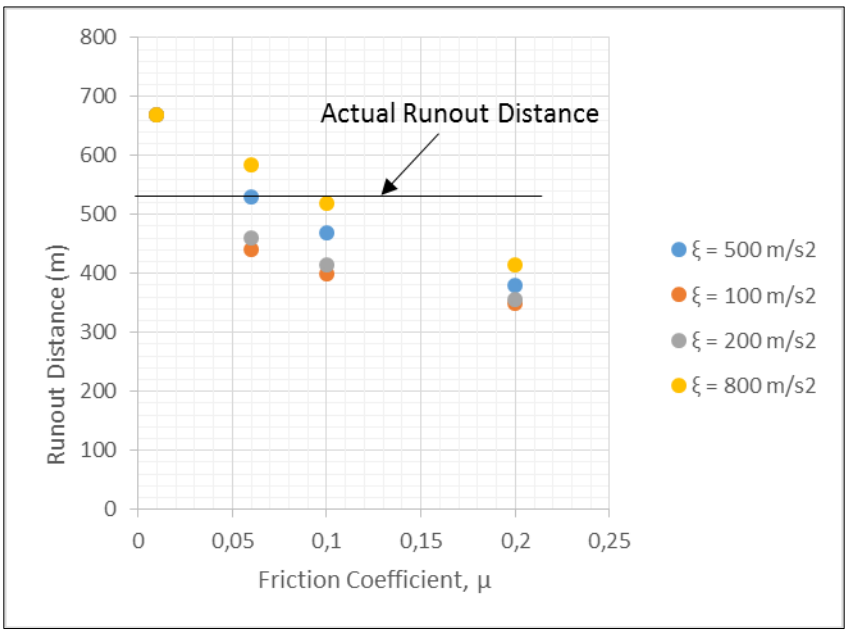

Figure 4-9 Runout distance as a function of friction coefficient, μ for variable ξ

While using the value of friction coefficient μ = 0.01, the debris flow overran the channel beyond the model flow size with runout distance exceeding 670 m (Figure 4-9). Hence only values greater than μ = 0.01 were used for rest of the sensitivity analysis.

Figure 4-10 shows that lesser values of turbulent coefficient, ξ reduced the runout distance. Values of ξ lower than 200 m/s^2 gave low runout distances unless the friction coefficient was decreased to a minimum value of 0.01, in which case different values of turbulent coefficient gave similar results of runout distance. This is because of the low frictional resistance to the flow due to μ = 0.01.

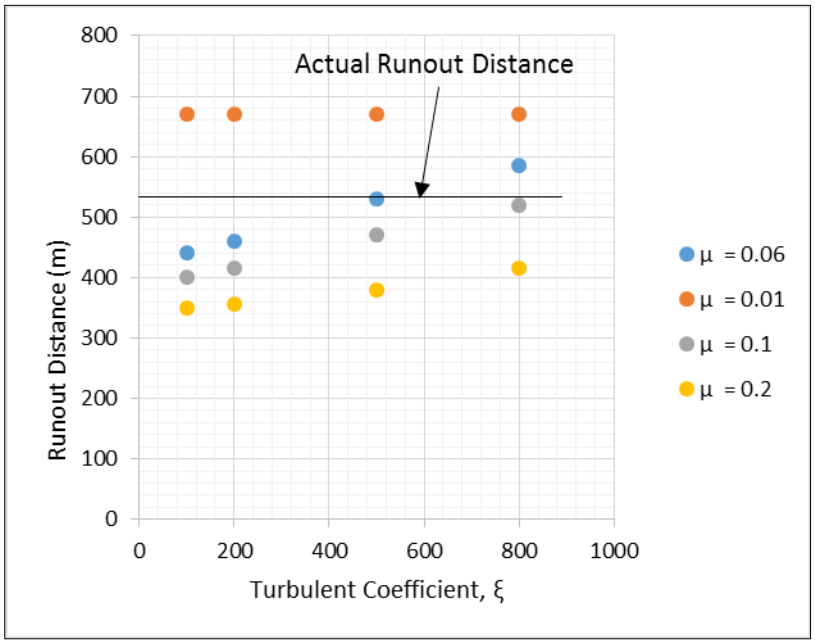

Figure 4-10 Runout distance as a function of turbulent coefficient, ξ for variable μ

In Figure 4-10, for all cases except μ = 0.01, the runout distance was less than the calibrated runout distance of 530 m for ξ < 500 m/s^2. This distance increased when increasing the value of ξ beyond 500 m/s^2.

From Figure 4-9 and Figure 4-10, it is evident that both the friction coefficient, μ and turbulent coefficient, ξ affect the runout distance. Change in values of μ greatly affects the runout distance. On the other hand, the effect of turbulent coefficient is found to be smaller compared to that of the friction coefficient.

In the next section, sensitivity analysis of each of the Voellmy coefficients was performed individually. This makes it clearer to see the dependence of runout distance on either of the friction coefficient and the turbulent coefficient.

4.6.2.1 Sensitivity to the Friction Coefficient μ

The sensitivity analysis performed above shows that increase in the value of friction coefficient decreases the runout distance of the debris flow. This is shown in Figure 4-11 for a single set

of ξ values. When the friction coefficient μ increases, the basal friction of the flow also increases resisting the flow and hence shortening the runout distance. In this part, the friction coefficient was varied between 0.01 and 0.2 keeping the other input parameters constant and using the calibrated value of ξ = 500 m/s^2.

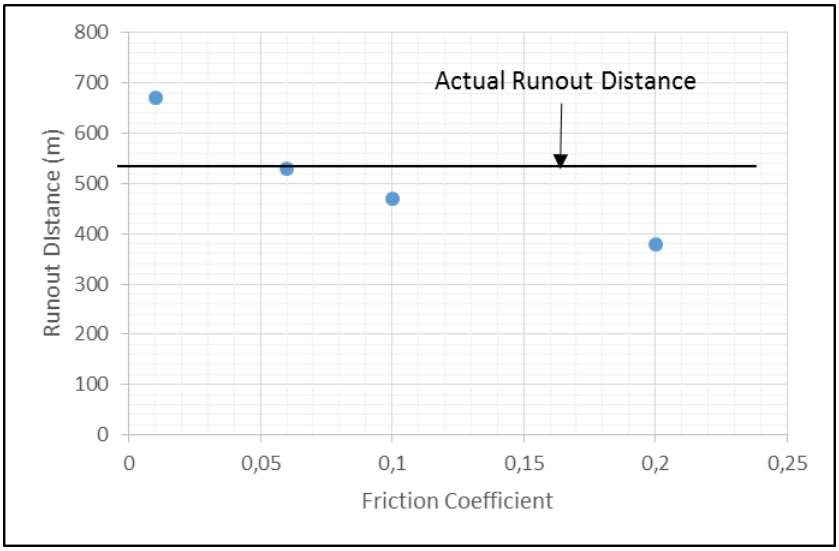

Figure 4-11 Runout distance as a function of friction coefficient, μ for ξ = 500m/s^2

μ with values greater than or equal to 0.2 caused the debris flow to stop before reaching the deposition zone in the laboratory model with runout distance lesser than 400 m. Similarly, when the simulations were performed with the values of μ set to the absolute minimum of 0.01, the debris flow overrode the channel and flowed beyond the defined dimensions of the laboratory model. There was also a huge lateral spread during these simulations confirming to the least resistance against the flow.

4.6.2.2 Sensitivity to the Turbulent Coefficient ξ

The turbulent coefficient has an inverse relationship to the basal friction as given by the Voellmy model law and as the turbulent coefficient increases, the basal friction decreases lengthening the runout distance and vice versa.

To see the effect of turbulent coefficient, additional simulations were performed with ξ = 100 m/s^2, ξ = 200 m/s^2, ξ = 800 m/s^2 for the calibrated value of μ = 0.06. Keeping all the other input parameters constant, the results are plotted below (Figure 4-12). Figure 4-12 shows how the runout distance of the debris flow changes with changing values of the turbulent coefficient.

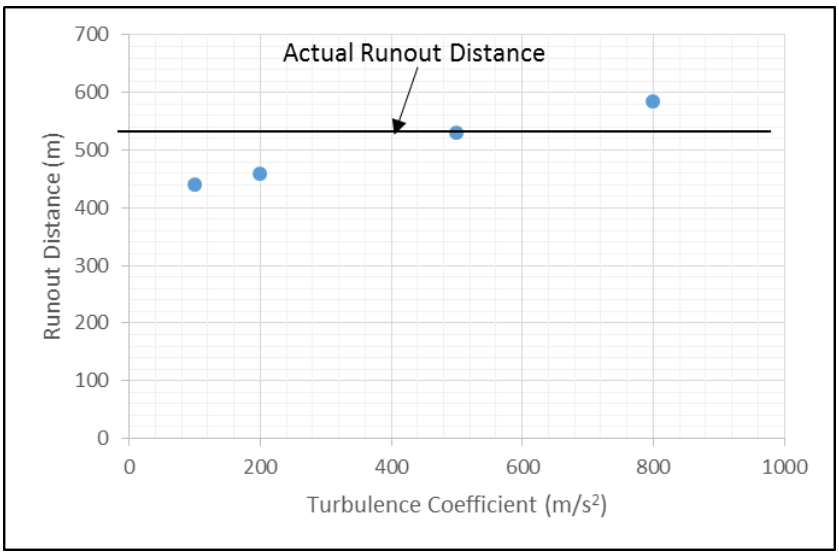

Figure 4-12 Runout distance as a function of turbulent coefficient, ξ for μ = 0.06

For a constant value of μ = 0.06, increase in the runout distance of the flow with increasing ξ values and vice versa can be seen from Figure 4-12. When ξ was increased from its calibrated value of 500 m/s^2, the runout distance increased to about 600 m. Similarly, when decreasing ξ to 100 m/s^2, the runout distance decreased from its calibrated value of 530 m to around 450 m.

4.7 Discussions

Among the three governing rheological parameters of Voellmy Salm model, the value of cohesion was kept zero during all simulations and the effects of remaining two friction parameters were analysed.

The Voellmy Salm model splits the total basal resistance into a velocity independent friction coefficient μ and a velocity dependent turbulent coefficient ξ. These are the two main parameters of the model controlling the flow of the material. The decrease in runout distance of the flow by increasing the friction coefficient and decreasing the turbulent coefficient shows the dependency of the runout distance on the two friction parameters. By increasing the friction coefficient, the frictional resistance provided by the channel bed increases reducing the runout distance. Similarly reduced values of turbulent coefficient result in lower flow velocities stopping the flow at shorter runout distances.

Previous studies have concluded that the runout distance is influenced mostly by the friction coefficient relative to the turbulent coefficient whereas the turbulent coefficient mainly affects the velocity of the flow (Borstad and McClung, 2009). This theory was reaffirmed by this case study where it can be seen that the runout distance of the debris flow was more sensitive to the

friction coefficient compared to the turbulent coefficient. Due to the unavailability of the velocity data, the effects on the velocity was not analysed focusing only on the runout distance of the flow.

As a whole, the Voellmy Salm model employed in RAMMS can be applied to represent debris flows accurately although the calibration of the model is a difficult task as it has been found in this study. Different sets of rheological parameters were chosen to match the model with the calibrated runout distance of the laboratory physical model. Parametric study of the different Voellmy coefficients, μ and ξ in this case should be conducted and these values differ according to different flow conditions. Therefore, one must be careful in selecting a representative value for all cases, as each set of parameters is only a representative of that case. This limits the capability of RAMMS in predicting the rheological parameters of the flow unless the flow conditions are identical to that of a previously calibrated site.

5 Simulation of Almåskroken Debris Flow

5.1 Background

On August 13, 2013, around four o' clock in the afternoon, a debris flow took place in Almåskroken, Midtre Gauldal Municipality in Sør-Trøndelag (Figure 5-1). This blocked the Fv 30 road and damaged a building. Based on field observations, a lot of water flowed on the slopes, both in the channel bed and the side slopes. In the side terrains, water flowed in fast-flowing streams, and came out of the ground at several places. The average slope angle is in excess of 25 degrees with steeper slopes up to around 35 degrees (L'Heureux and Gjelsvik, 2013). Fortunately, no lives were lost due to the accident but there were major damages to the roads and railways line.

Figure 5-1 Overview location of Almåskroken debris flow (Google-Maps, 2016)

The debris flow deposited over new steep slopes and entered a stream at the end. Some parts of the flow accumulated over the intact forest floor on the flatter portion below the initiating landslide. The deposit materials were mainly soil, boulders and trees which the flow had carried on its way down. This mixing of water changed the landslide into a debris flow and the floating of deposit ended up in river Gaula. The debris flow deposits crossed both Fv 30 and the railway track, destroyed a farm on its downward flow to the river as shown in Figure 5-2. The width of the flow was up to about 40-50 m at the road. The debris flow deposits consisted of a mixture of water, soil, stones and trees. (L'Heureux and Gjelsvik, 2013)

Figure 5-2 Almåskroken debris flow towards south-east (Leth-Olsen et al., 2013)

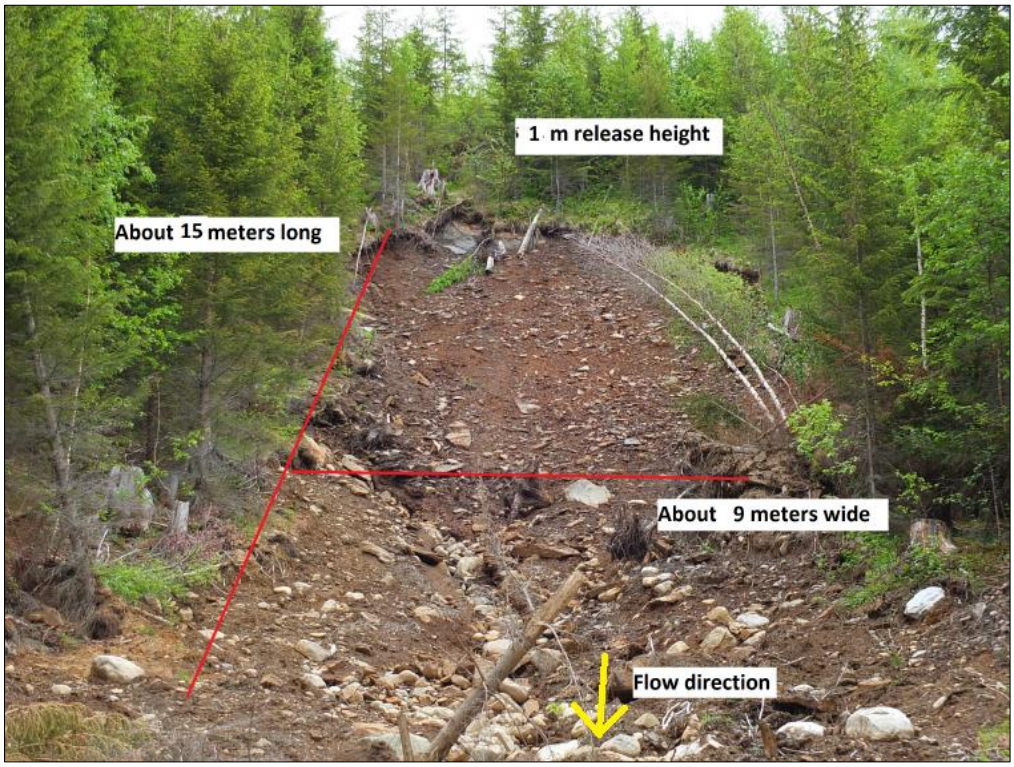

Figure 5-3 Initiation volume of the release area (Frekhaug, 2015)

On the days before the flow, 30 mm of rainfall occurred and a lot of water was observed in the flow path subsequently after the debris flow. The release area has an inclination of about 30 degrees and this inclination decreases just below the release area. As shown in Figure 5-3, the release area has a width of approximately 9 m and a length of 15 m. A constant release height of 1 m is taken throughout the whole release area. These field observations approximate the release volume of the initiating slide as 135 m^3 (Frekhaug, 2015). The flow flattens to around 17 degrees below the release area before it steepens again. The flow channel is about 50 m wide. There is presence of trees and scoured rock along the flow. No evident channel is visible

except for a slight depression. Deposition of the flow sediment started to take place when the slope decreased below 18 degrees and continued into the river. The amount of material deposited in the river is unknown so with a reasonable uncertainty, the total runout distance of the debris flow was approximated 355 m and the final volume of the deposited bed sediments was estimated to be 4000 m^3. (Frekhaug, 2015)

5.2 Application of Input Parameters

A 2-m resolution DEM of the Almåskroken site was provided by Martine Frekhaug with the help of ArcGIS. She had previously used RAMMS to predict the runout distance without the inclusion of entrainment. Additionally, other input parameters are to be defined for the simulation of the flow. As there were no data available on the density and the strength of the material, a suitable value of ρ = 2000 kg/m^3 and Cu = 0 kPa were adopted from different literatures (Bartelt et al., 2013, Pudasaini and Hutter, 2007). The release volume was identified with the help of previous observations carried out in the field (Figure 5-4). A block release of 135 m^3 was selected for the release volume. This was done by selecting an area on the DEM itself which was representative of the debris flow site, followed by appointing a suitable release height (Figure 5-5). The Voellmy friction coefficients were calibrated against the measured runout distance by performing a number of simulations on a trial and error basis.

Figure 5-4 Flow Path, Release Area and Entrainment Path of the Flow (Frekhaug, 2015)

Since there are trees and other vegetation present in the study area, a different set of friction parameters can be defined for those regions based on available literature (Bartelt et al., 2013) . The forest areas were identified from the maps and pictures of the site (Figure 5-6). To account for the influence of forest, the friction parameters were adapted consequently. The friction coefficient, μ was increased by 0.02-0.05 while the turbulent friction, ξ was reduced typically to the values of 400 m/s^2 (Christen et al., 2010a, Feistl et al., 2012).

In addition to above, the automatically defined calculation domain was replaced by a user-defined calculation domain as shown in Figure 5-5. This helps to decrease the simulation time without affecting the results.

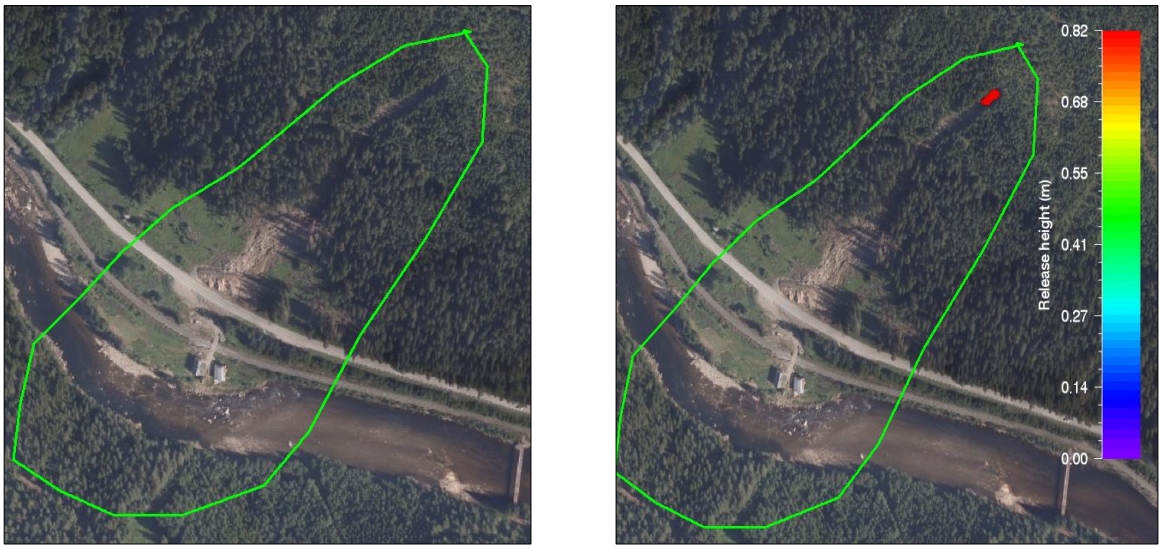

Figure 5-5 User defined Calculation Domain (Left) and Release Area (Right) as defined in RAMMS

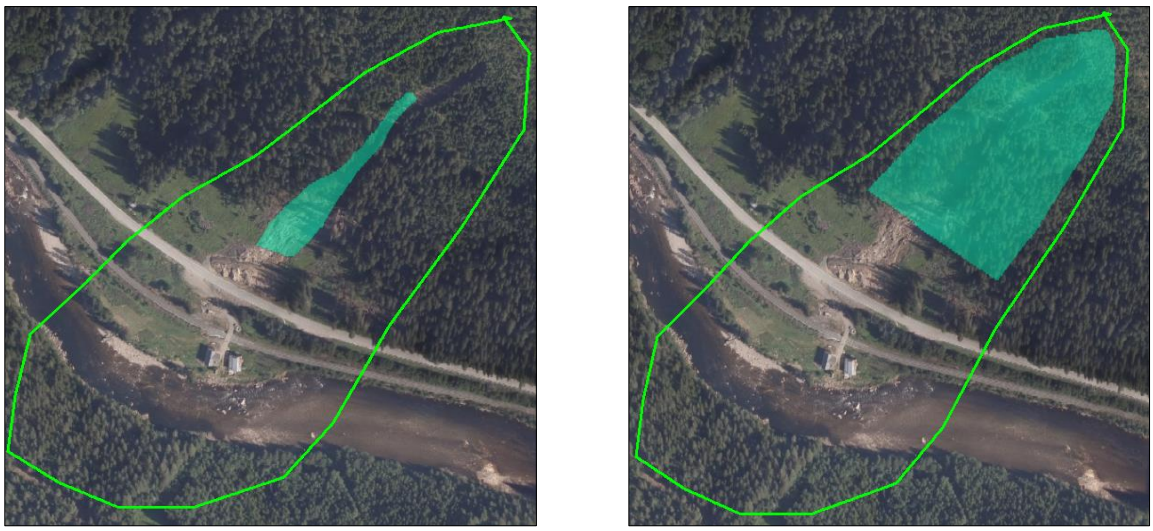

Figure 5-6 Entrainment Path (Left) and Forest Area (Right) as defined in RAMMS

To include the effect of entrainment, RAMMS provides an option of defining three different layers along the terrain bed from which material can be entrained. In this study, a single layer with constant depth and density was selected. The entrainment zone was defined with the help of the flow path and assigning a depth of 1-m and the same density of 2000 kg/m^3 as the rest of the materials as estimated from field observations (Figure 5-6). This entrainment depth of 1 m is the layer depth that has been eroded by the debris flow.

The rest of the parameters were kept constant according to their default values in RAMMS during all the simulations.

5.3 Assessment of Output Results

The runout distance observed in the site is the most convenient output parameter for analysis of the output results as it can be easily measured with accuracy. The observed runout distance for Almåskroken debris flow was estimated around 355 m. Although the debris flow may deposit into several small channels during deposition, the flow distance of the main channel is considered as the runout distance.

To account for entrainment, the deposited volume given by the numerical model can be another convenient parameter in addition to the runout distance, flow velocity and impact pressure. The effect of entrainment can be studied with the help of the final deposited volume of the debris flow, which in this case was estimated to be around 4000 m^3. The calculated deposit volume of the debris flow obtained from the simulation can be compared against the actual debris flow final deposit volume to calibrate the entrainment parameters. Both the runout distance and the deposit volume are reasonable approximations and not exact measurements (Frekhaug, 2015).

5.4 Sensitivity Analysis of the Rheological Parameters

The sensitivity analysis of the Voellmy coefficients for the Almåskroken debris flow was carried out to study their influence on the modelled outputs, mainly the runout distance. The Almåskroken debris flow represents the characteristics of a less channelized, granular and small debris flow so the applicability of the VS model to represent debris flows can be assessed. The sensitivity analysis was performed in the same way as done for the laboratory model, by varying one of the coefficients within a certain change while keeping the other one constant.

5.5 Sensitivity Analysis of the Entrainment Parameters

Similar to the rheological parameters, the sensitivity of the entrainment parameters, the entrainment coefficient K, was carried out keeping the Voellmy coefficients constant. This

helps to study the effect of sediment entrainment on the debris flow. Christen et al. (2010b) has previously studied the effect of entrainment process in RAMMS with K varying in the range of 0-5. Here, the effect of varying entrainment parameters was studied by defining an entrainment zone and varying the entrainment coefficient, K from 0 to 10 (M. Christen, Personal Communication, April 21, 2016). The sensitivity to the entrainment depth can also be checked by assigning an entrainment depth different from 1 m as assigned in this case.

5.6 Results

5.6.1 Model Calibration

Before starting any simulation and analysis in RAMMS, the values of the varying input parameters, μ, ξ and K need to be established. These values are adjusted until the simulation results match with the field observations. Several number of simulations were performed using different set of friction and turbulent coefficients unless their optimal values were obtained. For Almåskroken debris flow, the best-fit Voellmy friction coefficients were $\mu = 0.08$ and $\xi = 500$ m/s^2. An entrainment coefficient K = 5 was selected along with the best fit coefficients. With these parameters, the runout distance of the flow was successfully simulated but RAMMS was not able to simulate the final deposit volume. Hence, the runout distance was used for the calibration of the simulated model and the sensitivity analysis. Separate values for the forested terrain were provided as $\mu = 0.1$ and $\xi = 400$ m/s^2. In this section, the results obtained from the simulation with the calibrated values of $\mu = 0.08$, $\xi = 500$ m/s^2 and K = 5 are presented.

The velocity of the flow varied from 2 m/s to 8 m/s with a mean velocity of 4 m/s. Although there was no available data regarding the velocity of the debris flow, the maximum velocity of debris flows vary between 5-10 m/s (Norem and Sandersen, 2012) which is consistent with the simulated flow velocity. A plot of the maximum flow velocity along the terrain is shown in Figure 5-7. Additionally, a profile can be drawn along the center of the flow to generate line plots.

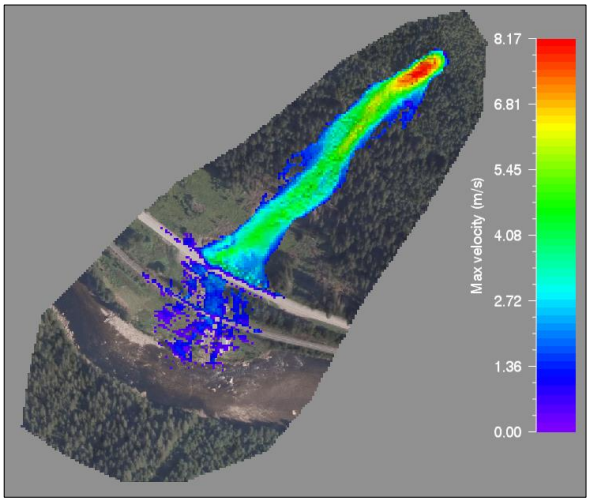

Figure 5-7 Maximum velocity of the flow along the terrain

The next output parameter generated by RAMMS is the flow height or the deposition height. The simulation gave a varied flow height of the deposit with maximum flow height up to 1.16 m at the beginning of the flow. At the deposition area, the flow height reduced to 0.1-0.2 m (Figure 5-8).

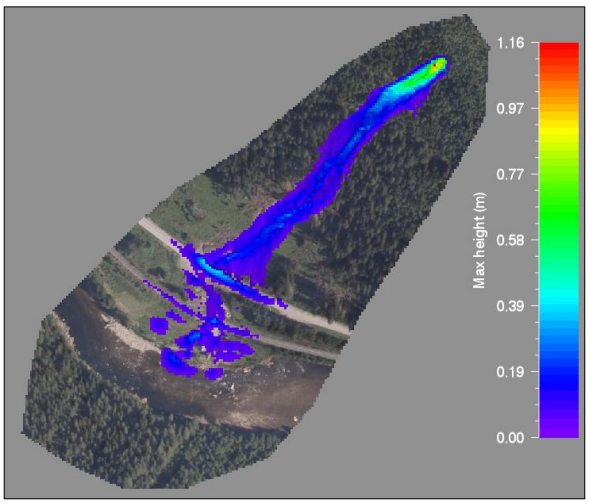

Figure 5-8 Maximum height of the flow along the terrain

RAMMS can also be used to simulate the impact pressure generated by the debris flow as shown in Figure 5-9. This tool can be important especially for the design of structures which might fall in the path of the flow. It can be used to design the mitigating structures for the flow like dams. The simulated flow generated a maximum pressure of 133.5 kPa.

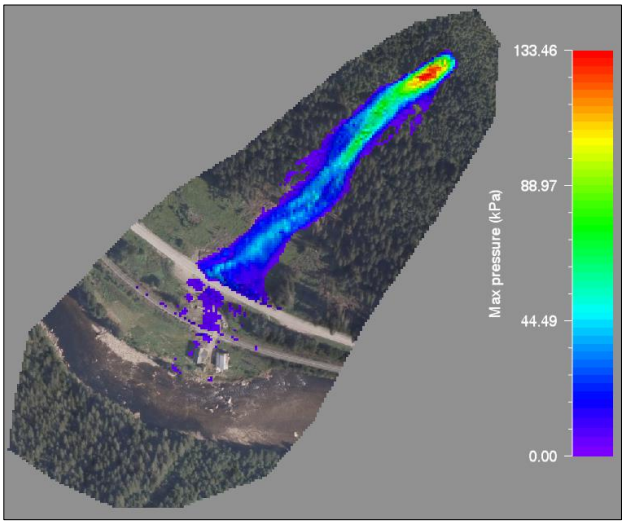

Figure 5-9 Maximum Impact Pressure of the flow

Another important output parameter in RAMMS simulation is the volume of entrained materials caused by the flow. In the field, a release volume of 135 m^3 was calculated and the deposit volume was estimated to be around 4000 m^3. During the simulation, the same release volume of 135 m^3 was selected and the deposit volume was found to be 100.26 m^3 (Figure 5-10). This deposit volume is much lower than the deposit volume observed in the field.

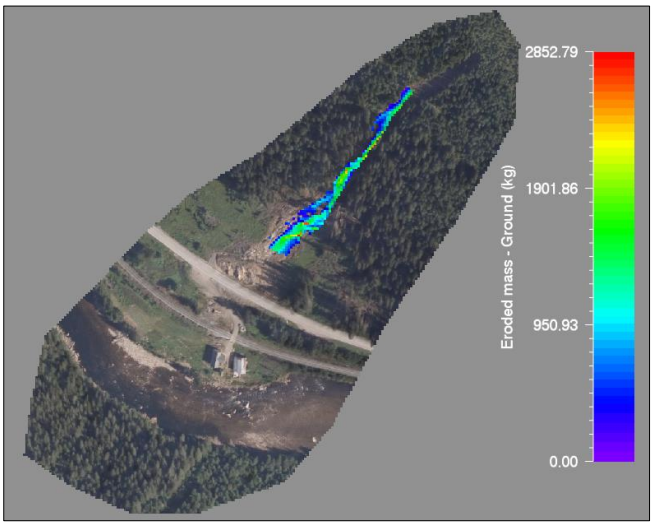

Figure 5-10 Eroded mass by the flow

Figure 5-11 shows the development of the flow along the channel as the simulation takes place. The flow took the path of the entrainment channel, increasing the flow velocity and the flow height in the steeper part. This evolution of the flow is similar to the one which occurred in the field (Figure 5-4) and can be simulated accurately by RAMMS.

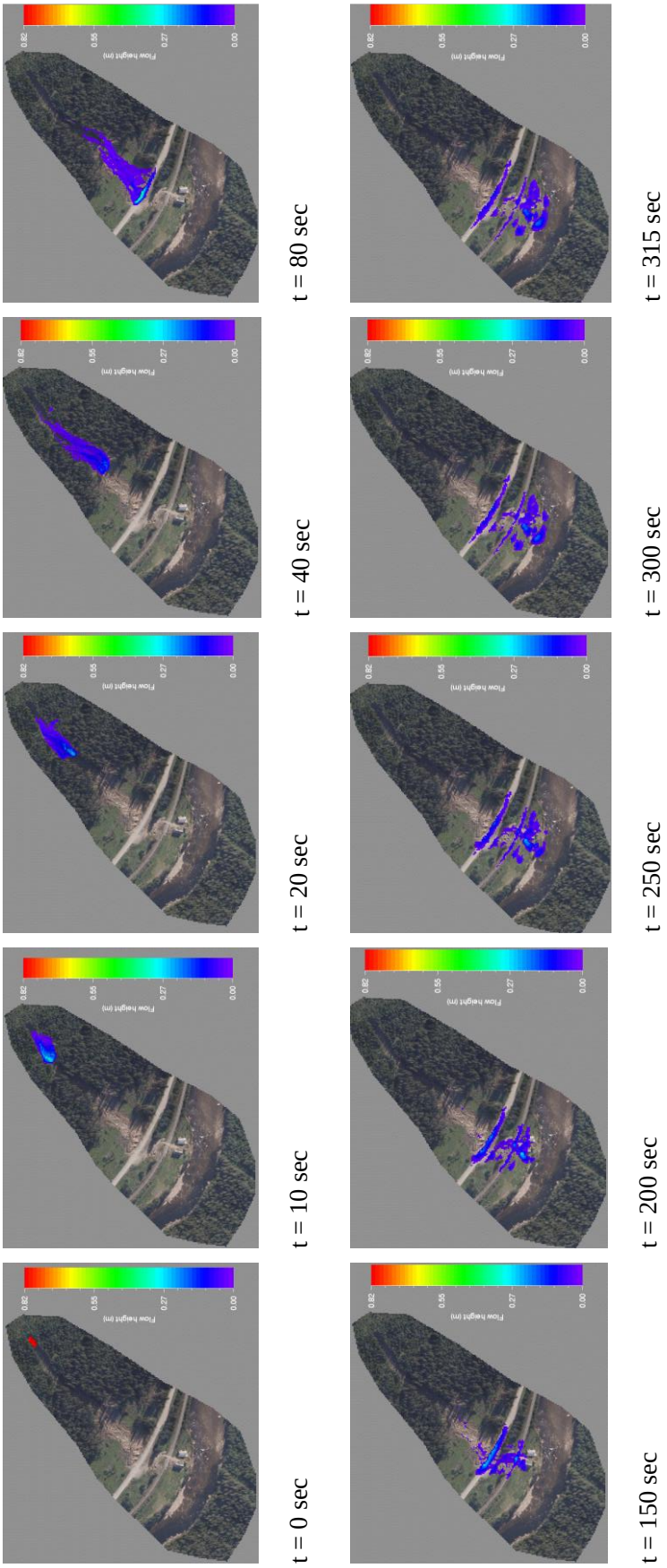

Figure 5-11 Development of the Flow Pattern in RAMMS

The flow pattern simulated above in RAMMS followed the original flow path of the debris event that took place in the Almåskroken. In the beginning, the flow was confined in a narrow path below the release zone where the slope is steeper. As the terrain flattened, the flow spread in lateral direction before it deposited near the road and the railway track. Some parts of the debris flow entered the river towards the end of the simulation (Figure 5-11).

A line can be drawn along the mid-section of the flow which can be used to generate the line plots of the maximum flow height and maximum velocity of the flow along the runout distance. Line plots of other output parameters can also be simulated similarly and it can be animated according to the different time steps of the simulation.

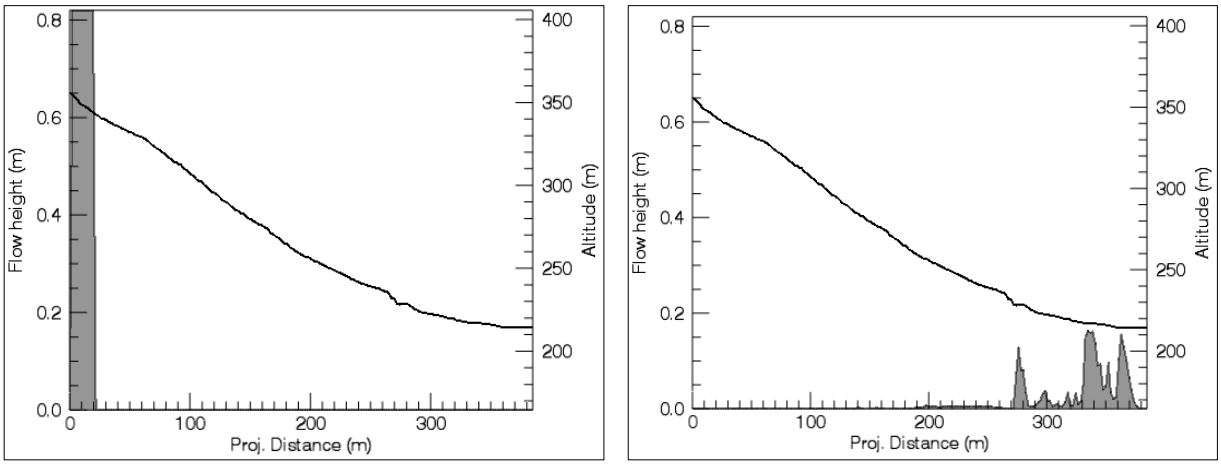

Figure 5-12 Flow Height vs Projected Runout Distance with μ = 0.08 and ξ = 500 m/s²

The above selected input parameters were able to replicate the total runout distance of 355 m of the Almåskroken debris flow successfully as plotted in Figure 5-12. However, a large discrepancy occurred on the amount of deposit volume between the simulated model and the filed observations.

5.6.2 Sensitivity Analysis of the Rheological Parameters

To assess the sensitivity of the results to the input rheological parameters, a number of simulations were made by defining different values of μ and ξ. Instead of carrying out a detailed sensitivity analysis as in the case of physical models, a brief one was carried out here by varying the rheological parameters to their minimum and maximum values. The effect of this change on the simulated runout distance was also determined.

5.6.2.1 Sensitivity to the Friction Coefficient μ

Two different simulations were carried out keeping all the other parameters constant except the friction coefficient, μ. The value of μ was changed to its minimum value, 0.01 and the maximum value used in this study, 0.2. The runout distance using a value of μ = 0.01 was found to be 400 m, an increase of 45 m (Figure 5-13). The flow spread laterally and crossed the entire width of the river due to the low frictional resistance.

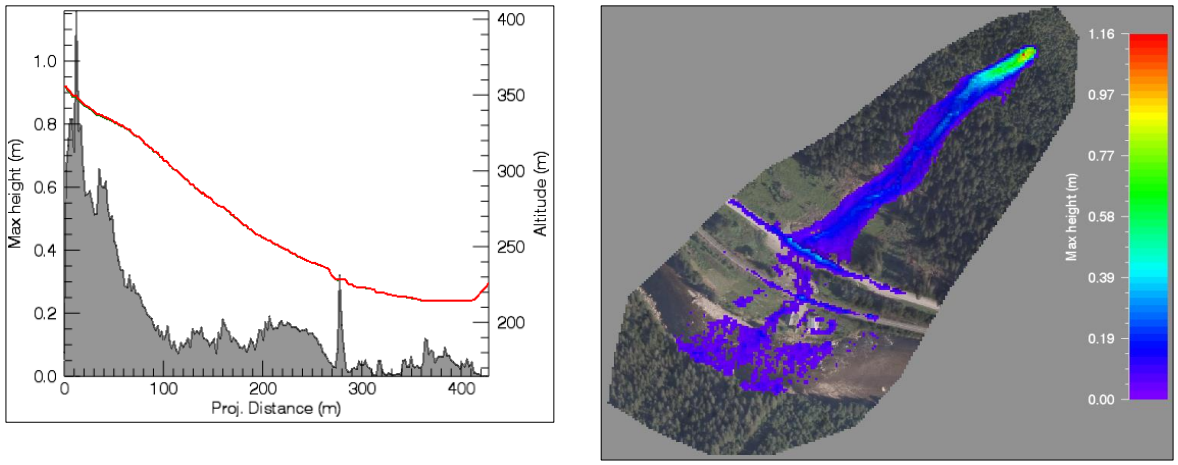

Figure 5-13 A plot of the runout distance using μ = 0.01 and ξ = 500 m/s^2 (Left). Plot of the flow pattern (Right).

When the value of μ was increased to 0.2, the runout distance of the flow changed to 320 m, a decrease of 35 m. The flow had a low mobility in both the longitudinal and the transverse direction and stopped before it started to deposit in the river as shown in Figure 5-14.

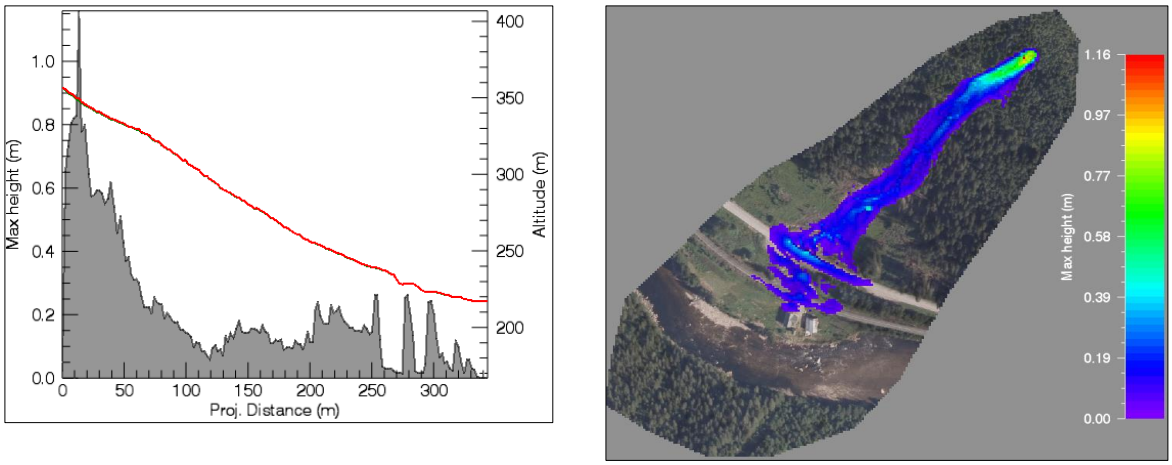

Figure 5-14 A plot of the runout distance using μ = 0.2 and ξ = 500 m/s^2 (Left). Plot of the flow pattern (Right).

5.6.2.2 Sensitivity to the Turbulent Coefficient ξ

Similarly, another two simulations were performed varying the values of the turbulent coefficient keeping all the other input parameters constant. In the first simulation, the value of ξ was changed from 500 to 100 m/s^2 and the runout distance changed to around 360 m, a 5 m increase from the calibrated runout distance. The flow pattern was similar to that of the calibrated simulation (Figure 5-15).

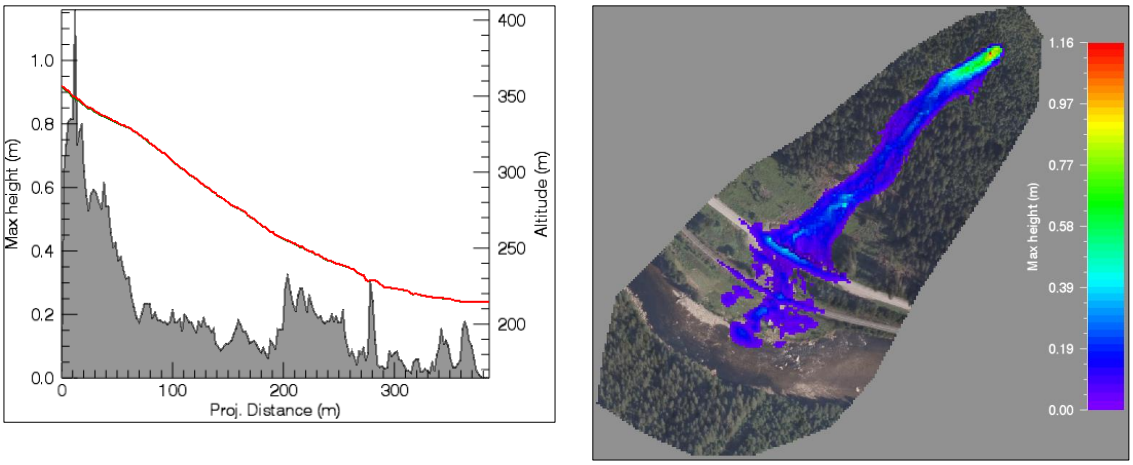

Figure 5-15 A plot of the runout distance using μ = 0.08 and ξ = 100 m/s^2 (Left). Plot of the flow pattern (Right).

A second simulation was carried out by changing the value of ξ from 500 to 800 m/s^2 and this simulation had a similar runout distance to the previous one with ξ = 100 m/s^2 of 360 m, a 5 m increase from the original runout distance of 355 m (Figure 5-16).

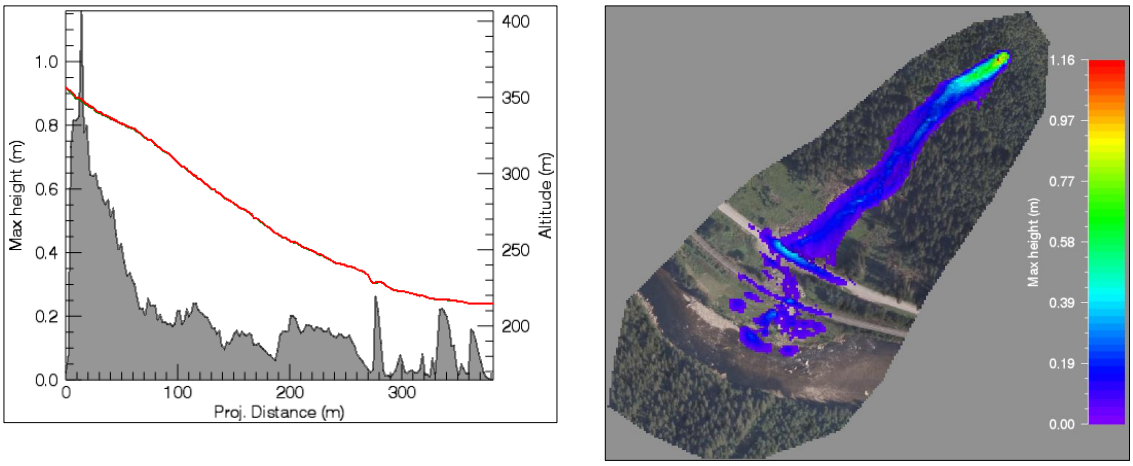

Figure 5-16 A plot of the runout distance using μ = 0.08 and ξ = 800 m/s^2 (Left). Plot of the flow pattern (Right).

In addition to the runout distance, the eroded volume also went through some change but not much compared to the runout distance. The eroded volume changed from 95 m^3 to 125 m^3 when μ and ξ were varied between their extreme values compared to the original eroded volume of approximately 3865 m^3.

5.6.3 Sensitivity Analysis of the Entrainment Parameters

A major feature of RAMMS simulation is to model the entrainment of the erodible materials in the channel bed. This has been enabled in this case by defining an entrainable layer with a fixed density, a fixed depth and an entrainment coefficient K. This coefficient K affects the amount of entrained materials in the flow. The effect on the runout distance and the eroded volume was studied by varying the values of K from 0 to 10.

5.6.3.1 Sensitivity to the Entrainment Coefficient K

The results of the sensitivity analysis of the runout distance of the flow with respect to the entrainment coefficient K are plotted in Figure 5-17. As K was varied between 0 and 10, the runout distance changed from 300 m to 375 m. For K = 0 with no entrainment, the runout distance had the lowest value of 300 m that is 55 m shorter than the original distance. When K = 10, the runout distance increased to 375 m, a 20 m increase from its original value of 355 m.

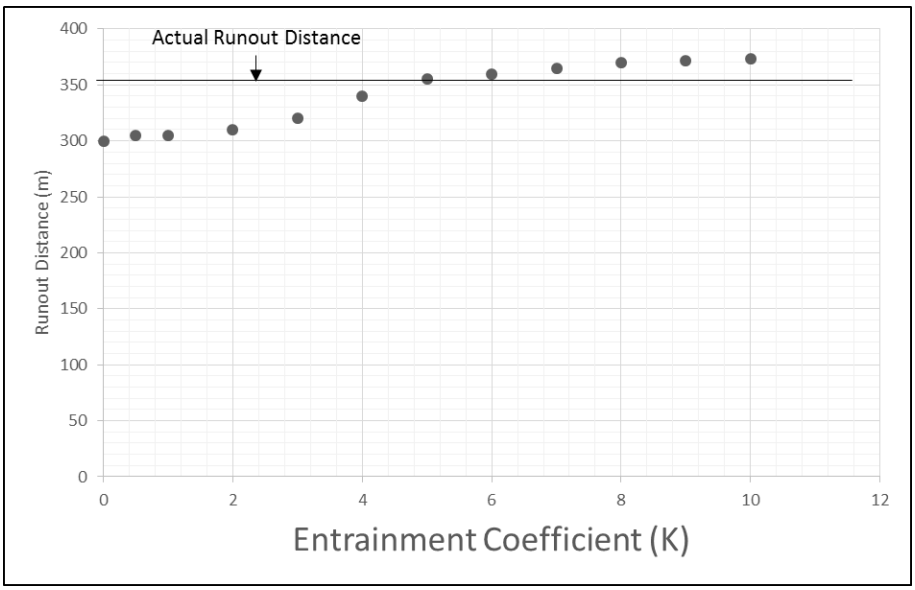

Figure 5-17 Runout distance as a function of entrainment coefficient, K for μ = 0.08 and ξ = 500m /s^2

Figure 5-18 shows the variation of the eroded volume with the entrainment coefficient, K. Although the simulations were not able to replicate successfully the final deposit volume of

4000 m^3, the plot shows that the eroded volume is largely influenced by the entrainment coefficient. Without any entrainment, there was not any eroded volume so the volume of the deposited material was equal to the initiating release volume of 135 m^3. The eroded volume increased to more than 1000 m^3 when the entrainment coefficient was increased to 10.

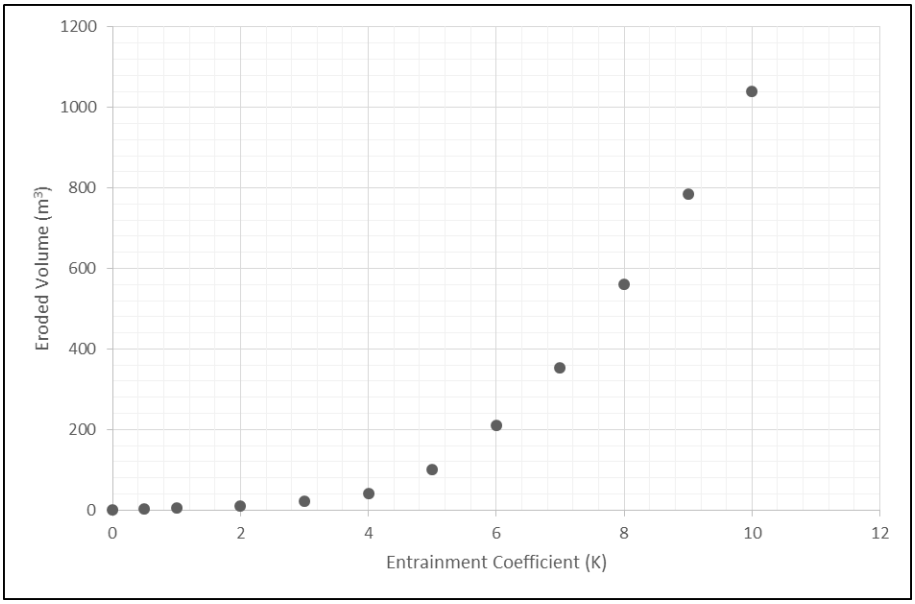

Figure 5-18 Eroded volume as a function of entrainment coefficient, K for μ = 0.08 and ξ = 500m /s²

To check the effect of other entrainment parameters, a separate simulation was carried out with all constant inputs of $\mu = 0.08$, $\xi = 500$ m/s^2, K = 5 and by changing only the entrainment depth from 1 m to 2 m once and then to 0.5 m. Irrespective of the change in the entrainment depth, the amount of the eroded volume stayed constant for entrainment depths of 0.5 m, 1 m and 2 m. The same 100.26 m^3 of material was eroded for $\mu = 0.08$, $\xi = 500$ m/s^2, K = 5 whether the depth of the entrainment zone was changed from 1 m to 2 m or 0.5 m. A possible reason for this might be due to the selection of the velocity driven law in RAMMS for erosion. If the momentum driven law is chosen instead of the velocity driven law, different results might occur because the momentum driven law also considers the mass of the material in addition the velocity of the flow.

5.7 Discussions

RAMMS is able to simulate the numerical modelling of Almåskroken debris flow that took place on August 13, 2013 at Midtre Gauldal in Sør-Trøndelag. The effect of the rheological parameters on the runout distance is similar that of the laboratory model; change in μ affects the runout distance whereas change in the turbulent coefficient affects the velocity of the flow.

Another analysis carried out during the simulation of Almåskroken debris flow was to study the effect of entrainment parameter in addition to the rheological parameters, μ and ξ. Similarly, the effect of varying rheological parameters on the entrainment volume was also observed.

It is evident that the change in the rheological parameters affects the runout distance and other aspects of the flow like the deposit height and the flow velocity. However, it appears that the amount of the eroded volume of entrainment materials does not change a lot due to changing μ and ξ. Sensitivity analysis of the friction coefficients showed that while the runout distance changed from 320 m to 400 m due to the change in the Voellmy friction coefficients, the variation in the eroded volume was less than 30 m^3.

On the other hand, entrainment parameters which in this study is defined by the entrainment coefficient K, plays an important role in determining both the runout distance as well as the volume of eroded materials as shown by the simulations carried out in this study. The eroded volume increased as the value of K was increased from 0 to 10. The runout distance of the flow subsequently increases as more materials are being entrained. The runout distance of the flow changed from 300 m without any entrainment to 375 m by providing K = 10. Similarly, approximately 1040 m^3 of bed materials was being entrained with K = 10 compared to the eroded volume of only 100 m^3 obtained K = 5 keeping constant values of the friction coefficients as μ = 0.08 and ξ = 500 m/s^2. The flow with all of these simulations was never able to produce the final deposit volume of 4000 m^3 as observed in the field. A possible reason for this is the minimal volume of the release area compared to that of the volume of entrainment bed sediments (M. Christen, Personal Communication, April 21, 2016). Previous versions of RAMMS were also more suited to the simulation of debris flows with high release volumes in the order of 10000-100,000 m^3 (Engelke, 2012). Simulations with larger release volume were carried out which resulted in an increase of eroded volume of bed materials but it was not analyzed in detail due to limited time. Secondly, the velocity driven law was selected for erosion law while defining entrainment in the simulation which means that entrainment is proportional to the velocity of the debris flow. For smaller velocities, the entrainment rate and the entrainment volume will be small. Moreover, some studies have shown that correlation of erosion and velocity does not give good results and velocity driven and momentum driven erosion laws do not consider processes like particle fluctuations on a smaller scale which is true in this case of small initiating release volume (Deubelbeiss et al., 2011).

A third option of velocity squared driven law for defining erosion is also available during simulation in RAMMS and upto 3438 m^3 of deposited volume was able to be modelled

choosing this option and a value of K = 5 but this brought about a significant increase in the runout distance of the flow and was not studied further. A possible suggestion would be to carry out a new model calibration from the beginning with a new set of friction coefficient μ, turbulent coefficient ξ and entrainment coefficient K choosing the erosion law of velocity squared driven law instead of the default velocity driven law.

6 Conclusions and Recommendations

6.1 Summary

The main aim of the thesis was to understand the mechanism of entrainment in debris flows and is presented as a literature review followed by back calculation of debris flows. For this purpose, an extended literature study was first conducted to investigate debris flows and the general morphology and physics of debris flows. The entrainment of bed sediments in debris flows was then studied with the help of analytical, physical and numerical approaches. A brief explanation of the analytical and physical approaches to investigate entrainment in the flow was presented. The rest of the study focused on the numerical approaches to debris flow modelling and the inclusion of entrainment in these numerical models.

The dynamic numerical software, RAMMS was used to model the debris flows. A short description of other numerical models, DAN3D, MassMov2D and FLO2D with their principles and governing equations is given prior to discussing in detail the working principle of RAMMS. To give a better understanding of functioning of RAMMS, the governing equations were derived and the erosion laws used for the entrainment model in RAMMS were presented.

For the next part of the thesis, attempts were made to carry out the simulation of a physical model prepared in the laboratory and of a real case debris flow event that took place in Almåskroken, Norway. For the simulation of the physical model, entrainment was not included and a simple calibration of the Voellmy friction coefficients by means of a back calculation was performed with RAMMS. A parametric study of the friction coefficients was conducted and the applicability of the Voellmy Salm model to model the debris flow numerically was assessed. The change in the input rheological parameters especially the friction coefficient, μ was found to affect the flow runout distance. The turbulent coefficient, ξ on the other hand did not influence the runout distance as much as the friction coefficient. RAMMS was successfully able to simulate the runout distance and the flow height of the debris flow represented by the physical model prepared in the laboratory using the values of $\mu = 0.06$ and $\xi = 500$ m/s^2. This leads to the conclusion that with the help of reasonable assumptions and individual calibration of the right input parameters, the Voellmy Salm model in RAMMS can be used to simulate debris flows accurately.

For the back calculation of the Almåskroken debris flow event, the entrainment module was used in RAMMS in an attempt to calibrate the final runout distance and the deposit volume. The runout distance was replicated accurately using the above-mentioned Voellmy Salm

rheological model but the final deposit volume could not be simulated correctly using the default velocity driven erosion law. The velocity squared driven erosion law gave better results for the eroded volume. The input parameters used for the above simulation were $\mu = 0.08$, $\xi = 500$ m/s^2 and K = 5. The effect of the rheological parameters was similar to the case of physical models. The entrainment coefficient, K played an important role in the volume of eroded materials.

The results from these simulations indicated that different set of parameters are suitable for different flow conditions and separate calibrations should be carried out for each debris flows. Thus, it is difficult to use RAMMS for the exact prediction of the output parameters like the runout distance, flow velocity as parameters used for one debris flow might not be suitable for another. However, a range of 0.05-0.2 for the friction coefficient, μ and 150 m/s^2 to 600 m/s^2 for the turbulent coefficient, ξ seems appropriate for the Voellmy friction coefficients as tested in this study for debris flows. The appropriate range for the entrainment coefficient K is harder to fix due to the difficulty in replicating the deposit volume as was found in this study.

6.2 Conclusions

As summarized, entrainment determines the final volume of the debris flows. Different researchers have previously tried to analyze the process of entrainment. Due to the limited knowledge of the physical processes involved in the phenomenon, most of the numerical models include entrainment in a very simplified manner through the help of calibration or through user defined erosion rates. In the case of RAMMS, it employs a rate controlled history dependent approach for entrainment governed by an entrainment coefficient, K.

RAMMS has a very well designed and easy to use graphical interface. It can work independently without the use of other software. Besides, there is no need to create and import files from a different program. The option of superimposing aerial photographs and topographic maps over the DEM makes the simulation and the output results look more realistic. The time required to finish the simulation of the model is quick in the order of a few minutes.

The output results of RAMMS are well visualized and sophisticated. Different output parameters, for instance the flow height and the flow velocity can be simulated and analysed separately. The simulation can be stopped and viewed with the help of the time step slider at the bottom of the user interface. GIF animations can be created of a particular time step or of

the entire simulated flow. Furthermore, the results of the simulation can be exported as ESRI files.

One of the most important feature of RAMMS is its ability to model entrainment in the debris flow through different erosion laws. Since entrainment plays a major role in the final deposit volume and the destruction caused by the debris flow and the risk it possesses, inclusion of entrainment in the simulation gives a more realistic prediction of the runout distances and the flow heights and flow velocities. Not a lot of numerical models include entrainment in the flow so RAMMS has an added advantage. Although the simulation of the Almåskroken debris flow was not able to replicate the final erosion volume successfully, some amount of entrainment still occurred in the flow.

In conclusion, whilst RAMMS can be an appropriate tool to back calculate simple debris flows with insignificant entrainment; more research needs to be done to study the effect of entrainment on the flow and implement it in the simulation of the flow. Back-calculation of flows where entrainment played a huge factor with other numerical models or through empirical methods and comparison with the results obtained from RAMMS can prove to be a good check to assess the entrainment module in RAMMS.

6.3 Limitations

During the course of this thesis, there were some limitations. Some are regarding the scarcity of data but most of these limitations are of the software, RAMMS.

1. Only one rheological model, the Voellmy Salm model is included in RAMMS. There is no choice for selection of other rheological models unlike other numerical software.
2. RAMMS does not account for the effect of pore water pressure.
3. The simulation results are dependent on the resolution of the DEM.
4. Erosion is simulated only in the channel bed and not on the side slopes. This makes it inconvenient to run a simulation in the case of channelized flow where erosion might occur not only on the channel bed but also on the walls of the channel.
5. Entrainment is defined in an empirical way with the help of entrainment coefficient, K and it is difficult to calibrate this parameter.

6.4 Further Work

To overcome the limitations specified above, some recommendations are provided below on which further work can be done.

1. As RAMMS has been found to be more suitable for debris flow which are initiated by high release volume in the order of 10000-100000 m^3, simulation of debris flows with larger initiating release volume may give good erosion results.
2. For better entrainment results, simulation with other erosion laws, especially the velocity squared driven law for entrainment can be carried out.
3. Further study on the entrainment process in RAMMS possibly by conducting physical modelling of debris flows including entrainment in the laboratory is recommended.
4. Modelling of a debris flow and its interaction with pre-existing or newly planned mitigation structures can be useful for risk and hazard assessment.
5. Simulation with other numerical models for debris flow modelling and comparison with the results from RAMMS is another way to assess its suitability for dynamic modelling.

BIBLIOGRAPHY

AYOTTE, D. & HUNGR, O. Calibration of a runout prediction model for debris-flows and avalanches. Proceedings of the 2nd International Conference on Debris-Flow Hazards Mitigation: Mechanics, Prediction, and Assessment, Taipei, Taiwan. Edited by GF Wieczorek and ND Naeser. AA Balkema, Rotterdam, 2000. 505-514.

BAGNOLD, R. 1966. An approach to the sediment transport problem. *General Physics Geological Survey, Prof. paper*.

BARBOLINI, M., BIANCARDI, A., CAPPABIANCA, F., NATALE, L. & PAGLIARDI, M. 2005. Laboratory study of erosion processes in snow avalanches. *Cold Regions Science and Technology,* 43**,** 1-9.

BARTELT, P., BUEHLER, Y., CHRISTEN, M., DEUBELBEISS, Y., GRAF, C., MCARDELL, B., SALZ, M. & SCHNEIDER, M. 2013. A numerical model for debris flows in research and practice- User Manual v1.5 Debris Flow.

BARTELT, P. & BUSER, O. 2010. Frictional relaxation in avalanches. *Annals of Glaciology,* 51**,** 98-104.

BEGUERÍA, S., VAN ASCH, T. W., MALET, J. & GRÖNDAHL, S. 2009a. A GIS-based numerical model for simulating the kinematics of mud and debris flows over complex terrain.

BEGUERÍA, S., VAN HEES, M. J. & GEERTSEMA, M. 2009b. Comparison of three landslide runout models on the Turnoff Creek rock avalanche, British Columbia. *Landslide processes: from geomorphology mapping to dynamic modelling. CERG Editions, Strasbourg***,** 243-247.

BERGER, C., MCARDELL, B. W., FRITSCHI, B. & SCHLUNEGGER, F. 2010. A novel method for measuring the timing of bed erosion during debris flows and floods. *Water resources research,* 46.

BIANCO, G. & FRANZI, L. 2000. Estimation of debris flow volumes from storm events.

BLANC, T., PASTOR, M., DREMPETIC, M. S. V. & HADDAD, B. 2011. Depth integrated modelling of fast landslide propagation. *European Journal of Environmental and Civil Engineering,* 15**,** 51-72.

BORSTAD, C. P. & MCCLUNG, D. 2009. Sensitivity analyses in snow avalanche dynamics modeling and implications when modeling extreme events. *Canadian Geotechnical Journal,* 46**,** 1024-1033.

BOVIS, M. J. & JAKOB, M. 1999. The role of debris supply conditions in predicting debris flow activity. *Earth surface processes and landforms,* 24**,** 1039-1054.

BRUNSDEN, D. 1999. Some geomorphological considerations for the future development of landslide models. *Geomorphology,* 30**,** 13-24.

CANNON, S. H., KIRKHAM, R. M. & PARISE, M. 2001. Wildfire-related debris-flow initiation processes, Storm King Mountain, Colorado. *Geomorphology,* 39**,** 171-188.

CESCA, M. & D'AGOSTINO, V. Comparison between FLO-2D and RAMMS in debris flow Modeling: a case study in the Dolomites. International Conference on Monitoring simulation, prevention and remediation of Dense and Debris flow II, 2006. 161-168.

CHEN, H. & LEE, C. 2000. Numerical simulation of debris flows. *Canadian Geotechnical Journal,* 37**,** 146-160.

CHEN, H. & LEE, C. 2003. A dynamic model for rainfall-induced landslides on natural slopes. *Geomorphology,* 51**,** 269-288.

CHEN, H. & LEE, C. 2004. Geohazards of slope mass movement and its prevention in Hong Kong. *Engineering Geology,* 76**,** 3-25.

CHRISTEN, M., BARTELT, P. & KOWALSKI, J. 2010a. Back calculation of the In den Arelen avalanche with RAMMS: interpretation of model results. *Annals of Glaciology,* 51**,** 161-168.

CHRISTEN, M., BARTELT, P., KOWALSKI, J. & STOFFEL, L. Calculation of dense snow avalanches in three-dimensional terrain with the numerical simulation program RAMMS. Proceedings Whistler 2008 International Snow Science Workshop September 21-27, 2008, 2008. 709.

CHRISTEN, M., KOWALSKI, J. & BARTELT, P. 2010b. RAMMS: Numerical simulation of dense snow avalanches in three-dimensional terrain. *Cold Regions Science and Technology,* 63**,** 1-14.

COE, J. A., KINNER, D. A. & GODT, J. W. 2008. Initiation conditions for debris flows generated by runoff at Chalk Cliffs, central Colorado. *Geomorphology,* 96**,** 270-297.

COSTA, J. E. 1988. Rheologic, geomorphic, and sedimentologic differentiation of water floods, hyperconcentrated flows, and debris flows. *Flood Geomorphology. John Wiley & Sons New York. 1988. p 113-122. 5 fig, 2 tab, 54 ref.*

CRUDEN, D. M. & VARNES, D. J. 1996. Landslides: investigation and mitigation. Chapter 3-Landslide types and processes. *Transportation research board special report*.

DAI, F., LEE, C. & NGAI, Y. Y. 2002. Landslide risk assessment and management: an overview. *Engineering geology,* 64**,** 65-87.

DEUBELBEISS, Y., MCARDELL, B. & GRAF, C. Dynamic Modelling of Erosion and Deposition Processes in Debris Flows With Application to Real Debris Flow Events in Switzerland. AGU Fall Meeting Abstracts, 2011. 0813.

DI SANTOLO, A. S. & EVANGELISTA, A. 2009. Some observations on the prediction of the dynamic parameters of debris flows in pyroclastic deposits in the Campania region of Italy. *Natural hazards,* 50**,** 605-622.

EASTERBROOK, D. J. 1999. *Surface processes and landforms*, Pearson College Division.

EGLIT, M. & DEMIDOV, K. 2005. Mathematical modeling of snow entrainment in avalanche motion. *Cold Regions Science and Technology,* 43**,** 10-23.

ENGELKE, C. 2012. Empirical and dynamical modeling of debris flow events close to Longyearbyen and Svea, Svalbard.

FANNIN, J. & BOWMAN, E. 2007. Debris flows-entrainment, deposition and travel distance.

FEISTL, T., BEBI, P., BÜHLER, Y., CHRISTEN, M., TEICH, M. & BARTELT, P. Stopping behavior of snow avalanches in forests. Proceedings of the International Snow Science Workshop ISSW. Anchorage, Alaska, 2012. 420-426.

FRANZI, L. & BIANCO, G. 2001. A statistical method to predict debris flow deposited volumes on a debris fan. *Physics and Chemistry of the Earth, Part C: Solar, Terrestrial & Planetary Science,* 26**,** 683-688.

FREKHAUG, M. H. 2015. An assessment of prediction tools to Norwegian debris flows.

GARCÍA-MARTÍNEZ, R. & LÓPEZ, J. L. 2005. Debris flows of December 1999 in Venezuela. *Debris-flow Hazards and Related Phenomena.* Springer.

GLADE, T. 2005. Linking debris-flow hazard assessments with geomorphology. *Geomorphology,* 66**,** 189-213.

GODT, J. W. & COE, J. A. 2007. Alpine debris flows triggered by a 28 July 1999 thunderstorm in the central Front Range, Colorado. *Geomorphology,* 84**,** 80-97.

GOOGLE-MAPS 2016. maps.google.com.

HÅLAND, G. 2012. Skred og skredsikring. I J. *Aurstad, Ø. Larsen, G. Refsdal, G. Berntsen, I. Hoff, & B. O. Lerfald, Lærebok, Drift og vedlikehold av veger*.

HILLER, P. & JENSSEN, I. 2009. Modellforsøk med flomskred mot bruer. Trondheim: Institutt for vann- og miljøteknikk, NTNU.

HUNGR, O. 1995. A model for the runout analysis of rapid flow slides, debris flows, and avalanches. *Canadian Geotechnical Journal,* 32**,** 610-623.

HUNGR, O. & EVANS, S. Rock avalanche runout prediction using a dynamic model. Proceedings of the 7th International Symposium on Landslides, Trondheim, Norway, 1996. 21.

HUNGR, O., EVANS, S., BOVIS, M. & HUTCHINSON, J. 2001. A review of the classification of landslides of the flow type. *Environmental & Engineering Geoscience,* 7**,** 221-238.

HUNGR, O. & JAKOB, D. M. 2005. *Debris-flow hazards and related phenomena*, Springer.

HUNGR, O., MCDOUGALL, S. & BOVIS, M. 2005. Entrainment of material by debris flows. *Debris-flow hazards and related phenomena.* Springer.

HUSSIN, H. Y. 2011. *Probabilistic run-out modeling of a debris flow in Barcelonnette, France.* M. Sc. thesis, Faculty of Geo-Information Science and Earth Observation (ITC), University of Twente, Enschede, Netherlands, 94 pp.

HUTCHINSON, J. 1986. A sliding-consolidation model for flow slides. *Canadian Geotechnical Journal,* 23**,** 115-126.

HUTCHINSON, J. & BHANDARI, R. 1971. Undrained loading, a fundamental mechanism of mudflows and other mass movements. *Geotechnique,* 21**,** 353-358.

IVERSON, R. M. 1997. The physics of debris flows. *Reviews of geophysics,* 35**,** 245-296.

IVERSON, R. M. 2005. Debris-flow mechanics. *Debris-flow hazards and related phenomena.* Springer.

IVERSON, R. M. 2012. Elementary theory of bed-sediment entrainment by debris flows and avalanches. *Journal of Geophysical Research: Earth Surface,* 117.

IVERSON, R. M. 2014. Debris flows: behaviour and hazard assessment. *Geology Today,* 30**,** 15-20.

IVERSON, R. M., SCHILLING, S. P. & VALLANCE, J. W. 1998. Objective delineation of lahar-inundation hazard zones. *Geological Society of America Bulletin,* 110**,** 972-984.

JAEDICKE, C., LIED, K. & KRONHOLM, K. 2009. Integrated database for rapid mass movements in Norway. *Natural Hazards and Earth System Science,* 9**,** 469-479.

JOHNSON, A. M. 1970. *Physical processes in geology: A method for interpretation of natural phenomena; intrusions in igneous rocks, fractures, and folds, flow of debris and ice*, Freeman, Cooper.

KING, J. 1996. Tsing Shan debris flow. *Special Project Report SPR,* 6**,** 133.

L'HEUREUX, J.-S. & GJELSVIK, V. 2013. Flomskred ved Almåskroken: Befaring og vurdering av skredområdet

LAACHE, E. 2016. Masters Thesis, NTNU (In Progress).

LETH-OLSEN, L., JUUL BURAN, B. & KJELLMARK, O. J. 2013. 'Vet ikke om togsporet er skadd'. Available at: http://www.adressa.no/nyheter/sortrondelag/article8098415.ece (Accessed: 10.05.2016).

LUNA, B. Q. 2007. Assessment and modelling of two lahars caused by" Hurricane Stan" at Atitlan, Guatemala, October 2005.

LUNA, B. Q., VAN WESTEN, C., JETTEN, V., CEPEDA, J., STUMPF, A., MALET, J., MEDINA-CETINA, Z. & VAN ASCH, T. A preliminary compilation of calibrated rheological parameters used in dynamic simulations of landslide run-out. Mountain risks: bringing science to society. Proceedings of the Mountain Risks International Conference. Firenze, Italy: CERG Strasbourg, 2010. 255-260.

MCDOUGALL, S. 2006. *A new continuum dynamic model for the analysis of extremely rapid landslide motion across complex 3D terrain.* University of British Columbia.

MCDOUGALL, S. & HUNGR, O. 2004. A model for the analysis of rapid landslide motion across three-dimensional terrain. *Canadian Geotechnical Journal,* 41**,** 1084-1097.

MIZUYAMA, T., KOBASHI, S. & OU, G. Prediction of debris flow peak discharge. Proceedings of the International Symposium Interpraevent, Bern, Switzerland, 1992. 99-108.

MORGENSTERN, N. & SANGREY, D. A. 1978. Methods of stability analysis. *Transportation Research Board Special Report*.

NETTLETON, I., MARTIN, S., HENCHER, S. & MOORE, R. 2005. 4 DEBRIS FLOW TYPES AND MECHANISMS.

NOREM, H. & SANDERSEN, F. 2012. Flom-og sørpeskred. *Project report" Klima og Transport", SVV report, Oslo,* 73.

O'BRIEN, J., JULIEN, P. & FULLERTON, W. 1993. Two-dimensional water flood and mudflow simulation. *Journal of hydraulic engineering,* 119**,** 244-261.

PAPA, M., EGASHIRA, S. & ITOH, T. 2004. Critical conditions of bed sediment entrainment due to debris flow. *Natural Hazards and Earth System Science,* 4**,** 469-474.

PUDASAINI, S. P. & HUTTER, K. 2007. *Avalanche dynamics: dynamics of rapid flows of dense granular avalanches*, Springer Science & Business Media.

QUAN, L. 2012. Dynamic numerical run-out modeling for quantitative landslide risk assessment. *Thesis of University of Twente, ITC,* 206**,** 1-237.

REID, M. E., IVERSON, R. M., LOGAN, M., LAHUSEN, R. G., GODT, J. W. & GRISWOLD, J. P. 2011. Entrainment of bed sediment by debris flows: Results from large-scale experiments. *Debris-flow Hazards Mitigation, Mechanics, Prediction, and Assessment***,** 367-374.

RICKENMANN, D. 1999. Empirical relationships for debris flows. *Natural hazards,* 19**,** 47-77.

RICKENMANN, D. 2005. Runout prediction methods. *Debris-flow hazards and related phenomena.* Springer.

RICKENMANN, D., LAIGLE, D., MCARDELL, B. & HÜBL, J. 2006. Comparison of 2D debris-flow simulation models with field events. *Computational Geosciences,* 10**,** 241-264.

RICKENMANN, D., WEBER, D. & STEPANOV, B. 2003. Erosion by debris flows in field and laboratory experiments. *Debris-flow hazards mitigation: mechanics, prediction, and assessment***,** 883-894.

SALM, B. 1993. Flow, flow transition and runout distances of flowing avalanches. *Annals of Glaciology,* 18**,** 221-221.

SALM, B., GUBLER, H. U. & BURKARD, A. 1990. *Berechnung von Fliesslawinen: eine Anleitung für Praktiker mit Beispielen*, Eidgenössisches Institut für Schnee-und Lawinenforschung, Weissfluhjoch/Davos.

SASSA, K. The mechanism of debris flows. Proc. of 11th Int. Conf. on SMFE, 1985. 1173-1176.

SAVAGE, S. B. & HUTTER, K. 1989. The motion of a finite mass of granular material down a rough incline. *Journal of fluid mechanics,* 199**,** 177-215.

SCHILLING, S. P. & IVERSON, R. M. Automated, reproducible delineation of zones at risk from inundation by large volcanic debris flows. Proceedings of the 1997 1st International Conference on Debris-Flow Hazards Mitigation: Mechanics, Prediction, and Assessment, 1997. 176-186.

SCHOWALTER, W. R. 1978. *Mechanics of non-Newtonian fluids*, Pergamon press Oxford.

SCHRAML, K., THOMSCHITZ, B., MCARDELL, B., GRAF, C. & KAITNA, R. 2015. Modeling debris-flow runout patterns on two alpine fans with different dynamic simulation models. *Natural Hazards and Earth System Sciences Discussions,* 3**,** 1397-1425.

SOVILLA, B., BURLANDO, P. & BARTELT, P. 2006. Field experiments and numerical modeling of mass entrainment in snow avalanches. *Journal of Geophysical Research: Earth Surface,* 111.

STINY, J. 1910. Die Muren [Debris flows]. *Wagnerschen Univ., Buchhandlung, Innsbruck, Austria.[English translation, EBA Consult., Vancouver, Canada, 1997.]*.

TAKAHASHI, T. 1978. Mechanical characteristics of debris flow. *Journal of the Hydraulics Division,* 104**,** 1153-1169.

TAKAHASHI, T. 2014. *Debris flow: mechanics, prediction and countermeasures*, CRC press.

THAKUR, V., NIGUSSIE, D. & DEGAGO, S. 2014. A preliminary study of rheological models for run-out distance modelling of sensitive clay debris. *Numerical Methods in Geotechnical Engineering,* 1**,** 115.

VAN WESTEN, C. 2009. Multi-hazard risk assessment. *Distance education course Guide book. Bangkok, United Nations University-ITC*.

VARNES, D. J. 1978. Slope movement types and processes. *Transportation Research Board Special Report*.

VOELLMY, A. 1955. Uber die Zerstorungskraft von Lawinen. Schweiz. Bauzeitung, Jahrg. 73, S. 159-165, 212-217, 246-249, 280-285. *English as: On the destructive force of avalanches. 63p. Alta Avalanche Study Center, Transl,* 2**,** 1964.

WANG, G., SASSA, K. & FUKUOKA, H. 2003. Downslope volume enlargement of a debris slide–debris flow in the 1999 Hiroshima, Japan, rainstorm. *Engineering geology,* 69**,** 309-330.

YANG, M. 2016. Masters Thesis, NTNU (In Progress).

YIFRU, A. L. 2014. Assessment of Rheological Models for Run-out Distance Modeling of Sensitive Clay Slides, Focusing on Voellmy Rheology.

Appendix A

Sample Grid data used for DEM in RAMMS-2D Debris Flow

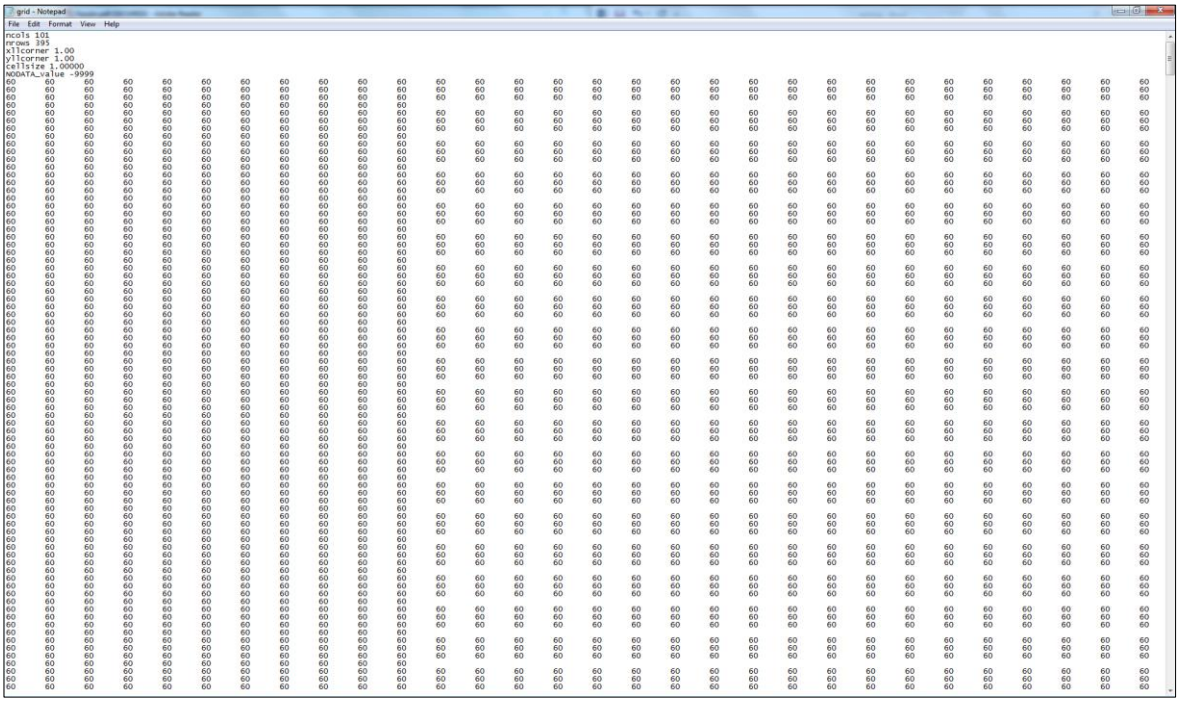

Appendix B

A detailed explanation on the simulation procedure of RAMMS:

1. Before starting the simulation in RAMMS, general preference should be set up for directories which will contain all the files for the DEM along with the aerial photos and topographic maps. This makes the whole simulation process convenient during the model run.

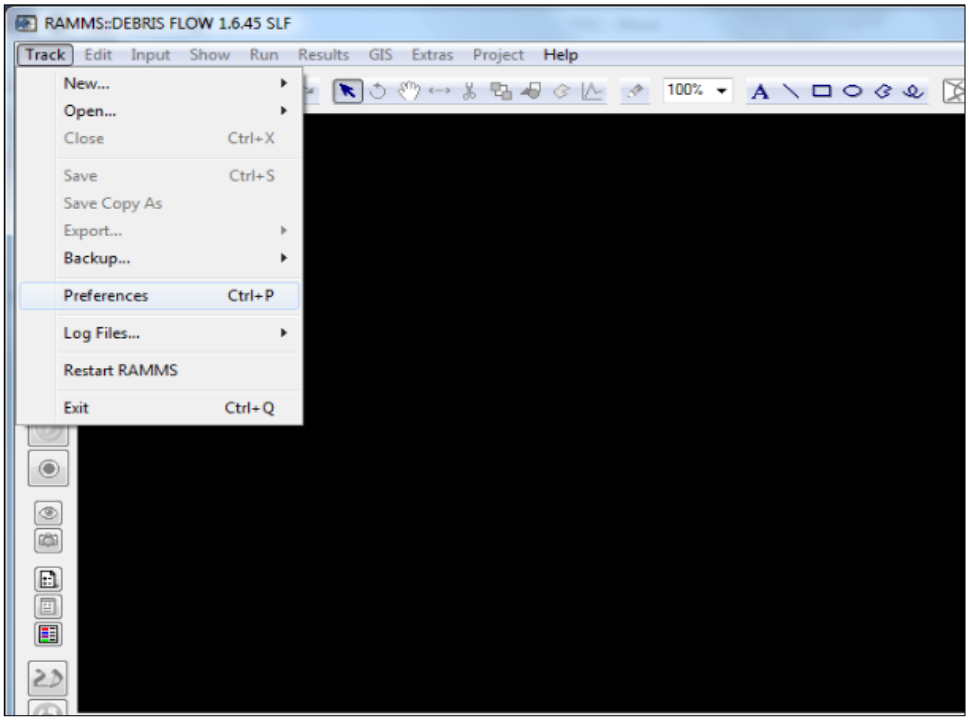

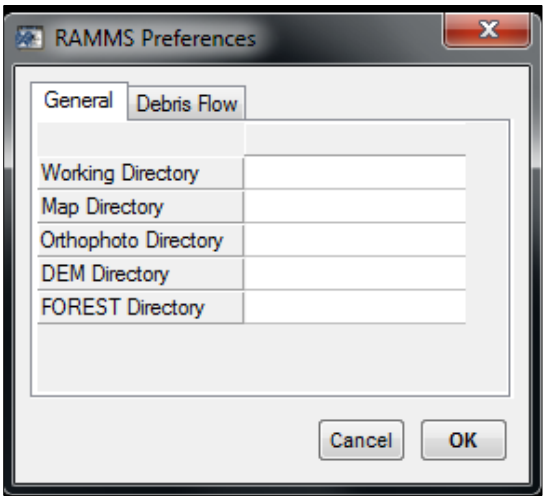

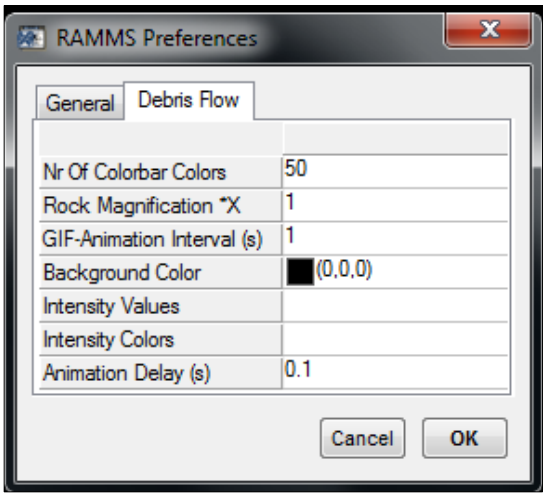

2. After the preferences have been setup, it is time to start a new project in RAMMS.

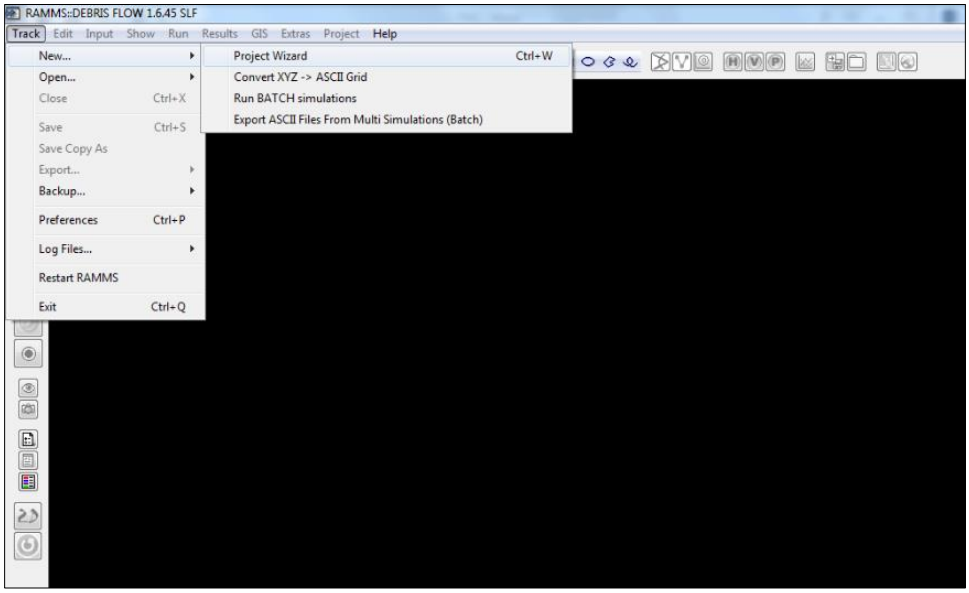

3. The new project wizard looks like below where one can define the project name and location. The DEM prepared in EXCEL can be imported in the next window and the gird resolution is fixed depending on the resolution of the DEM itself. This imported DEM must be in the ASCII grid format.

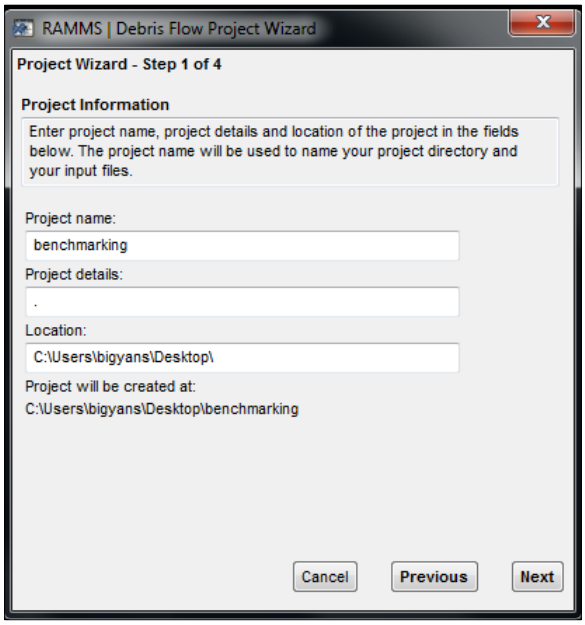

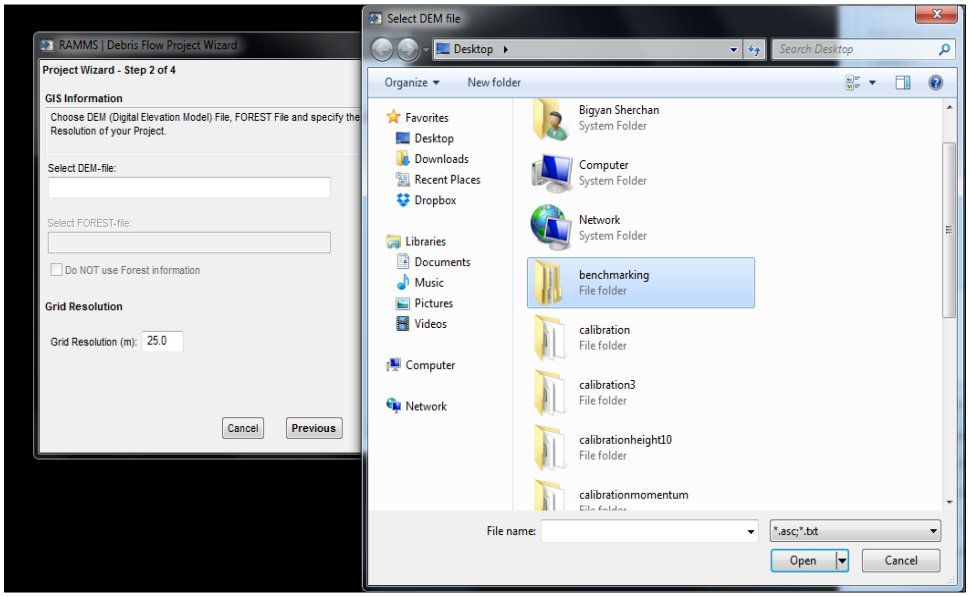

4. RAMMS then automatically defines the co-ordinates of the project boundary and creates a project.

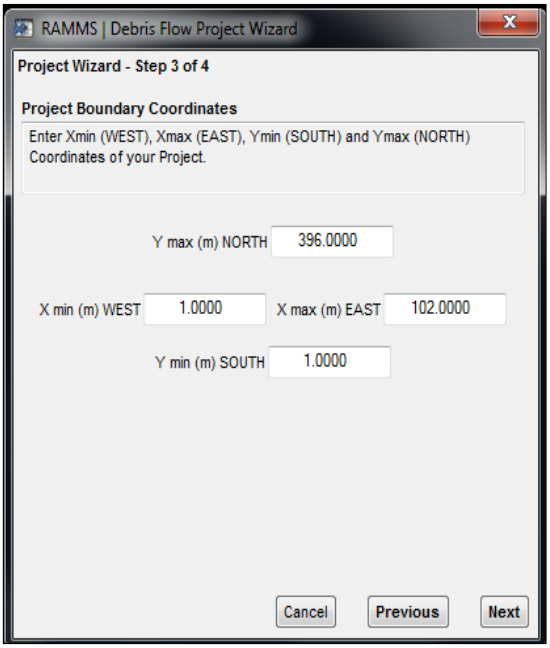

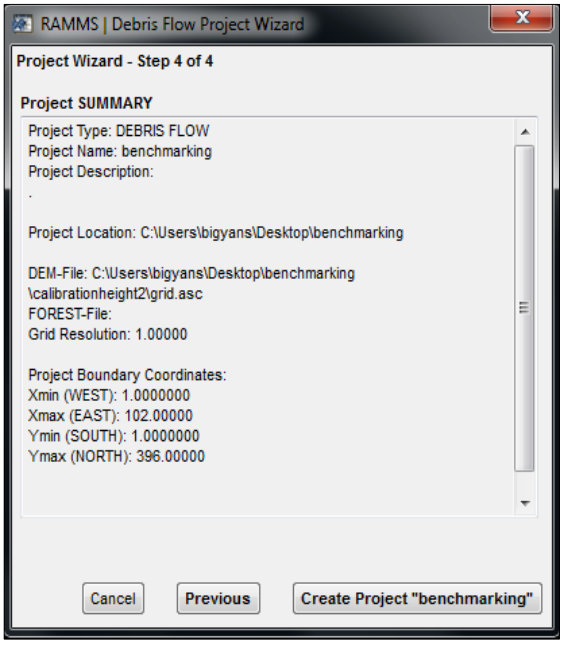

5. There is an option of importing topographic maps and aerial images over the DEM. After the completion of the project, the 3D representation of the DEM and the photograph, if available is shown on the screen. The user can switch between the 3D and 2D mode. The 2D mode is required while drawing the release area and fixing a calculation domain.

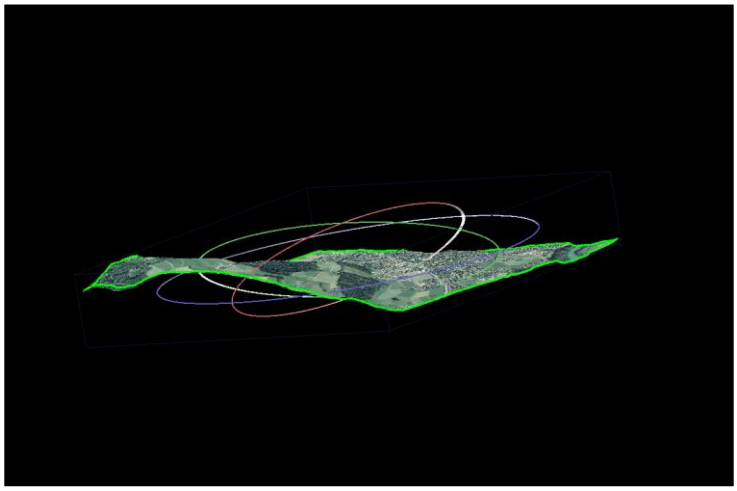

6. By default, RAMMS sets up an automatic calculation domain enclosing the whole project boundary. The user can modify this domain according to their needs.

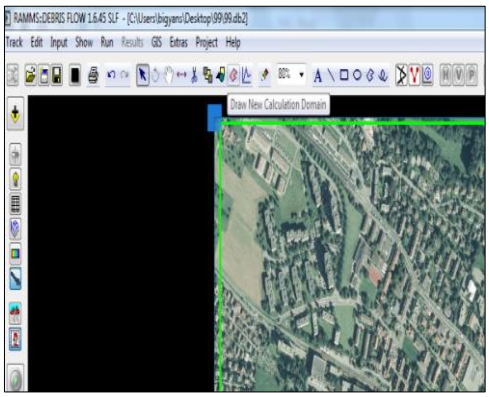

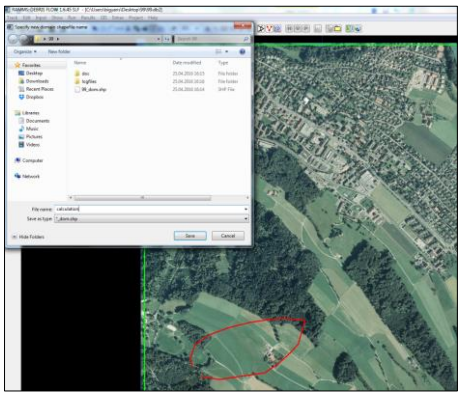

7. Similarly, a release area can be drawn in the same way by drawing a polygon shape. The release height is fixed later which gives the initiating volume of the slide.

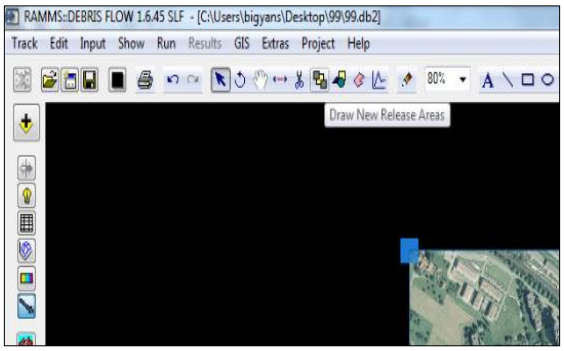

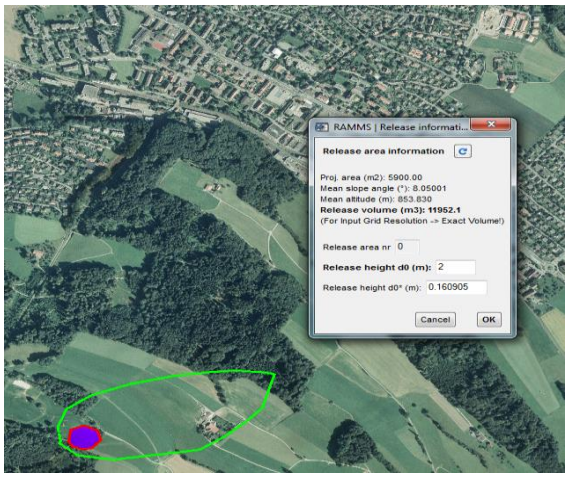

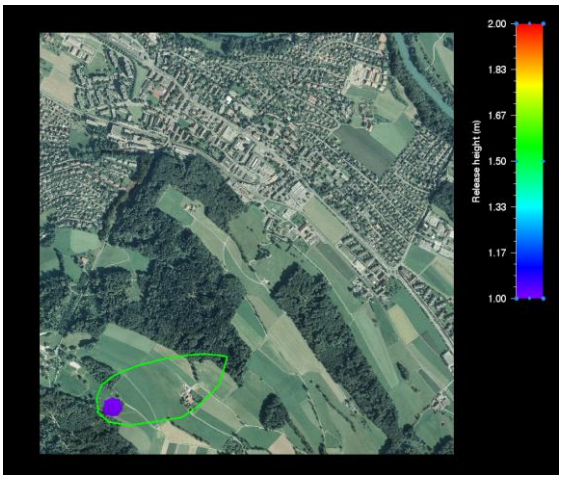

8. After the release area, calculation domain and the entrainment polygons have been defined, it is time to start the debris flow calculation run. The other input parameters can be defined along the simulation process. The user specifies the different simulation parameters like the grid resolution, end time, and number of dump steps. These are kept to their default values for this research. Similarly, the density of the terrain and the earth pressure coefficient (lambda) is defined. The numerical scheme is kept at second order with a default cutoff height of 0.00001 m.

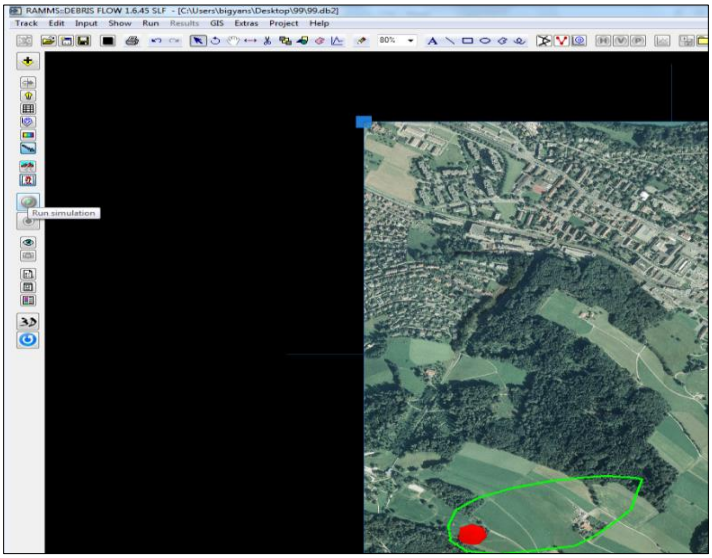

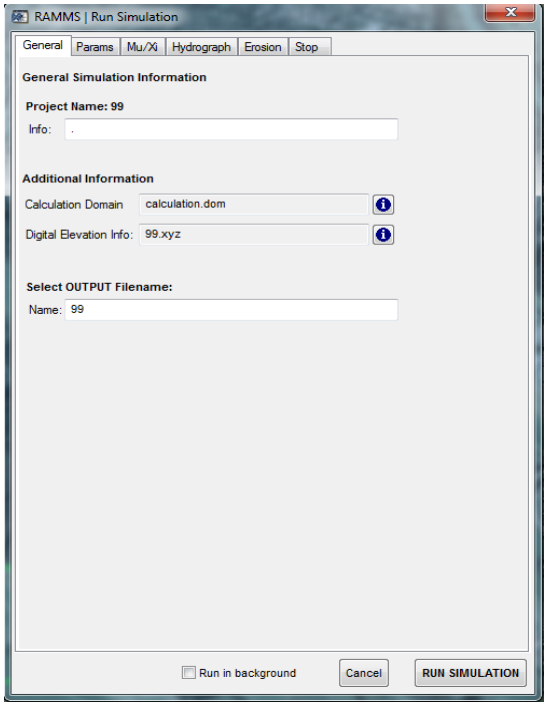

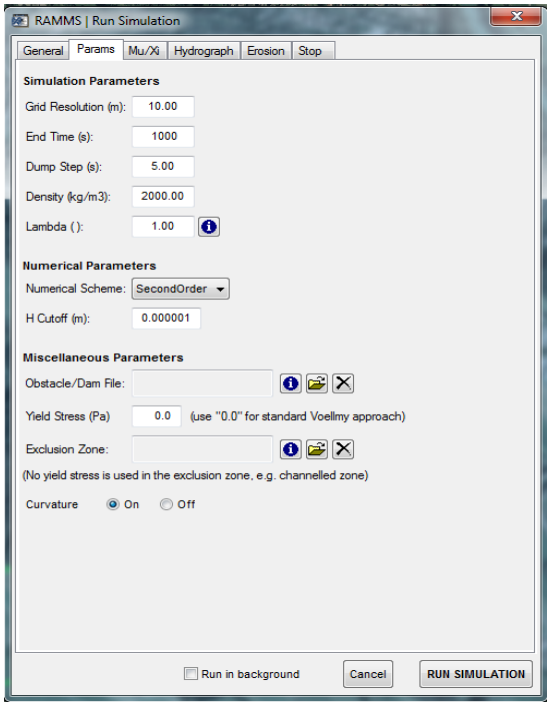

9. Then it is time to define the different friction parameters, friction parameter, μ and the turbulent coefficient, ξ. These are in accordance with the calibration of the Voellmy model used in RAMMS.

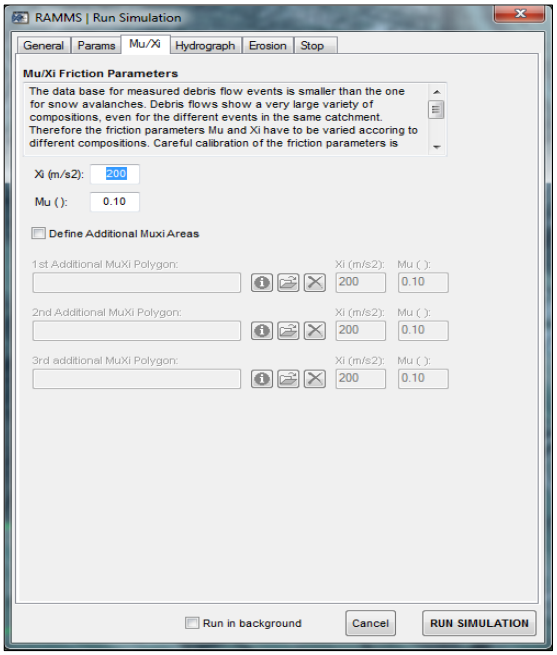

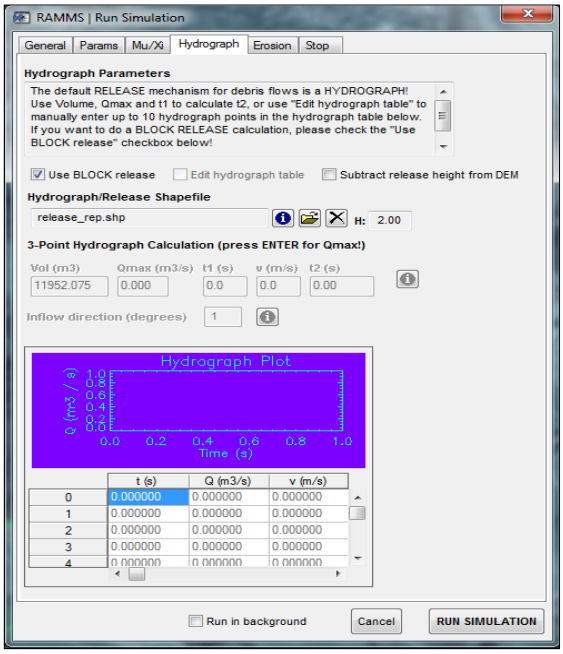

10. Entrainment is included in this version of RAMMS. To define entrainment, another polygon has to be drawn to define the area where entrainment occurs. Any number of polygons can be drawn to include entrainment, depending on where entrainment occurs in the terrain. To include the entrainment, the polygon shape file is loaded with an input depth, the density of the entrainment zone and the entrainment coefficient, K.

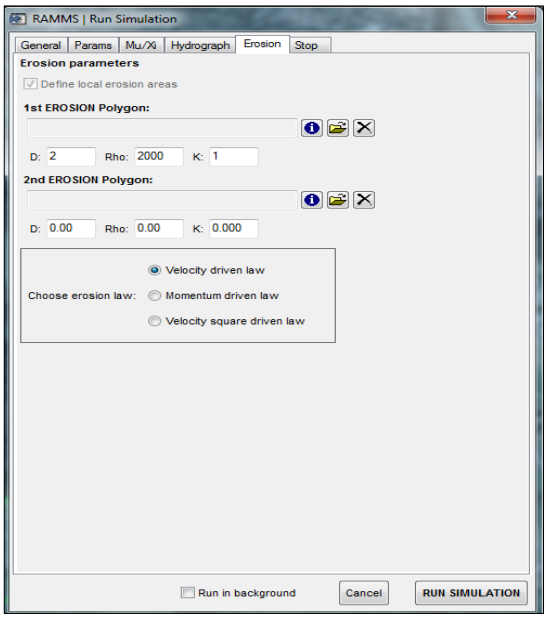

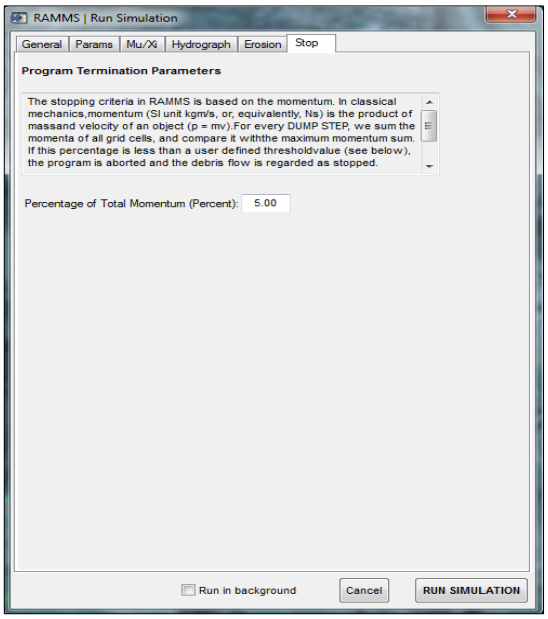

11. The next step is to define the stopping criteria. Once the calculation is started, the flow is calculated at each dump step. At the end of the simulation, RAMMS produces an output log file giving the various output parameters, the overall maximum height, the

overall maximum velocity and the overall maximum pressure to name a few. These parameters can also be viewed in the RAMMS window by selecting the required parameter from the Results drop down menu.

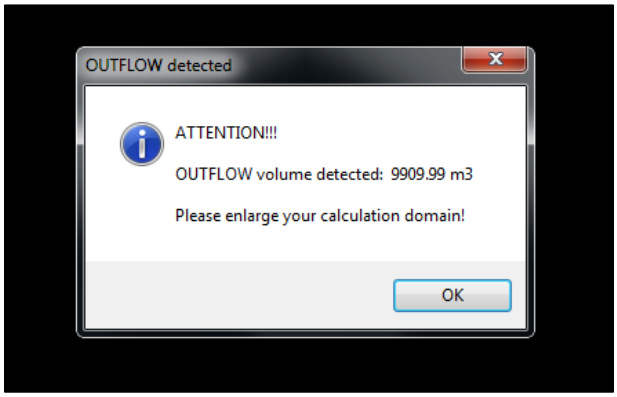

12. In case the debris flows outside of the calculation domain, RAMMS shows an attention window. This outflow volume is the part of the release volume that is blocked by or passing across the calculation domain and occurs due to placing of the release volume on top of the given terrain which allows it to flow in every direction. To solve this error, the calculation domain should be enlarged.

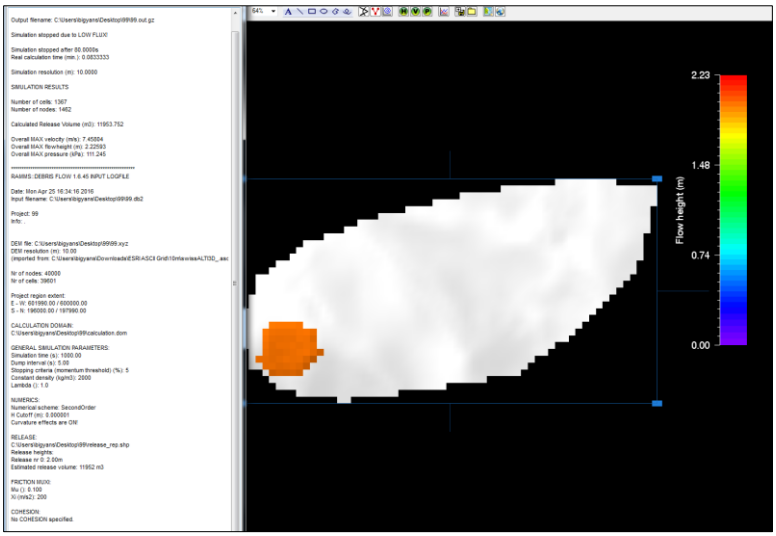

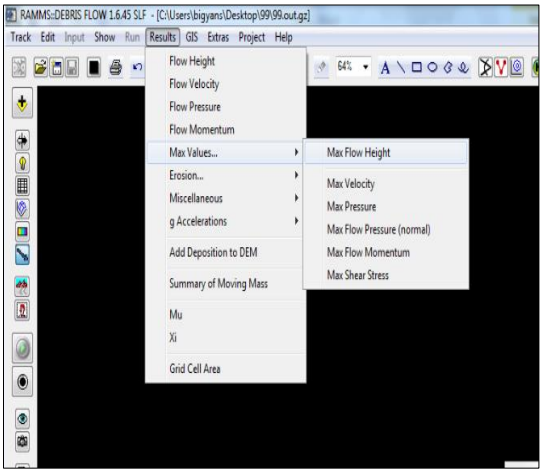

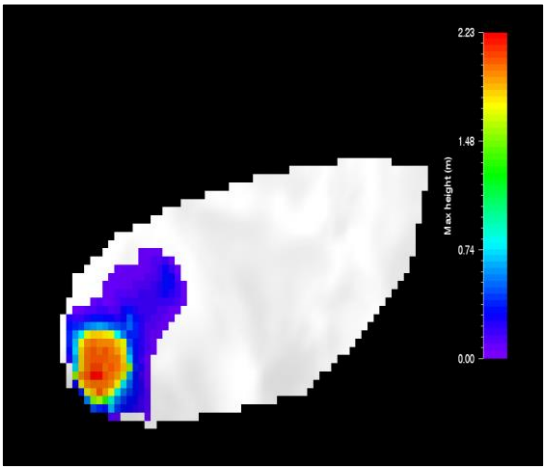

13. There is the possibility of viewing the debris flow at different time steps. By sliding through the dump step bar at the bottom of the window, the position of the flow at different time intervals can be viewed.

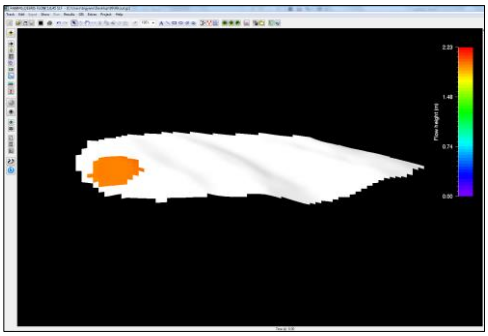

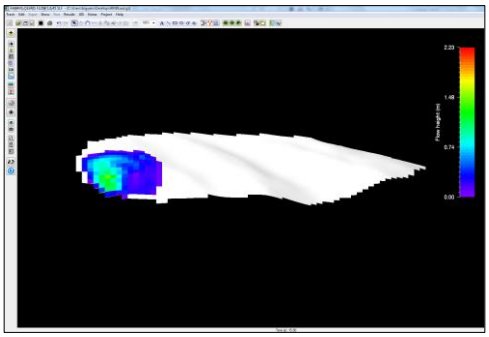

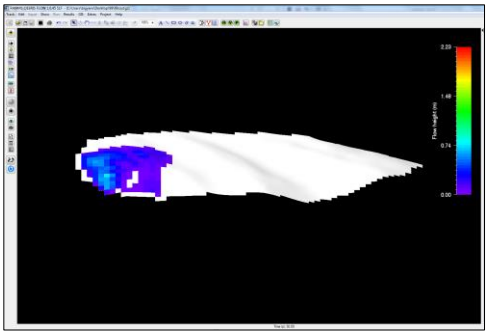

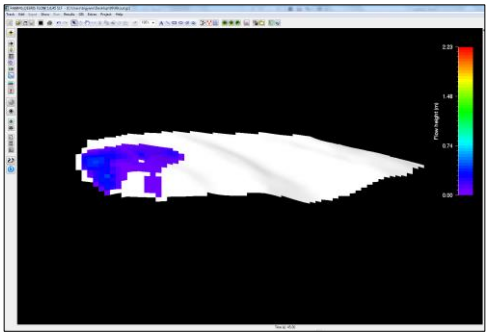

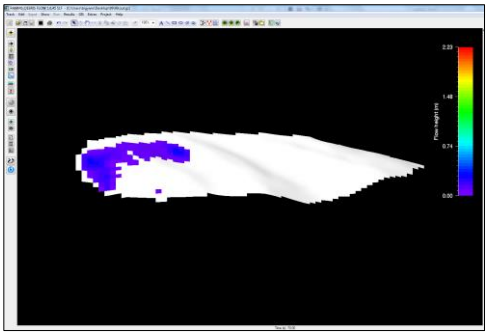

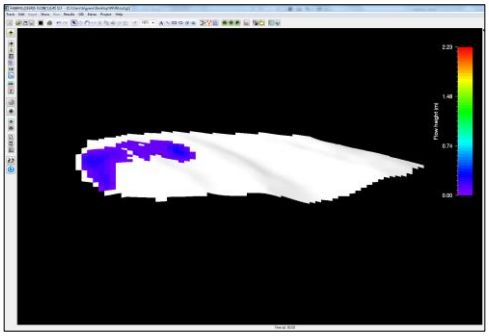

14. Additionally, profile and cross-sections can be drawn along the flow to show line and time plots.

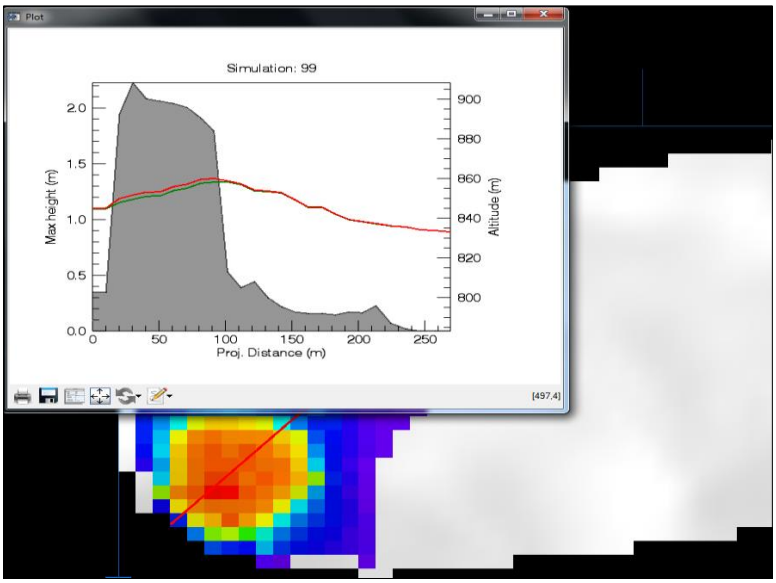

Appendix C

Benchmarking

Background

A sample DEM of a chute was prepared in EXCEL by defining the x, y and z co-ordinates of the chute. The chute has an inclination of 21.8 degrees, so that it can be a sample representative of debris flows which have inclination ranging from 20-30 degrees. This DEM was used to carry out the simulations in RAMMS which are described below.

The DEM prepared in EXCEL can be imported in RAMMS and the grid resolution is fixed depending on the resolution of the DEM itself. This imported DEM must be in the ASCII grid format. RAMMS then automatically defines the co-ordinates of the project boundary and creates a project.

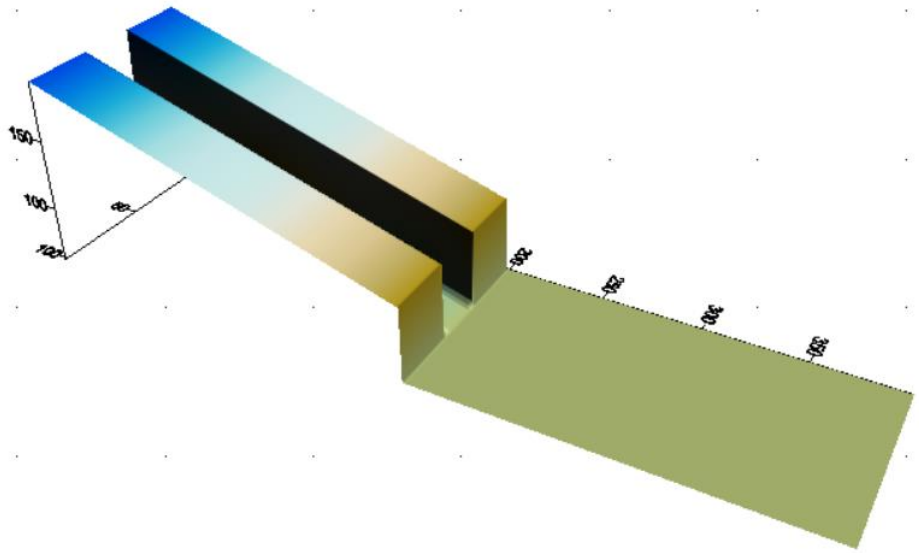

Simple model used for benchmarking of RAMMS software

Application of input parameters

After the definition of the topography of the flow, the next step is the application of input parameters. The first parameter is the definition of initiation zone which gives the release volume. In this case, two different release volumes were considered to see the effect on the results. This was achieved by varying only the release height, keeping the same release area. Two release areas with release volume 732 m^3 and 3660 m^3 with release height 2 m and 10 m respectively were considered for benchmarking. The density of the debris flow along with the rest of the terrain was kept constant with a value of 2000 kg/m^3 as it is representative of the

debris flow (Bartelt et al., 2013). The cohesion of the material was not specified as the flow materials were assumed to be having near zero cohesive strength (Pudasaini and Hutter, 2007).

The next input parameters are the friction parameters. Selection of appropriate values for the Voellmy friction coefficients is an important step. As there were no specific criteria for this simulation, the friction parameters were kept constant throughout the simulation and their values were chosen as recommended in the user manual, $\mu = 0.2$ and $\xi = 200$ m/s^2.

Another important input parameter is the definition of entrainment zone and assignment of relevant values for entrainment. The entrainment zone along with its depth and the density of the entrainment zone was kept constant varying the entrainment coefficient, K. The depth of the entrainment zone was provided 1 m for preliminary modelling having the same density, 2000 kg/m^3 with K = 1.

The rest of the parameters were kept constant according to their default values in RAMMS during all the simulations.

Assessment of output results

The most significant outputs for debris flow results are the runout distance, flow velocity, impact pressure and the deposited volume. As there were no fixed results in this case for model calibration, sensitivity analysis of varying input parameters, the release volume and the entrainment coefficient K specifically, on the runout distance and the deposited volume was studied during every simulation.

Results

The analysis result for the runout distance and the flow velocity is shown in the following figures. Simulation results of maximum flow heights and maximum velocities against the projected runout distance for two different release volumes, 732 m^3 and 3660 m^3 are presented one after another. As seen in the plots, the flow heights and flow velocities are dependent on the release volume, determined by the release height. There was only a slight difference in the total runout distance for the two different release volumes.

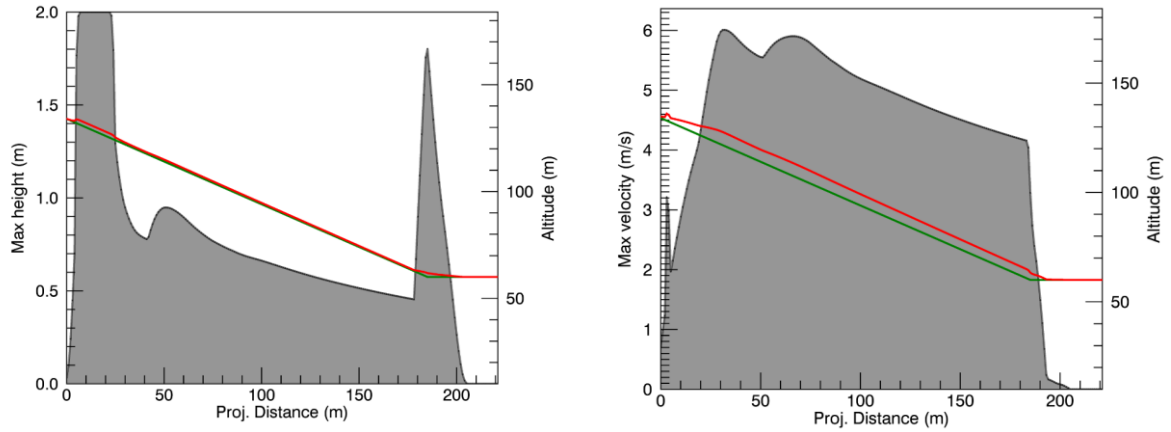

Flow height and Runout distance for a release height of 2 m and release volume of 732 m^3.

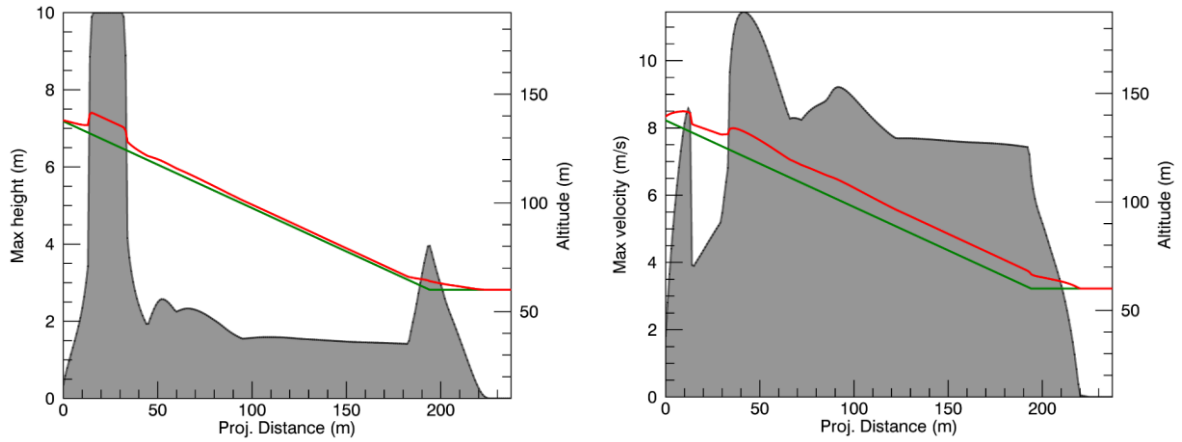

Flow height and Runout distance for a release height of 10 m and release volume of 3660 m^3.

For a release volume of 732 m^3, the maximum flow height along the runout was around 1.75 m at the beginning of the deposition zone where the channel flattens. The maximum velocity during the entire flow duration was 6 m/s which decreased to below 4 m/s towards the end of the flow. The runout distance of the flow was around 205 m.

When the release volume was increased to 3660 m^3, there was not a significant change in the runout distance; it only increased to nearly 222 m. The maximum flow height changed to around 4 m in the deposition zone. The flow had a maximum velocity of more than 11 m/s from its inception and it gradually decreased to 6-8 m/s before coming to a stop at the end.

Because of entrainment, less than 5 m^3 of bed materials was eroded for both cases of different release volumes. This is a result of applying an entrainment coefficient of K = 1, keeping μ = 0.2 and ξ = 200 m/s^2. When this value was increased to K = 5, there was a large variation in the eroded volume. For the first release volume of 732 m^3, 25 m^3 of bed materials was eroded whilst more than 57 m^3 of bed materials was entrained with a release volume of 3660 m^3. Both

these eroded volumes are lower than the available 100 m^3 of sediment volume that can be entrained.

Discussions

From the results above, it can be seen that the increase in release volume of the initiating landslide will increase the runout distance, flow height and velocity of the debris flow. There was not a significant change in the runout distance and this can be accounted by the low release volume of the initiation area (M. Christen, Personal Communication, April 21, 2016).

The entrainment volume is governed in RAMMS by the entrainment coefficient, K. As this value was increased, the eroded volume simultaneously increased. The eroded volume did not change for both release volumes with lower values of K up to 1. Upon increasing the value of K beyond 1, 3660 m^3 of the initiating slide eroded greater volume than that by 732 m^3. One distinct feature in all these cases is the final eroded volume did not reach its maximum value. The maximum eroded volume which is given by the release volume of 3660 m^3 with K = 5 was around 60 m^3 out of 100 m^3 of available volume that can be eroded in total. This has again been accounted to the lower release volumes in general. RAMMS is more suited to the simulations of debris flows with initiation volume in order of 10000-10000 m^3.

Appendix D

NTNU
Det skapende universitet

MASTERKONTRAKT
- uttak av masteroppgave

1. Studentens personalia

Etternavn, fornavn **Sherchan, Bigyan**	Fødselsdato **29. nov 1988**
E-post **bigyansherchan@gmail.com**	Telefon **47145383**

2. Studieopplysninger

Fakultet **Fakultet for ingeniørvitenskap og teknologi**
Institutt **Institutt for geologi og bergteknikk**
Studieprogram **Geotechnics and Geohazards**

3. Masteroppgave

Oppstartsdato **15. jan 2016**	Innleveringsfrist **10. jun 2016**
Oppgavens (foreløpige) tittel **Debris Flow** **Entrainment of bed sediments by debris flow**	
Oppgavetekst/Problembeskrivelse A lot of landslides occur in Norway every year. As a result of this, debris flow may occur. Even though the initiating landslides are small, the resulting debris flow may bring along with it entrainment of large amount of materials. This study will look into the different mechanisms of debris flow conducted by numerical, analytical and empirical techniques.	
Hovedveileder ved institutt **Professor Steinar Nordal**	Medveileder(e) ved institutt **Ashenafi Lulseged Yifru**
Merknader **1 uke ekstra p.g.a påske.**	

4. Underskrift

Student: Jeg erklærer herved at jeg har satt meg inn i gjeldende bestemmelser for mastergradsstudiet og at jeg oppfyller kravene for adgang til å påbegynne oppgaven, herunder eventuelle praksiskrav.

Partene er gjort kjent med avtalens vilkår, samt kapitlene i studiehåndboken om generelle regler og aktuell studieplan for masterstudiet.

Trondheim, 14 January 2016

Sted og dato

Student

Hovedveileder

Originalen lagres i NTNUs elektroniske arkiv. Kopi av avtalen sendes til instituttet og studenten.